SIMULATED PLUME DEVELOPMENT AND DECOMMISSIONING USING THE BREAKTHROUGH CURVES OF FIVE CATIONS

A Thesis Submitted to the College of

Graduate Studies and Research

In Partial Fulfillment of the Requirements

For the Degree of Master of Science

In the Department of Chemical and Biological Engineering

University of Saskatchewan

Saskatoon

By

CRYSTAL D. RINAS

Permission to Use

In presenting this thesis in partial fulfilment of the requirements for a Postgraduate degree from the University of Saskatchewan, I agree that the Libraries of this University may make it freely available for inspection. I further agree that permission for copying of this thesis in any manner, in whole or in part, for scholarly purposes may be granted by the professor or professors who supervised my thesis work or, in their absence, by the Head of the Department or the Dean of the College in which my thesis work was done. It is understood that any copying or publication or use of this thesis or parts thereof for financial gain shall not be allowed without my written permission. It is also understood that due recognition shall be given to me and to the University of Saskatchewan in any scholarly use which may be made of any material in my thesis.

Requests for permission to copy or to make other use of material in this thesis in whole or part should be addressed to:

Head of the Department of Chemical and Biological Engineering

University of Saskatchewan

Saskatoon, Saskatchewan S7N 5A9

ABSTRACT

The primary objective of this research was to investigate multicomponent transport of five major cations, Ca^{2+}, Mg^{2+}, NH_4^+, K^+ and Na^+, in laboratory soil columns. The soil columns were packed with soils from two different sites and were equilibrated with fresh groundwater from each respective site. Experimental data was obtained by flushing a simulated contaminant through the soil columns. The soil columns were then flushed with fresh groundwater to simulate decommissioning activities. The breakthrough data and soil exchange capacities obtained from both tests were used to identify key processes affecting the transport of the geochemical species.

During the simulated contaminant flushing stage, NH_4^+ and K^+ replaced Ca^{2+} and Mg^{2+} on the soil exchange sites. Breakthrough of NH_4^+ was attenuated by factors of 3.2 and 6 for Sites 1 and 2 soils, respectively. Breakthrough of K^+ was attenuated by factors of 3.2 and 5.4 for Sites 1 and 2 soils, respectively. Generally, ions with higher valency will exchange for those of lower valency, but in this case the majority of the ions (NH_4^+ and K^+) in the solution has a lower valency and will exchange with those of higher valency by mass action. Ca^{2+} was the first to be replaced, followed by Mg^{2+} once the ionic strength of the solution increased.

The displacement of calcium and magnesium created a concentration pulse of these cations that coincides with the chloride breakthrough curve. Calcium and magnesium concentrations reached up to approximately 275% and 2000%, respectively, higher than the freshwater originally in the column.

During the freshwater flushing stage, freshwater infiltrated the soil columns to assess the permanency of contaminant attenuation and to identify the geochemical mechanisms of contaminant release. Concentrations of NH_4^+ and K^+ declined quickly. Ninety-five percent of attenuated NH_4^+ was released by the soil. Therefore, the attenuation of NH_4^+ is reversible but this occurs over several pore volumes at concentrations lower than those in the simulated contaminant and therefore would not result in a mass loading to the environment. Cation exchange was identified as the mechanism responsible for the release of the adsorbed ammonium and potassium into the soil pore water.

ACKNOWLEDGMENTS

First and foremost I would like to thank Dr. Terrance Fonstad for giving me the opportunity to pursue this M.Sc. Degree. I am truly thankful for his guidance, patience and friendship. I would also like to thank my graduate advisory committee: Dr. Charles Maulé and Dr. Huiqing Guo as well as Dr. Angela Bedard-Haughn for their careful review of this thesis.

I would like to thank Civil Engineering laboratory technicians Alex Kozlow and Doug Fisher for kindly lending their assistance and tools.

Financial support for this project was provided by Saskatchewan Agriculture and Food Agricultural Development Fund for which I am thankful.

My parents, Walter and Sandra Halliday, as always, have been a huge support to me. Thank you both for your love and support throughout all of my academic pursuits.

DEDICATION

This "pieces" is dedicated to my husband, Darrell Rinas and my son, Carson Rinas. Thank you both for your love, support and patience.

TABLE OF CONTENTS

page

LIST OF TABLES

LIST OF FIGURES

CHAPTER 1
INTRODUCTION

1.1 Background

In 2008, the Saskatchewan pork industry produced a total of 2.6 million pigs, the highest number of pigs produced in the province historically (Saskatchewan Pork 2011). Since 1995, this was an increase of 1.8 million pigs. As the industry expanded, there was added pressure for it to be environmentally sustainable. In 2009, difficult market conditions have caused this number to drop to 1.9 million pigs (Saskatchewan Pork 2011). This introduced an additional environmental concern regarding the decommissioning of hog production facilities that are no longer operational. The foremost environmental concern regarding hog production facilities is the storage of liquid manure.

Waste from hog production facilities is commonly stored in earthen manure storages (EMS). Contaminant seepage from earthen manure storages is considered a threat to the surrounding groundwater resources. Engineered earthen manure storages are designed to protect surface and groundwater by properly siting the storage and using highly impermeable construction materials which reduce the potential for seepage from the storage. Seepage problems can occur with storages that were not built to current standards or when lined storages are not maintained properly.

When earthen manure storages are no longer operational, the remaining waste should be properly removed. Decommissioning concerns are raised when a storage was not built or operated properly and seepage occurred allowing the movement of contaminants into the soil below. This

creates a mass of contaminants that are adsorbed onto the soil particles beneath the earthen manure storage that are not removed during decommissioning. No research targeting the closure of earthen manure storages and the fate of adsorbed contaminant is available in the literature.

Liquid hog manure contains significant amounts of the following inorganic ions: ammonium-nitrogen (NH_4^+), potassium (K^+), bicarbonate (HCO_3^-), chloride (Cl^-), sodium (Na^+) and sulphate (SO_4^{2-}) (Fonstad 2004). Seepage of these inorganic species into surrounding soils can constitute a groundwater contamination problem. The species of foremost concern is NH_4^+. Ammonium can be converted to nitrate-nitrogen (NO_3^-) in an aerobic environment. Groundwater containing NO_3^- is a health risk because it can cause methemoglobinemia when ingested by infants.

This study was initiated in the hog industry, but its application is not limited to this industry. Multicomponent contaminant seepage is not only seen in the case of earthen manure storages, but is also seen in cases of seawater intrusions (Beekman and Appelo 1990) and landfill leachate plumes (Erskine 2000; Thorton et al. 2001)

In the case of contaminant seepage from various sources, often high concentrations of multiple inorganic chemical species are involved. When several species are present, complex breakthrough patterns can occur as the species progress through the subsurface (Voegelin et al. 2000; Vulava et al. 2002). These complex breakthrough patterns are due to the adsorption of cations on clay particle surfaces and subsequent precipitation/dissolution reactions and changes in soil structure. These reactions cause a separation of the ions known as a chromatographic sequence.

Chromatographic sequences can be replicated in laboratory soil column tests. Soil column testing refers to the measurement of the transport parameters describing the migration of a chemical species through soil under controlled laboratory conditions (Shackelford 1995). Initially, steady-state flow is established, followed by the introduction of a continuous contaminate source of known concentration. The effluent is then periodically collected and the concentration analyzed. The measured effluent breakthrough curves are then evaluated. Most laboratory soil column tests consist of binary ion exchange, where one cation is replaced by another, such as the replacement of calcium (Ca^{2+}) by Na^{+} by Vulava et al. (2002) or the exchange of K^{+} with Ca^{2+} by Griffioen et al. (1992). Laboratory soil column tests by Beekman and Appelo (1990), Cerník et al. (1994) and Thorton et al. (2000) have consisted of three or more cations. Fonstad (2004) conducted laboratory soil column tests using five cations, Ca^{2+}, magnesium (Mg^{2+}), Na^{+}, K^{+} and NH_4^{+}.

By evaluating column breakthrough curves, transport parameters including attenuation factors can be determined. These parameters are required for geochemical contaminant transport models. Improving the accuracy of these models will result in more accurate predictions of contaminant transport.

1.2 Research Objectives

The primary objective of this research was to investigate multicomponent transport of five major cations, Ca^{2+}, Mg^{2+}, NH_4^{+}, K^{+} and Na^{+}, in laboratory soil columns. The soil columns were

packed with soils from two different sites and were equilibrated with fresh groundwater from each respective site. Experimental data was obtained by flushing a simulated contaminant through soil columns. Following this, the soil columns were flushed with fresh groundwater to simulate decommissioning activities. The breakthrough data and soil exchange capacities obtained from both tests were used to identify key processes affecting the transport of the geochemical species. Specific objectives included:

1) confirming the attenuation of ammonium and potassium using column breakthrough curves during the simulated plume development; and

2) determine the potential for desorption of ammonium and potassium using column breakthrough curves from the post decommissioning simulation.

Secondary objectives included evaluating two different methods to determine the partitioning of cations on soil exchange sites.

Improved knowledge of transport mechanisms will allow for more accurate predictions and risk assessment of the environmental performance of waste storages. A better understanding of environmental performance will increase public assurance and acceptance of hog production facilities.

CHAPTER 2
LITERATURE REVIEW

2.1 Earthen Manure Storages and Leachate

Saskatchewan industries have a responsibility to ensure all industrial operations are environmentally sustainable. This responsibility extends to all industries from agriculture to mining to public works. In the last decade, industries in Canada have realized the importance of ensuring their operations are environmentally sustainable. This is not only a social responsibility, but the governed regulations require specific standards to be followed. In the case of protecting groundwater resources from a contaminant source, often a contaminant transport model is required. The accuracy of their models depends on the accuracy of their input parameters. This study examines the mechanisms of contaminant transport from earthen manure storages, the results of which can be used to improve contaminant transport modeling.

In the agricultural industry, earthen manure storages (EMS) are a common facility to store liquid hog manure. They are cost effective and more common than concrete or steel above ground storage facilities. Today, many engineered earthen manure storages are lined with clay soils to protect groundwater by preventing lateral and vertical contaminant seepage. Seepage problems can occur with earthen manure storages that were not built to today's standards or when the lined storages are not operated properly.

In Saskatchewan, regulations provision is not made for the attenuation capacity of underlying soils of an EMS. Instead, the environmental performance of an EMS accounts for the existing

site conditions and mode of transport mechanisms that govern seepage of contaminants from the storage (i.e. sites are assigned one of three categories: geologically secure, geologically variable and geologically sensitive based on the ground water velocity, hydraulic gradients, and geologic conditions) (Saskatchewan Agriculture Food and Rural Revitalization 2005).

Numerous research studies have been conducted to study the seepage of contaminants from earthen manure storages into the groundwater system. Most of these studies have focused on if and how much earthen manure storages leak, how soil type affects seepage rates, and the sealing effect caused by animal waste. These studies have continuously shown that when EMS are constructed improperly without an impermeable liner or when the liner has been eroded or cracked, a contaminant plume develops beneath the storage (Cirvalo et al. 1979; McMillan and Woodbury 2000; Ritter and Chirnside 1990; Westerman et al. 1995). The extent of the contaminant plume varies with age, soil type, and water table depth with the worst type scenario being an earthen manure storage constructed without a liner on a sandy soil with a high water table. In Saskatchewan, this type of site would be considered geologically sensitive.

When a livestock operation shuts down and the earthen manure storage is decommissioned, risks to the groundwater system remain. There has been limited research specifically targeting the transport of contaminant plumes once closure of an earthen manure storage has taken place.

Jones (1999) presented a paper on the closure of earthen manure storages. In this paper, two closure procedures were recommended. The first was the elimination of the earthen manure structure by diverting all surface water runoff away from the storage, filling the lagoon with soil,

and establishing a vegetative cover to prevent erosion. The second was a conversion to a farm pond where the lagoon is rinsed with water, agitated, and the manure removed before being refilled with water. The problem with both of these methods is that poorly designed and constructed liners, as well as those that were badly eroded, may have already allowed significant movement of contaminants into the soil below the earthen structure. Both of the suggested decommissioning methods do not remove any existing contamination plumes beneath the earthen structure posing a risk of this plume to travel further into the groundwater system.

Fonstad (2004) identified that the composition of earthen manure storage leachate was not readily available in the literature. By taking samples from various types of hog production facilities and various depths of an earthen manure storage, Fonstad (2004) was able to characterize the inorganic composition of earthen manure storage leachate.

Table 2.1 Composition of EMS leachate and landfill leachate composition.

Contaminant	Typical level in landfill leachate[1] (mg/L)	Typical level in swine manure leachate[2] (mg/L)	Typical level in swine manure leachate[3] (mg/L)
Ammonium (as N)	800	1977	3900
Potassium	780	1118	2000
Magnesium	250	92	100
Chloride	2000	2398	1350
Sodium	700	1918	750
Calcium	155	62	200
Sulphate	70	90	700
Bicarbonate(as $CaCO_3$)	n/a	7600	11700
Copper	0.1	n/a	0.1

[1]Typical levels taken from Erskine (2000); [2]Typical level taken from Thornton et al. (2005); [3]Typical level taken from Fonstad (2004).

In Table 2.1, NH_4^+ is the element with the greatest potential toxic impact on groundwater quality and occurs at relatively high concentrations in the leachate. The concern of NH_4^+ contamination

is the conversion of NH_4^+ to nitrate in oxidizing conditions. Once taken into the body, nitrates are converted into nitrites. The nitrite then reacts with oxyhemoglobin (the oxygen-carrying blood protein) to form metheglobin, which cannot carry oxygen. If a large enough amount of metheglobin is formed in the blood, body tissues may be deprived of oxygen. When this happens, infants can develop a blue coloration of their mucous membranes and possibly digestive and respiratory problems. This condition is also known as methemoglobinemia.

Earthen manure storages are only one potential source of groundwater contamination. The composition of landfill leachate is similar to the composition of EMS leachate. Table 2.1 lists the composition of landfill leachate from landfills taking predominantly domestic and commercial waste (Thorton et al. 2005). Ammonium is also the primary contaminant of concern arising from domestic waste landfills and is most likely to impact water resources via a groundwater pathway (Erkskine 2000).

2.2 Contaminant Transport Mechanisms

Once a leachate leaves a source, whether it be an EMS or landfill, its chemistry will be altered along its travel path. The most active processes are dilution, adsorption, exchange reactions, precipitation, and filtration (Islam et al. 2002). In the case of EMS, biochemical processes are likely to take place under anaerobic conditions (Islam et al. 2002). The transport of NH_4^+ is attenuated by two main processes: ion exchange and oxidation (Erskine 2000).

Ion exchange is an adsorption process where positive ions are attracted to negatively charged clay-mineral surfaces. Generally ions with higher valency will exchange for those of lower

valency. For example, the affinity for $Al^{3+} > Ca^{2+} > Mg^{2+} > K^{+}=NH_4^{+} > Na^{+}$ (Appelo and Postma 1999). For ions of same charge, the cation with the smallest hydrated radius is strongly absorbed because it is closest to the site of charge. For example, K^{+}, with a hydrated radius of 0.532 nm, will exchange for Na^{+}, hydration radius of 0.790 nm, on the exchange sites.

In the case of EMS leachate plumes and other types of contaminant transport, there are often many contaminant species involved. When several species are present, complex breakthrough patterns can occur as the plume progresses (Voegelin et al. 2000; Vulava et al. 2000). These complex breakthrough patterns occur due to the competitive adsorption of cations. Certain cations are preferred on the soil exchange sites. This preference is based on the ionic strength of the solution, mass action (high concentration of ion in solution), and ion valency (Fonstad 2004). The cations that are adsorbed by the soil do not transport as rapidly as unreactive anions such as chloride. This results in a separation of the ions as they appear in the plume known as a chromatographic sequence.

Chromatographic sequences are seen in the natural environment in the cases of seawater intrusions (Beekman and Appelo 1990), landfill leachate plumes (Thornton et al. 2000), earthen manure storage leachate plumes, and fertilization of soils with manures (Nunez-Delgado et al. 1997).

Extensive work has been published describing the adsorption of NH_4^{+} in multicomponent systems. Ceazan et al. (1989) investigated the attenuation of NH_4^{+} and K^{+} in a shallow sand and gravel aquifer by field scale observation of a sewage contaminant plume, small-scale tracer

injection tests and batch sorption experiments. In the small-scale tracer injection tests, attenuation of NH_4^+ was caused by cation exchange. Ammonium displaced Ca^{2+} and Mg^{2+} from aquifer sediments. They found that the replacement of aquifer cations was probably a mass action effect rather than selectivity because later flushing with NH_4^+ free groundwater easily liberated most of the adsorbed NH_4^+. Although the liberation of NH_4^+ was not the focus of their study, they stated it is important when considering the effect of decommissioning of an earthen manure storage site.

Thorton (2001, 2005) studied the attenuation of landfill leachate by clay liner materials and found that NH_4^+ in the leachate is attenuated by ion exchange. Breakthrough of major cations occurred as a series of fronts and resulted in the elution of Ca^{2+} and Mg^{2+} above input concentrations, but differential attenuation of Na^+, K^+, and NH_4^+. Calcium and Mg^{2+} stabilized at input leachate levels only when NH_4^+ and K^+ achieved final breakthrough in each column. The elution of major cations during leachate breakthrough were characteristic of those produced by multicomponent heterovalent ion-exchange reactions which results in the chromatographic displacement of native cations from the exchange complex by adsorption of leachate cations.

The second part of the Thornton's study included the permeation of the liners with oxygenated water to provide information on the reversibility of contaminant attenuation, plus the likely form and magnitude of contaminant loadings which might occur following a landfill oxygenation. They found that 26% to 52% of previously sorbed NH_4^+ was released depending on the soil material. They stated that attenuation is reversible but this release occurs over several pore

volumes at concentrations which are much lower than those in the leachate and therefore more manageable from a practical point of view.

Fonstad (2004) identified the need to investigate the release of adsorbed NH_4^+ once the source is removed and natural waters begin to infiltrate and leach the contaminant plume. He postulated that with higher ionic strengths and NH_4^+ and K^+ concentrations, both ions would be preferentially adsorbed. When the ionic strength of the solution was reduced, NH_4^+ and K^+ would be released as Ca^{2+} and Mg^{2+} would displace them on the soil exchange sites.

Chang and Donahue (2007) found that clay rich soil samples absorbed and/or desorbed major cations in the pore fluid using a radial-diffusion cell method. They found that the competition for the adsorption sites depended on constituent mole fraction, ionic charge and ionic size (hydrated radius). In particular, NH_4^+ dominated the adsorption sites because NH_4^+, with a high mole fraction in the source (45%), had more chances to occupy the sites compared to other co-existing cations. They also found that even though K^+ and NH_4^+ have the same hydrated radius, K^+ adsorption, when in competition with NH_4^+, was suppressed.

Cation exchange reactions in soils are commonly described using selectivity coefficients. The most popular equations describing how to calculate selectivity coefficients are the Vanselow, Gaines and Thomas, and Gapon equations (Vulava et al 2000).

The selectivity coefficient expresses the relative bonding strength of an exchanger for two cations. For the following reaction:

$$A + B\text{-}X \leftrightarrow A\text{-}X + B \quad (1)$$

the selectivity coefficient is:

$$K_{A/B} = ([A\text{-}X][B])/([B\text{-}X][A]) \quad (2)$$

where the square brackets denote activities.

The concentration of an ion in solution can be directly converted to activity by using the Debije-Huckel theory. Determining the activity of an adsorbed ion is more difficult. The Gaines-Thomas convention uses the equivalent fraction of the exchangeable cation for the activity of the adsorbed ions. The Vanselow convention uses molar fraction for the activity of the adsorbed ions. With the Gapon convention, the molar and equivalent fraction are identical because both are based on a single exchanger site with a charge of negative one.

Although it is possible to determine selectivity coefficients from breakthrough curves, it involves complex mathematics and has not been solved for systems with more than three cations (Appelo 1996). Fonstad (2004) showed that the ions on the exchange complex could be modeled using the solution chemistry and selectivity coefficients developed from column tests using five ions. The selectivity functions were determined using data of extractable and exchangeable ions from sectioning of the soil columns. Fonstad (2004) showed that the selectivity coefficients were a function of the ratio of monovalent to divalent cations in solution for clay till while the

coefficients varied as a function of the Ca^{2+} quantity on the exchange complex of a smectite clayey sand.

2.3 Soil Column Testing and Determining Transport Parameters

Soil column testing refers to the measurement of the transport parameters describing the migration of a chemical species through soil under controlled laboratory conditions (Shackelford 1995). Initially, steady-state flow is established, followed by the introduction of a continuous contaminate source of known concentration. The effluent is then periodically collected and the concentration analyzed. The measured effluent breakthrough curves are then evaluated.

The column of soil used in a column test is not representative of a natural situation but represents a natural situation as closely as possible in a laboratory setting. Column experiments are preferred over batch tests because the soil water ratios for the column test are more realistic than the batch test (Griffioen et al. 1992).

Darcy's law is used to analyze the flow of water through soil. For an experimental apparatus, such as a soil column shown in Figure 2.1, a circular cylinder has a cross section, A. The inflow rate is equal to the outflow rate, Q, the soil length is l, and h is the hydraulic head and dh/dl is the hydraulic gradient. K is the saturated hydraulic conductivity. All of these variables are incorporated experimentally into Darcy's Law (Freeze and Cherry 1979):

$$Q = -K \frac{dh}{dl} A \qquad (3)$$

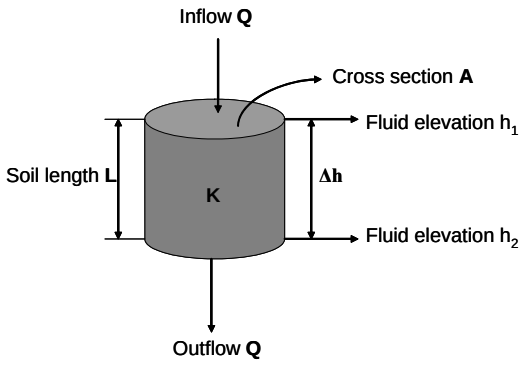

Figure 2.1. Soil column apparatus for the demonstration of Darcy's law.

The one dimensional Darcy velocity is defined as:

$$v = \frac{Q}{A} \tag{4}$$

The groundwater velocity (v), is calculated below:

$$\bar{v} = \frac{v}{n} \tag{5}$$

where n is the porosity.

Solute transport in groundwater is affected by a large number of physical, chemical and microbial processes and soil properties. The major processes include advection, diffusion and hydrodynamic dispersion, aqueous complexation, precipitation/dissolution, adsorption/desorption, microbial reactions, and redox transformations (Islam et al. 2001). The soil properties such as hydraulic conductivity, ion exchange capacity, and buffering capacity of the soil are also important in assessing the potential for groundwater pollution. The advection dispersion equation (ADE) is a well known equation that describes one dimensional solute transport of a miscible contaminant through a saturated homogeneous soil (Freeze and Cherry 1979).

$$D\frac{\partial^2 C}{\partial l^2} - \bar{v}\frac{\partial C}{\partial l} = R_d\frac{\partial C}{\partial t} \qquad (6)$$

where t= time; l= soil length; C= solute concentration in the soil pore water; R_d = attenuation factor; and D= hydrodynamic dispersion coefficient. The advection dispersion equation ignores microbial processes.

Diffusion, where ions move in the soil water in response to concentration gradients, and advection, where ions move with the soil water, are the two main processes that govern solute transport in soil. Differences in pore water velocities within individual pores and between pores of different sizes lead to an additional effect known as hydrodynamic dispersion, which results in a spreading of solute as the solute moves with the soil water. Because both diffusion and mechanical dispersion result in reduced solute concentration gradients they are often combined

in the mathematical description of solute transport, and referred to as the hydrodynamic dispersion coefficient.

The hydrodynamic dispersion coefficient, D, is given by (Freeze and Cherry 1979):

$$D = \alpha v + D^* \quad (7)$$

where α= longitudinal dispersivity of the soil; v= seepage velocity; D*= effective diffusion coefficient. The hydrodynamic dispersion coefficient accounts for spreading or apparent mixing of the solute migration front during transport.

Chemical diffusion, described by the effective diffusion coefficient, is a process where a chemical species moves from an area of higher concentration to an area of lower concentration. The coefficient of molecular diffusion is related to the coefficient of molecular diffusion for a species in free water as follows:

$$D^* = D_o \tau \quad (8)$$

where τ is a tortuosity factor. The coefficient of diffusion for most salts in free water is in the range of 1×10^{-10} to 2×10^{-10} m^2/s. A typical value cited in the literature is around 0.015 m^2/y (Goodall and Quiqley 1977; van der Kamp 1996).

Mechanical dispersion is mixing caused by local variations in velocity around some mean velocity of flow. Fluid flow and velocity are the main controls on the longitudinal dispersion in a column. Different properties that affect mechanical dispersion are pore size, path length, autocorrelation (all pores do not connect and a branch off of a normal flow path can take the contaminant away from the rest of the plume if the path does not reconnect), and pore friction (fluid moves faster in centre of pore than along the edges). The coefficient of mechanical dispersion has been related to travel distance, with the value of dispersivity ranging from 1/50 to 1/100 of the travel distance (Gelhar et al. 1992). Freeze and Cherry (1979) have noted that dispersion of reactive solutes generally is greater than the dispersion of nonreactive solutes.

A column Peclet number is a dimensionless parameter that is a measure of the relative amount of advective flow compared to diffusion controlled flow. The column Peclet number is defined as:

$$P_e = \frac{vd}{D_f} \tag{9}$$

where: d is the diameter of the particles in the column (m), D_f is the diffusion coefficient in pure water (m^2/s) and v is the Darcy velocity (m/s). At high Peclet numbers, advection dominates the transport process whereas diffusion dominates the transport process at low Peclet numbers (Appelo and Postma 1999). The Peclet number is dependent upon the scale of the system.

The attenuation factor, R_d, accounts for linear, reversible and instantaneous equilibrium adsorption of reactive solutes. For reactive (adsorbing) solutes, $R_d>1$, and for nonreactive

(nonadsorbing) solutes, R_d=1 on the basis that all of the pore space conducts flow. The process of attenuation acts simply to slow the velocity of the contaminant by a constant factor.

The effective porosity is the portion of the soil through which chemicals move (Stephens et al. 1998). Effective porosity is less than the total porosity, because even if the soil is fully saturated, not all of the water-filled pores are interconnected or contribute to flow (Stephens et al. 1998). The pores that do not contribute to flow are known as immobile or dead-end pores. The total porosity is defined as:

$$n = \frac{V_V}{V_T} \tag{10}$$

where: V_v is the volumn of the voids and V_T is the total volume of soil.

The effective porosity can be found using Equation (11) and a nonreactive tracer such as chloride. When the concentration is normalized, C/C_0=0.5 should occur when one pore volume of solution has flowed from the column. Using the measured elapsed time, $t_{0.5}$ at C/C_0=0.5, the column length, L, and Darcy velocity, v, the effective porosity can be calculated as (Stephens et al. 1998):

$$n_e = \frac{L}{t_{0.5}v} \tag{11}$$

Analytical solutions to the advection dispersion equation (6) have been derived for several different initial and boundary conditions. Based on the work of Ogata and Banks (1961) and modified to include attenuation factor the solution for a saturated homogeneous soil is:

$$\frac{C}{C_o} = 0.5\left\{erfc\left[\frac{R_d - \bar{v}t}{2\sqrt{DR_d t}}\right] + \exp\left(\frac{\bar{v}x}{D}\right) erfc\left[\frac{R_d - \bar{v}t}{2\sqrt{DR_d t}}\right]\right\} \quad (12)$$

for the following boundary conditions:

$C_{(x,t=0)}=0$; $C_{(x=0,t)}= C_0$;

where $C_{(x,t)}/ C_0$ = concentration of the chemical species at point x and time t relative to the source concentration; and erfc(z)= complementary error function. This is measured by instantaneous concentrations as a function of time at the end of the column.

This analytical solution can be used to estimate the solute transport parameters (longitudinal dispersivity and attenuation factor). Measurement of D and R_d is achieved by fitting theoretical curves of $C_{(x,t)}$, based on analytical solutions to (12) to measured curves of $C_{(x,t)}$ determined from laboratory column tests.

Although the ADE has been used extensively in literature, there is evidence that demonstrates consistent errors in the application of the equation. Kennedy and Lennox (2001) show that the ADE fails to describe tails in solute concentration breakthrough curves. Actual breakthrough

curves tend to have sharper leading tails followed by longer, smoother trailing tails. This theory is also supported by Levy and Berkowitz (2003) where they found that actual breakthrough curves have early breakthrough and late time tails compared to the ADE.

Cation exchange capacity (CEC) is a measure of the quantity of sites on soil surfaces that can retain positively charged ions by electrostatic forces. Cation exchange sites are found primarily on clay and organic surfaces. The cation exchange capacity (CEC) is an essential soil characteristic because it gives a measure of the soil's ability to adsorb cations. Dohrmann (2006) defines CEC as "a measure of the ability of clay or a soil to adsorb cations in such a form that they can be readily desorbed by competing ions".

The surfaces of clay mineral carry negative charges. These negative charges result in cations present in the soil pore water being attracted to the clay particles. The cations are not permanently held and if the pore water chemistry change they can be replaced by other cations. The cations are attracted to a clay mineral particle because of the negative surface charges but at the same time tend to move away from each other because of their thermal energy. The net effect is that the cations form a dispersed layer adjacent to the particle, the cation concentration decreasing with increasing distance from the surface until the concentration because equal to that in the pore water. The term diffuse double layer describes the negatively charged particle surface and the dispersed layer of cations.

The thickness of the diffuse double is layer is affected by valency, hydrated radius, and concentration of cations in solution (Teppen and Miller 2006; Chang and Donahue 2007). An

increase in valency results in a decrease in diffuse double layer thickness. Cations with a relatively small hydrated radius (K^+, NH_4^+) form a thin double layer, soil particles get close enough for short range attractive forces to cause flocculation. Cations with a relatively large hydrated radius (Ca^{2+}, Mg^{2+}) form thick double layer, soil particles cannot approach each other causing dispersion. Increasing the solution concentration can cause the thickness of the diffuse double layer to contract, whereas a dilute solution can cause the thickness of the diffuse double layer to expand.

The structure of soil can change due to a change in the diffuse double layer of clay minerals. When the concentration of the surrounding solution increases, the thickness of the diffuse double layer contracts and flocculation (edge to edge orientation of the clay particles) occurs. The smaller diffuse double layer results in a larger effective pore space which leads to an increased hydraulic conductivity. When an external, confining force is acting on a soil, a smaller diffuse double layer leads to a decrease in interparticle forces. The clay particles approach each other and the soil structure becomes more dense (Schmitz 2006). A smaller cross section is available to flow, and the hydraulic conductivity decreases.

A change in solution concentration was the cause of a change in dispersivity as described by (Beekman and Appelo 1990).

> During seawater displacement by fresh water the clay was in a flocculated state (fixed as a loosely built and permeable framework between the larger mineral grains due to the high salt content). An early breakthrough of fresh water, with fingering is caused by the contrast in solution density. The decrease in salinity caused an interlayer swelling of the clay, permeability decreases, mixing increases. During the exchange of Na for other cations (with a lower extent of hydration) the interlayer water is released and the permeability is restored.

Under saturated conditions, clay swelling and dispersion are the two processes that have been hypothesised to cause a reduction in hydraulic conductivity (Keren and Ben-hur 2003). Soil swelling caused by increased salinity can reduce hydraulic conductivity (Fetter 1999). As the diffuse double layer grows thicker, the hydraulic conductivity decreases, because clay minerals tend to expand and swell into the pore space. The diffuse double layer is thicker when it contains the monvalent ions and as such monovalent ions tend to weaken the bonds between clay particles. The effect of swelling is reversible if the saline water is flushed from the pores. However, if smaller particles break loose from the soil structure, they can be transported by water until they are carried into small pore throats, where they can be lodged. This causes a more or less irreversible reduction in hydraulic conductivity.

There are numerous methods for determining CEC and many papers have been devoted to the study of this process. The two most common methods are the ammonium acetate method (Lewis 1949) and the barium chloride method (Henderson and Duquette 1986). These methods may not be accurate when mineralogic components in soil such as carbonates are present because these minerals can become partially dissolved during exchange experiments (Dohrmann 2006; Wang et al. 2005).

Several authors have proposed methods to overcome the problem of mineral dissolution. Wang et al. (2005) discusses these different methods which include: suppressing the solubility of $CaCO_3$ by using water alcohol mixtures, removing the $CaCO_3$ by repeated washings, dissolving and re-precipitating the $CaCO_3$ as a less soluble phase, and using double extractions. Wang et al. (2005) describes these procedures as having a tendency to be inconsistent, excessively time

consuming, or having too many routine analytical steps, which make the procedures impractical and vulnerable to the introduction of errors.

Beekman and Appelo (1990) use a $BaCl_2$ extraction to determine composition of Na^+, K^+, Ca^{2+}, and Mg^{2+} on the exchange sites and then a subsequent $MgSO_4$ extraction to determine the CEC. In order to correct for dissolved salts, alkalinity measurement was subtracted from the Ca^{2+} measured and total CEC measured.

Ludwig and Kolbl (2002) tested two different methods of obtaining the exchange complex composition using the geochemical model PHREEQC. The exchange coefficients used in PHREEQC to model one-dimensional transport, inorganic complexation, and multiple cation exchange in a soil column were calculated using exchangeable cations obtained by a percolations with NH_4Cl and $BaCl_2$ and obtained by shaking with $BaCl_2$. They found that the amounts of exchangeable cations were best found by experiments with homogenized soil with percolation of $BaCl_2$ as PHREEQC was best able to predict concentrations of cations in solution phase.

The saturated hydraulic conductivity for glacial till typically ranges from $1x10^{-6}$ to $1x10^{-12}$ m/s and for silty sand the hydraulic conductivity typically ranges from $1x10^{-3}$ to $1x10^{-7}$ m/s (Freeze and Cherry 1979). The hydraulic conductivity of soil is directly affected by soil structure.

As calcium and magnesium are released from the soil, they appear before the leachate front. Thorton et al. (2000) saw 59% of the calcium desorbed from the soil was precipitated as $CaCO_3$. Bicarbonate was attenuated and mass balance calculations showed that 78 meq of Ca^{2+} and

alkalinity were removed during leachate breakthrough. At the leachate front and in another column they observed dissolution of native $CaCO_3$ by the leachate where more Ca^{2+} was eluted from the column than the amount of cations absorbed and total CEC.

The soil structure can also affect the breakthrough of normally unreactive species. The existence of dead-end or unconnected pore space can lead to an effective porosity in which all of the pore space does not contribute to fluid flow (Shackleford and Redmond 1995). One method commonly used to determine this effect is to measure the number of pore volumes of flow required for advective breakthrough. They found that the measured attenuation effect for Cl^- and the low flow rates (diffusion-dominated transport) preclude using chloride breakthrough curve for determining an effective porosity.

CHAPTER 3
MATERIALS AND METHODS

3.1 Soil Material

Soil samples were collected from two separate locations; Site 1 located near Saskatoon, Saskatchewan and Site 2 located near Kelvington, Saskatchewan. Each of these sites housed a hog production facility and earthen manure storages.

Soil from Site 1 was collected during the excavation of test holes ranging in depth from two to nine meters. The soil from Site 2 was collected during construction of the EMS. Soil characteristics of these soils were obtained during a separate study (Fonstad 2004). The soil samples were air-dried, tumbled and passed through a two millimeter sieve to ensure homogeneity before being packed into the columns.

The particle size analysis and x-ray diffraction analysis from Fonstad (2004) are shown in Table 3.1.

The soil from Site 1 is a silty-sand material with 9% clay that is composed of 70% smectite in the clay fraction. The CEC of Site 1, as determined by the conventional ammonium acetate displacement of $BaCl_2$ on both the saturation extract and squeezed extract methods, ranged from 8.3 meq/100g to 12.5 meq/100g. The high CEC of this primarily sandy soil is resultant of the large quantity of smectite in the clay fraction. Smectite has both external and internal surface area available for cation adsorption.

The soil from Site 2 is sandy-clay till material. It is composed of 20-30% smectite , 10-20% kaolinite and 40-50% quartz and feldspars in the clay fraction of the soil. The cation exchange capacity of Site 2, as determined by the conventional ammonium acetate displacement of $BaCl_2$ on both the saturation extract and squeezed extract samples, ranged from 8.8 meq/100g to 11.8 meq/100g.

Table 3.1. Soil characteristics of soils used in column experiments (Fonstad 2004).

	Site 1	Site 2
Particle Size Analysis		
% > 75 μm (% sand and gravel)	82	40
% < 75 μm (% fines)	18	60
% < 2 μm (% clay)	9	30
X-ray diffraction analysis[1]		
% smectite	70	20 - 30
% mica	10	5 - 10
% vermiculite	5 - 10	0 - 10
% chlorite	< 5	0 - 5
% kaolinite	< 5	10 - 20
% quartz and feldspars	< 5	40 - 50

[1]X-ray diffraction analysis completed on clay fraction of the soil sample.

3.2 Column Set-up

The column set up consisted of modified Tempe cells (Figure 3.1). Although Tempe cells are traditionally used to determine soil water characteristic curves, they were slightly modified to be used for column leaching experiments. A single Tempe cell set-up consisted of a Plexiglass cylinder with two removable Plexiglass end-plate assemblies mounted on both ends. The top and bottom end-plate assemblies were held together with five rods. Each end-plate assembly consists of a round doughnut shaped part that contains an o-ring and slides over the end of the column. The bottom plate contains a

high entry air disc with a pressure rating of one bar and an effective pore size of one micron. The high entry air disc was assumed to be inert. The cylinder had a 70 mm inside diameter and a 150 mm length.

Eight soil columns (four for each soil type) were initially prepared. The inner walls of the cylinder were covered with Dow Corning High-Vacuum Grease, a silicon based material that has an excellent resistance to water. The grease ensured that preferential flow did not occur along the sides of the cylinder. Standard Proctor moisture content and dry density for Site 1 soils was 14.7% and 1840 kg/m^3 as determined by the average of four Standard Proctor tests performed by P. Machibroda Engineering Ltd. in Saskatoon, Saskatchewan. Standard Proctor moisture content and dry density for Site 2 soils was 18% and 1710 kg/m^3 from Fonstad (2004). The soil was moistened to the above Standard Proctor moisture contents and was compacted into the modified Tempe cell to an approximate height of 80 mm. A screen was placed on the surface of the soil and a spring loaded disc was placed on top of the screen to ensure that the change in pore water concentration did not cause preferential flow paths. Consolidation will occur in one direction (vertically), not horizontally away from the sidewalls of the Tempe cell.

Figure 3.1. Prepared soil in a modified Tempe cell.

3.3 Soil Column Leaching

Column experiments were carried out in two stages. The first stage was to simulate the chemical changes in groundwater during creation of a contaminant plume. The second stage simulated the reintroduction of groundwater into the contaminant plume with the source of the plume removed. This was done in an attempt to replicate the decommissioning of the site.

Air pressure was applied to the top of a reservoir connected to four soil columns through plastic tubing and a copper manifold. The reservoir contained the column leachate (Figure 3.2). The leachate was forced through the soil column by the air pressure applied

to the solution in the reservoir. The reservoir solution was sampled occasionally to monitor any changes in reservoir chemistry. The pressure was set at 138 kPa (14 metres water head) for the Site 1 columns and 207 kPa (21 metres water head) for the Site 2 columns. The fluid exited the reservoir through plastic tubing, into a manifold, and then plastic tubing lead separately to each soil column (Figure 3.3). The soil column experiments took place at room temperature, approximately 23 ºC. Column effluent fractions were collected in a glass cylinder (Figure 3.4) connected to the bottom of each soil column by plastic tubing. Collection tubes were capped to attempt to reduce evaporation errors.

Figure 3.2. Reservoir for soil columns.

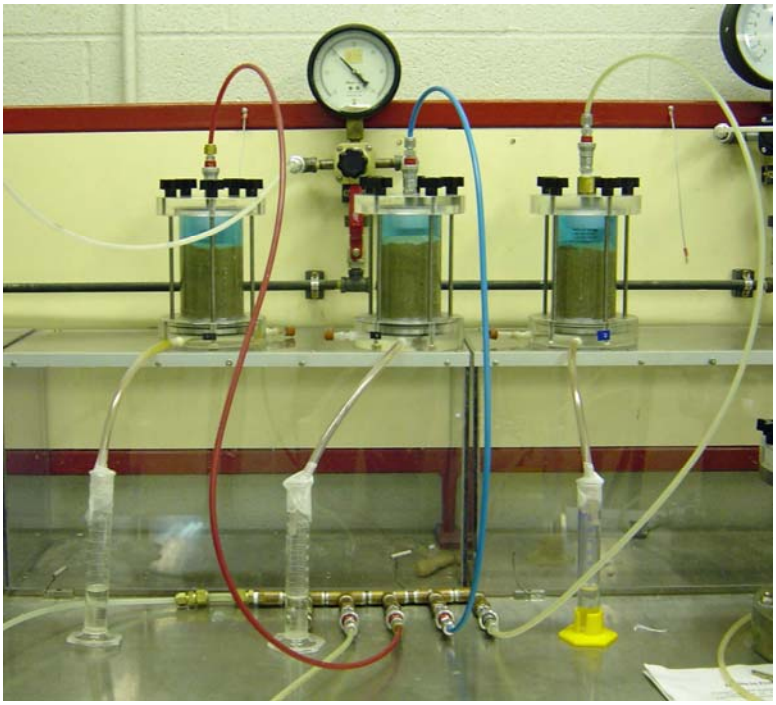

Figure 3.3. Column leaching set-up.

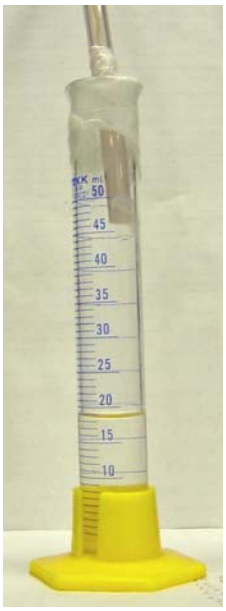

Figure 3.4. Column effluent fraction collector.

3.4 Column Conditioning

Initially, all the soil columns were conditioned with uncontaminated groundwater. The groundwater used to condition the Site 1 soil columns was collected from a background peizometer located up gradient to the existing EMS. The water was stored at 4 ºC until used in the experiment.

The groundwater used in the Site 2 soil columns was simulated by duplcating the chemistry of an uncontaminated piezometer at Site 2. A solution containing ions at concentrations corresponding to mean concentrations of groundwater was made by dissolving $NaCO_3$, $CaSO_4$, KCl, and $NaSO_4$ in deionized water to obtain the concentrations displayed in Table 3.1.

To condition the columns, the groundwater solution was passed through the column until the chemistry of column influent was equal to the chemistry of the column effluent. This was monitored by measuring the electrical conductivity of the column effluent until it had stabilized and then analyzing the ions in an effluent sample. Following this step, one column with Site 1 soil and one column with Site 2 soil were disassembled and the soil was used for soil exchange site analysis.

3.5 Leachate Flushing Stage

Once the columns were equilibrated with ground water, simulated EMS contaminate solution was applied to the remaining six columns for 131 days for Site 1 columns and 114 days for Site 2 columns (Table 3.2). The source chemistry of an EMS was simulated by using the chemistry given by Fonstad (2004), where a number of different EMS at hog

production facilities in Saskatchewan were sampled to obtain the chemistry of an EMS effluent. A solution containing ions at concentration corresponding to mean concentrations of EMS effluent were obtained by dissolving Na_2CO_3, $CaSO_4$, $MgSO_4$, KCl, NH_4HCO_3, and $NaSO_4$ in deionized water to obtain final concentrations shown in Table 3.3. The simulated contaminant solution was placed directly on top of the soil.

Table 3.2. Leachate flushing stage timeline.

Column	Start date	End date	Duration (days)
1, 2 & 3	May 3, 2005	September 12, 2005	131
4, 5 & 6	August 2, 2005	November 24, 2005	114

Table 3.3 Simulated contaminant composition.

Ion	Concentration ($mg\ L^{-1}$)
Cl^-	1640
HCO_3^-	12658
SO_4^{2-}	461
Ca^{2+}	36
Mg^{2+}	17
Na^+	1415
K^+	1736
NH_4^+	3466

After a sufficient number of pore volumes passed through the soil (column influent was equal to column effluent), the simulated contaminant solution was replaced in the reservoir, feed tubes and on top of the soil columns with the original groundwater

solution initially used to condition the columns. At this time, one more column of each soil type was dissembled for soil exchange site analysis.

3.6 Freshwater Flushing Stage

The freshwater was then leached through the soil columns to simulate decommissioning of the EMS. The column effluent was collected periodically and analyzed. The column leaching was stopped once the chemistry of the influent was equal to the chemistry of the effluent. The time it took for this to happen is listed in Table 3.4. The remaining soil columns were disassembled and analyzed to determine the chemistry of the soil exchange sites.

Table 3.4. Freshwater flushing stage timeline.

Column	Start date	End date	Duration (days)
2 & 3	September 15, 2005	May 15, 2006	242
4	November 28, 2005	May 15, 2006	167
6	November 28, 2005	April 4, 2006	126

3.7 Effluent Analysis

The pH, electrical conductivity, alkalinity, and NH_4^+ analysis were conducted immediately after the sample was collected.

Sodium and K^+ were analyzed using the flame photometric method (American Public Health Association, 1998). Chloride was analyzed using an argentometric method (American Public Health Association, 1998). Ammonium was analyzed using the tritrimetric method after the samples were carried through preliminary distillation (American Public Health Assocation, 1998). Calcium and Mg^{2+} were determined using EDTA Titrimetric Method (American Public Health Association, 1998). Alkalinity was determined using the titration method (American Public Health Association, 1998). Sulphate was determined using a Technicon auto analyzer.

Effluent concentrations were plotted as normalized concentration (13), corrected for the concentration of pore water initially in the soil at the start of each stage.

$$C / C_0 = \frac{C_e - C_i}{C_0 - C_i} \qquad (13)$$

Where C_e = concentration of column effluent, C_i = concentration of pore water initially in the soil column and C_0 = concentration of solution in the reservoir.

3.8 Soil Analysis

A total of six soil columns were disassembled at different stages during the column study. The soil was placed into plastic bags and stored at 4°C until further analysis. Table 3.5 lists the column names, soil type and the type of pore water the column was equilibrated with at the time of disassembly.

Table 3.5. Soil columns.

Column	Site	Soil Type	Equilibrated Pore Water
1C	1	Clayey silty-sand	Freshwater
1	1	Clayey silty-sand	Simulated contaminant
3	1	Clayey silty-sand	Freshwater
KC	2	Sandy clay	Freshwater
5	2	Sandy clay	Simulated contaminant
6	2	Sandy clay	Freshwater

Two different methods were used to separate the soil from the pore water before determining the CEC and are discussed in the following section.

3.8.1 Soil Soluble Chemistry Extraction

The first is an attempt to remove soluble salts by washing them the soil. The second method to extract soluble salts utilized a physical compression method. Each method is followed by a double adsorbed cation extraction. These methods were chosen by using the resources available at the study facility.

The first method to attempt to remove the soil pore water from the soil was a modification of the saturated paste salinity test for soils (Carter 1993). By saturating the soil with deionized water, it was predicted that the soluble salts would be sufficiently removed without affecting the partitioning of cations on the soil exchange sites. Instead of repeatedly washing the soil, using a one-time saturation would suppress the effects of changing the partitioning of cations on the soil exchange sites.

Approximately 200 g of soil was weighed and placed into a container. The total weight of the soil sample and container was recorded. The soil sample was brought to saturation using deionized water. Once saturated, the sample was allowed to stand for a minimum of four hours to ensure that the saturation criterion was still met. If the soil had stiffened, additional deionzed water was added and paste was mixed thoroughly. The container was weighed with the contents. The increase in weight (amount of water added) was recorded.

After the paste was allowed to stand for an additional four hours, it was transferred to a Buchner funnel fitted with highly retentive filter paper. A vacuum was applied and the extract were collected until air passed through the filter. Turbid filtrates were refiltered. The extracts were stored at 4°C until analyzed. The soil was retained for further testing.

3.8.2 Squeezed Extraction

The second method to attempt to remove the soil pore water from the soil was to mechanically squeeze the pore water from the soil before testing. Mechanical squeezing has been effectively used in the past to determine the composition of soil pore water. Bottcher et al. 1996 achieved water recovery between 30% and 50% of the total water content using a high-pressure squeezing device. It is important to note that they found an increase in dissolved ion concentrations at increasing pressures indicating that micro pore solutes have the highest concentrations of solutes.

Soil samples collected after column disassembly were sealed in plastic bags and held at 4°C to prevent moisture loss until testing.

A stainless steel squeezer was manufactured in the engineering shops. It consisted of three parts: the outer cylinder, bottom plate and piston. Soil directly from the soil columns was placed into a squeezing apparatus. Filter paper and a metal screen was placed on the bottom of the apparatus between the soil sample and the outlet.

An unmeasured force was applied to the piston by a commercially available hydraulic press. The pore water leaves the squeezer through the bottom plate through nylon tubing. A 50 cc syringe was contacted to the nylon tubing. Testing continued until no more pore water could be extracted (approximately 24 hours). The sample was stored at 4 ºC until analyzed.

3.8.3 CEC Determination

The partitioning of cations on the exchange sites and the total CEC was determined using two different methods using the soil samples from each method described above.

Step 1: Barium chloride

For each sample, approximately three grams of dried soil was weighed and placed in a 50 mL centrifuge tube. 30 mL of 0.1M barium chloride ($BaCl_2$) was added to each tube. The tubes were then shaken slowly on an end-over-end shaker at 15 rpm for two hours. The sample was then filtered with a No. 41 Whatman filter paper. The supernatant was then analyzed with an atomic adsorption spectrophotometer (AAS).

Step 2: Ammonium Acetate

The soil samples were leached with approximately 100 mL of deionized water, added in portions, to remove the excess barium. The soil sample was than leached with 190 mL of

ammonium acetate. The volume of the leachate was made up to 200 mL and the Ba concentration was determined using the AAS.

3.8 Data Analysis

The solute transport relationships of all columns were evaluated using an analytical solution of the advection-dispersion equation (Equation 7). This model was used to estimate the hydraulic parameters (velocity, dispersivity and kinematic porosity) of each column.

A mass balance was completed for each solute at the end of both the simulated contaminant flushing stage and the freshwater flushing stage. The measured concentrations of each solute was used to estimate the mass of solute eluted in the column effluent.

PHREEQC (Parkhurst and Appelo 1999) was used to characterize the leachate contaminant chemistry and the column effluent chemistry. PHREEQC is a computer program available from the United States Geological Survey and has the capability to provide speciation and saturation indices for chemical solutions based on data from various thermodynamic databases.

CHAPTER 4
RESULTS AND DISCUSSION

4.1 Solid Phase Composition

The soil samples were collected from the study sites and various properties were determined during a previous study (Fonstad, 2004).

4.2 Soil Cation Exchange Capacity

The moisture contents of the soil samples before and after squeezing the pore water from the sample are shown in Figure 4.1. The quantity of water extracted from the soils ranged from an average of 21.1% of the total water content for the soil from Site 1 and 17.7% of the total water content for the soil from Site 2. The remaining water was considered bound water.

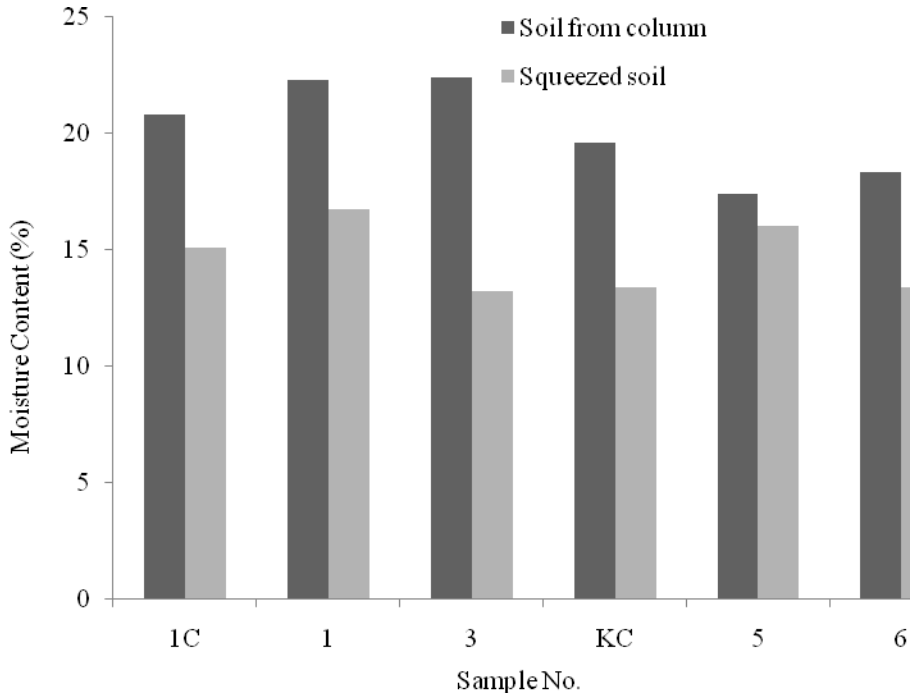

Figure 4.1. Moisture content of the soil samples before and after squeezing.

Tables 4.1 to 4.4 show the composition of cations on the soil exchange site as determined from the saturated paste extract method and the squeezed extract method.

Table 4.1. Saturation extract leached with $BaCl_2$

Sample	Ca^{2+} (meq/100g)	Mg^{2+} (meq/100g)	Na^{+} (meq/100g)	K^{+} (meq/100g)	NH_4^{+} (meq/100g)	CEC (meq/100g)
SC	6.6	5.4	0.3	0.5	0.0	**12.8**
S1	5.8	2.0	1.3	2.6	3.2	**14.9**
S3	6.4	3.6	0.3	0.9	0.7	**11.9**
KC	6.1	5.8	0.6	0.4	0.0	**12.9**
K5	4.6	0.7	1.2	2.5	4.9	**14.0**
K6	6.3	6.3	0.6	0.5	0.0	**13.7**

Table 4.2. Saturation extract leached with ammonium acetate displacement of $BaCl_2$.

Sample	CEC (meq/100g)
SC	**9.2**
S1	**12.5**
S3	**9.1**
KC	**9.6**
K5	**11.4**
K6	**11.8**

Table 4.3. Squeezed extract leached with $BaCl_2$.

Sample	Ca^{2+} (meq/100g)	Mg^{2+} (meq/100g)	Na^{+} (meq/100g)	K^{+} (meq/100g)	NH_4^{+} (meq/100g)	CEC (meq/100g)
SC	3.9	2.4	0.4	2.8	0.3	**9.8**
S1	1.5	0.6	0.1	2.7	1.2	**6.0**
S3	3.1	1.4	0.4	3.6	0.9	**9.4**
KC	3.1	1.8	0.6	2.9	0.0	**8.5**
K5	3.6	0.4	0.7	3.5	1.2	**9.5**
K6	2.0	1.6	0.6	2.7	0.1	**7.0**

Table 4.4. Squeezed extract leached with ammonium acetate displacement of $BaCl_2$.

Sample	CEC (meq/100g)
SC	**10.9**
S1	**10.4**
S3	**8.3**
KC	**9.9**
K5	**8.8**
K6	**11.7**

The saturated paste method resulted in overall higher cation exchange capacities compared to the squeezed samples. This is likely due to the dissolution of precipitates in the soil but cannot be checked since anions were not measured. In Figures 4.2 and 4.3, Ca^{2+} and Mg^{2+} concentrations are significantly higher in all samples, including the samples equilibrated with the simulated contaminant.

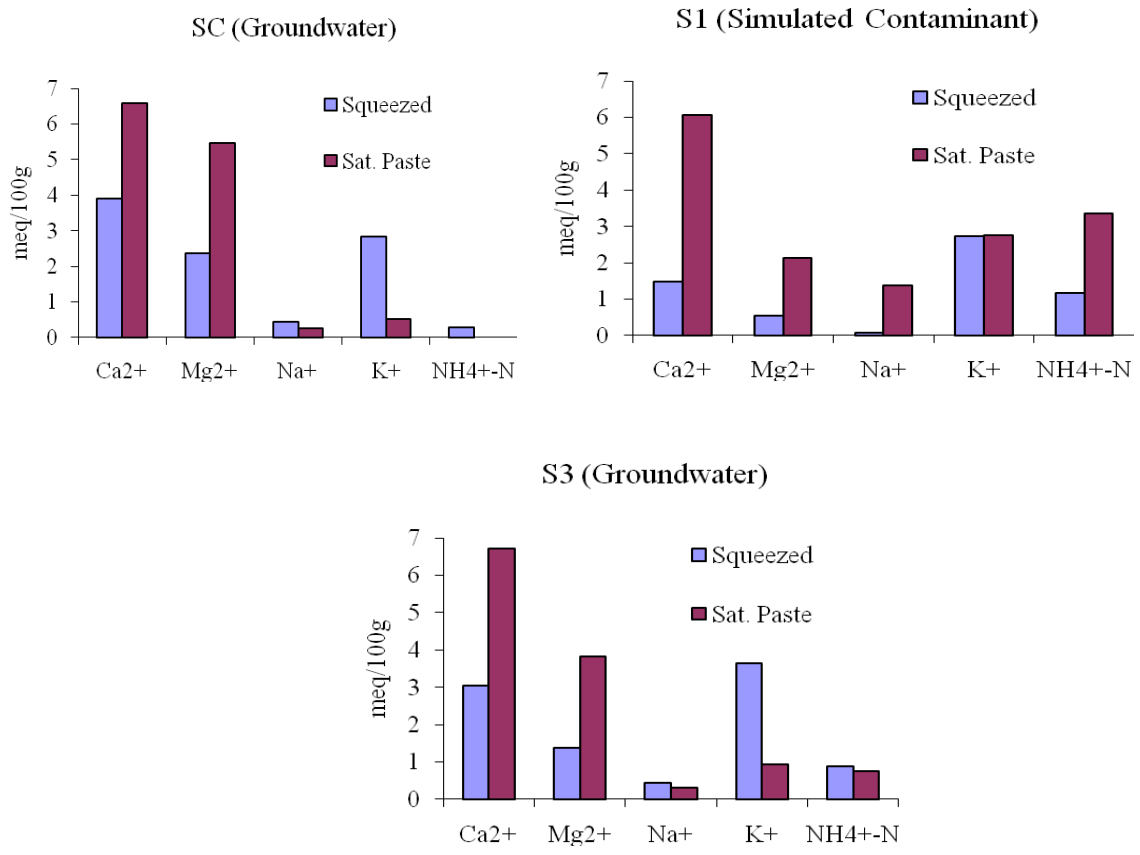

Figure 4.2. Partitioning of exchangeable cations on the soil exchange sites determined by ammonium acetate leaching for Site 1 columns.

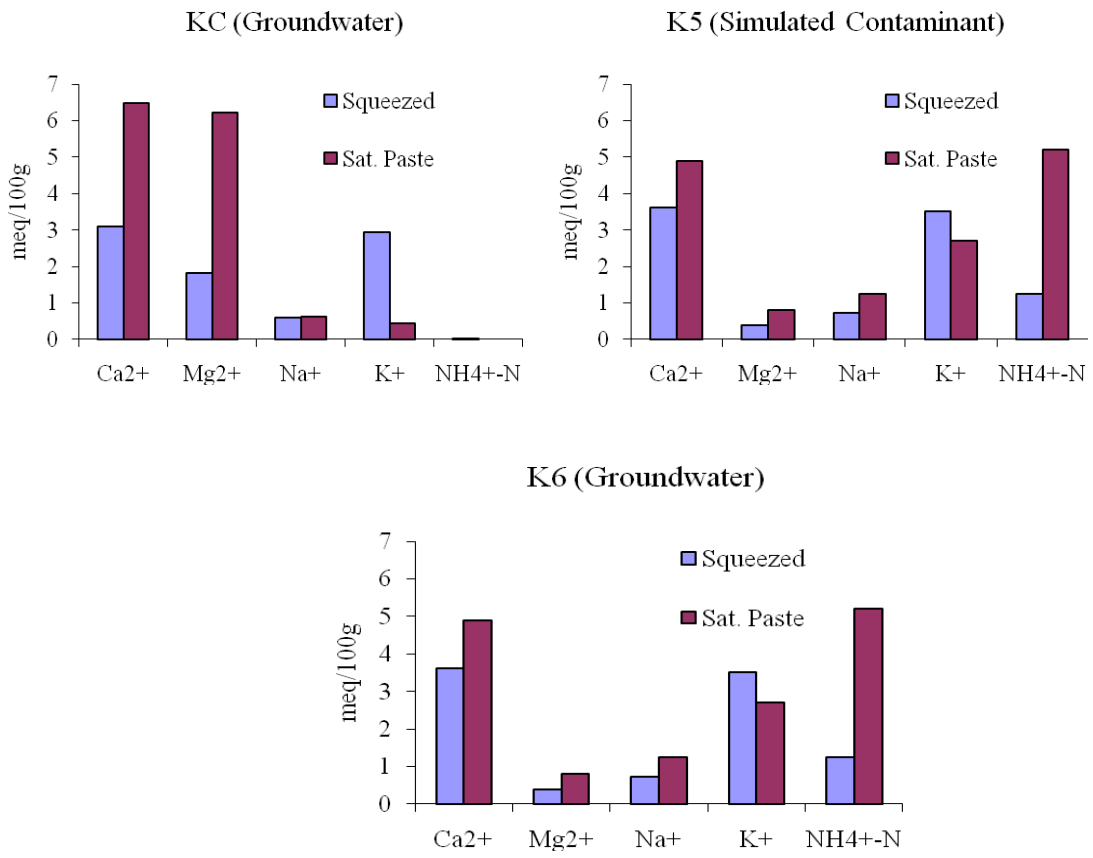

Figure 4.3. Partitioning of exchangeable cations on the soil exchange sites determined by ammonium acetate extraction for Site 2 columns.

The quantity of soil exchange sites occupied by K^+ was consistently higher for the squeezed samples. For the squeezed samples, the amount of K^+ on the soil exchange sites after the simulated contaminant flushing stage (S1) is lower than the amount originally on the soil (SC) which is not expected because K^+ was attenuated by the soil. This could be explained by the inability of $BaCl_2$ to effectively replace K on the soil exchange sites for this particular clay structure. Barium chloride may be ineffective because Ba^{2+} has a larger hydrated radius and K^+ could be trapped in the interlayers of the smectite clay. The CEC of the soil from S1 was only 6.0 meq/100g compared to SC and S3 which had a CEC of 9.8 meq/100g and 9.4 meq/100 g,

respectively, which indicates that the method may not have been successful at liberating all cations from the soil exchange sites.

Both methods are known to possibly change the composition of cations on the exchange site. The saturated paste method introduces a dilute solution which can cause a change of partitioning of cations on the soil exchange sites. Squeezing the pore water out of the soil sample, can result in a pressure filtrate that has a higher ion concentration than the original pore water (Appelo and Postma 1999). This is caused by anion exclusion which initially dilutes the filtrate followed by higher concentrations when the diffuse double layer expands and allows the anions to pass through. It was not possible to measure the effect of either of these composition changes, but it is important to consider them as possible reasons why the two methods resulted in different exchange compositions.

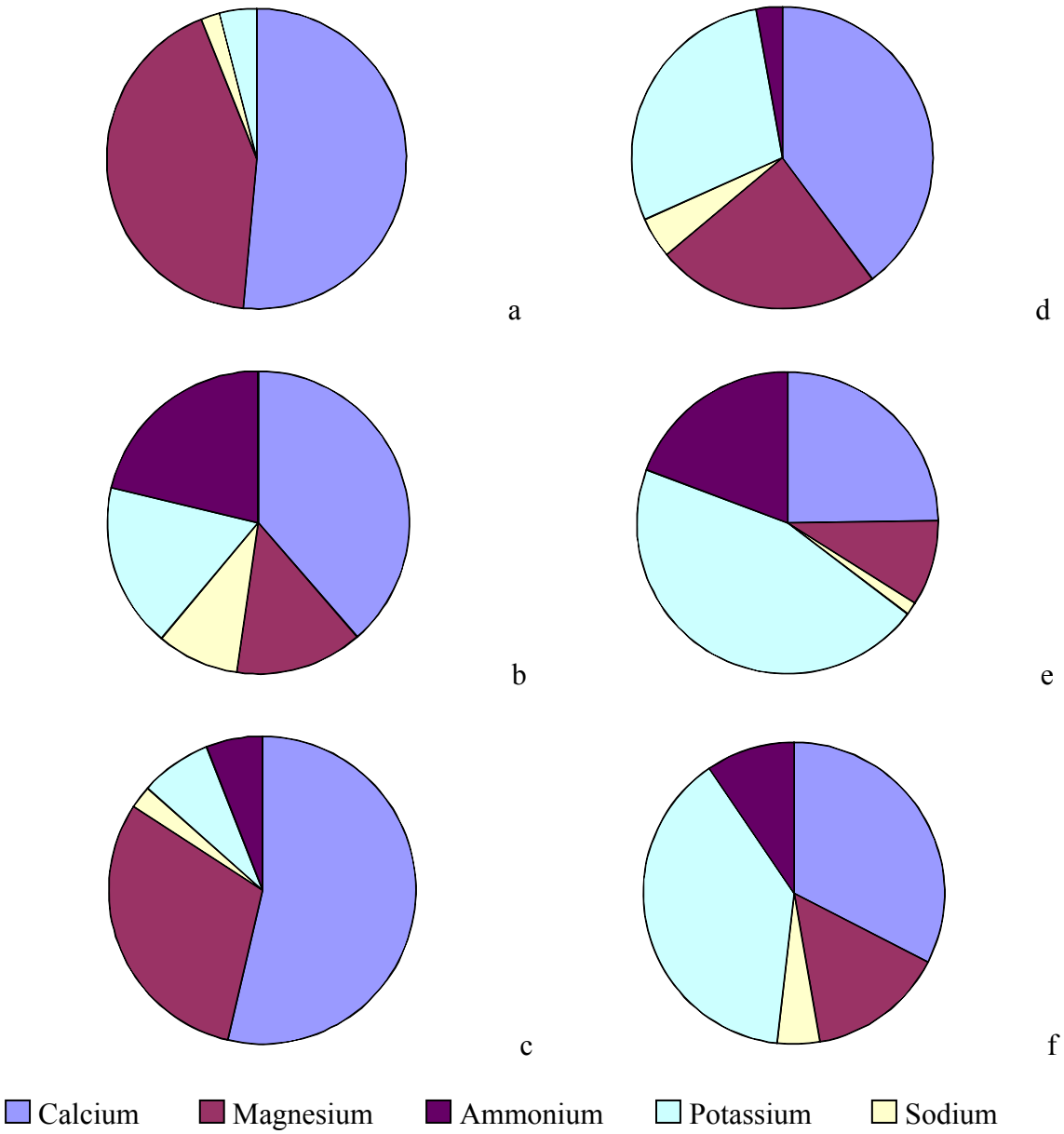

Figure 4.4. Distribution of Site 1 exchangeable cations as using saturated paste pore water extraction a) before simulated contaminant leaching b)after simulated contaminant leaching c) after freshwater leaching and using squeezed pore water extraction d) before simulated contaminant leaching e) after simulated contaminant leaching f) after freshwater leaching.

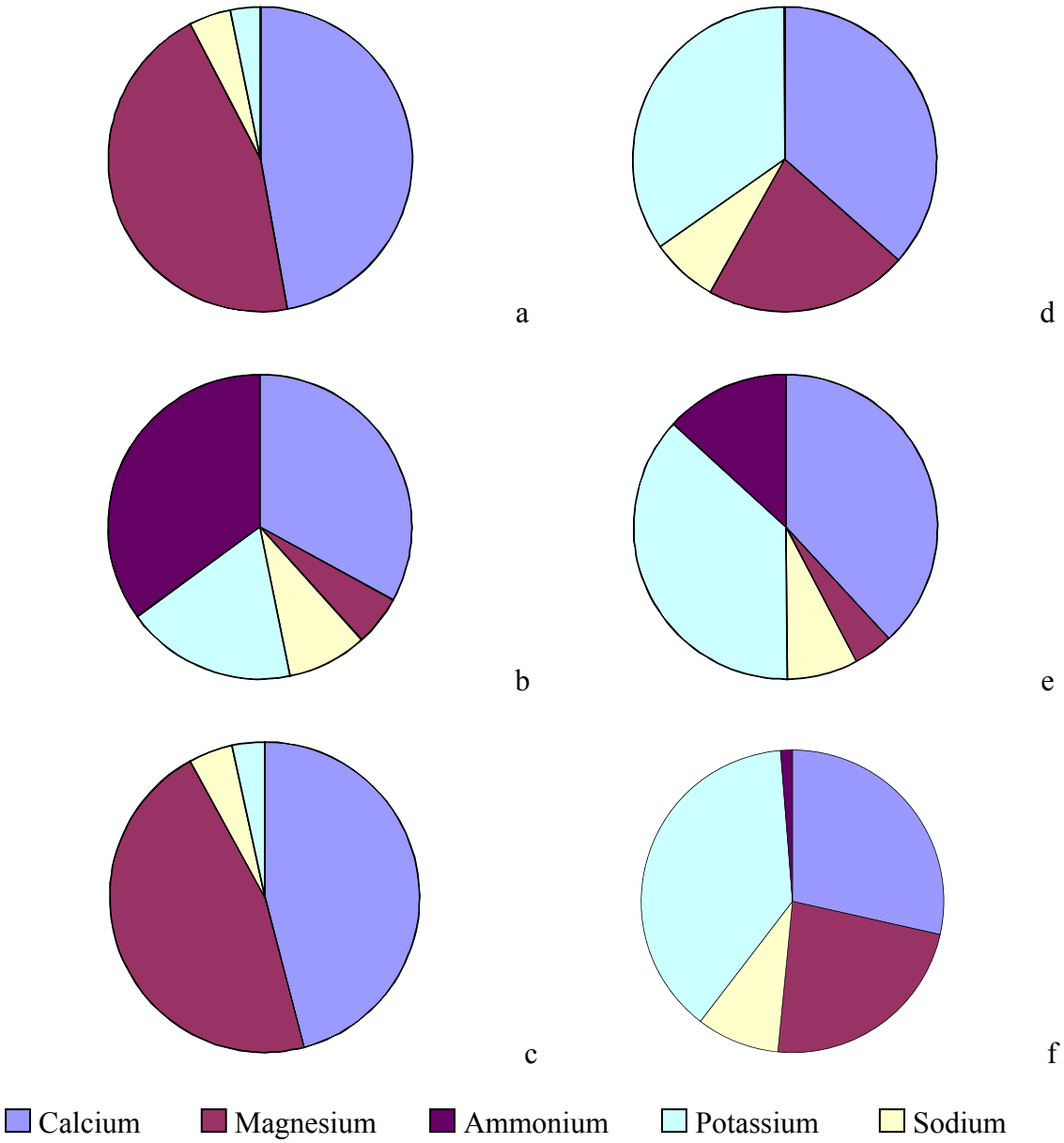

Figure 4.5. Distribution of Site 2 exchangeable cations as using saturated paste pore water extraction a) before simulated contaminant leaching b) after simulated contaminant leaching c) after freshwater leaching and using squeezed pore water extraction d) before simulated contaminant leaching e) after simulated contaminant leaching f) after freshwater leaching.

Figures 4.4 and 4.5 show the proportion of each cation on the soil a and d) before the simulated contaminant leaching, b and e) after the simulated contaminant leaching and c and f) after freshwater leaching using both the saturated paste pore water extraction and squeezed pore water extraction methods. The proportion of cations after each stage is different between the two methods. The saturated paste pore water extraction consistently results in a higher amount of Ca^{2+} and Mg^{2+} and less Na^{+} on the soil exchange sites at all three stages. After the simulated contaminant flushing stage, the saturated paste samples had less K^{+} and more Ca^{2+} on the soil exchange sites than the squeezed samples. Even though each method yields different results, the proportion of cations on the soil exchange sites was very similar at each stage. The two different soils were also very similar if the same method was used. The significance of these similarities is that regardless of the method used to measure the quantity of cations on the soil exchange sites, the partitioning of cations goes back to the original partitioning on the exchange even after flushing with the simulated contaminant and completely changing the partitioning of cations in-between.

The saturated paste samples are a closer representation when compared to the results of the column breakthrough effluent study; therefore, the saturated paste method was used when comparing the CEC analysis to the column breakthrough mass balance calculation.

4.3 Reservoir Chemistry

Samples were taken regularly throughout the column breakthrough study to confirm the chemistry of the influent solution. The sample was taken from the tubing at the point where it

immediately entered the column. Table 4.6 contains the average for each constituent of the column influent solution.

Table 4.6. Average measured chemistry results for column influent solutions.

Ion	Site 1 Groundwater mg L^{-1}	Site 2 Groundwater mg L^{-1}	Simulated Contaminant mg L^{-1}
Anions			
Cl^-	190	190	1640
HCO_3^-	347	44	11817
SO_4^{2-}	58	4200	560
Cations			
Ca^{2+}	128	470	11
Mg^{2+}	56	650	21
Na^+	36	380	913
K^+	65	75	1926
NH_4^+	0	0	2936
Cu	0	0	111

The saturation indices for calcite dolomite and gypsum as calculated by PHREEQC for each average influent solution are listed in Table 4.7. The SI of calcite for the simulated contaminant was 1.17; therefore, calcite precipitation was expected. This is likely a result of the high HCO_3^- concentration required to balance the NH_4^+ in the solution. Calcite and dolomite were undersaturated in Site 2 groundwater.

Table 4.7. Saturation indices for column influent solutions.

	Site 1 Groundwater mg L^{-1}	Site 2 Groundwater mg L^{-1}	Simulated Contaminant mg L^{-1}
Calcite	1.55	-0.72	1.17
Dolomite	2.99	-1.01	3.31
Gypsum	-1.84	0.01	-3.07

The measured pore volume of each soil column was determined by the difference in weight from a sample of saturated soil from the column dried to the determine moisture content and applying the moisture content to the entire mass of soil in the column.

Table 4.8. Pore volume determination.

Column Number	Measured Pore Volume (mL)
Column 1	129
Column 2	120
Column 3	132
Column 4	116
Column 5	118
Column 6	130

During the study, it was noted that the simulated contaminant fluid was a bright blue colour after leaving the manifold. This was likely caused by the corrosion of the copper manifold by the NH_4^+ salts in the simulated contaminant solution. At this point, the copper manifold was removed and replaced with a polyvinylchloride manifold. It was decided to analyze for copper in both the column influent and effluent to account for its effect on the results. The simulated contaminant had 111 mg/L (3.5 meq/L) of copper in solution, which was considered insignificant for ion exchange reactions compared to the high concentration of NH_4^+ (210 meq/L) and K^+ (50 meq/L) in solution.

4.4 Freshwater Equilibration Stage

The Site 1 and Site 2 columns were conditioned with groundwater for three months from February 3, 2005 until May 3, 2005. The electrical conductivity of the effluent was stable for approximately one month before the groundwater was replaced with simulated contaminant solution for the simulated contaminant flushing stage of the column experiments.

4.5 Simulated Contaminant Flushing Stage

The simulated contaminant flushing stage started on May 3, 2005. It continued until September 12, 2005. Time is measured in days from the start of the simulated contaminant flushing stage.

All three columns for Site 1 experienced a decrease in flow rate from approximately 40 ml/day to 25 ml/day over 10 days during the simulated contaminant flushing stage (Figure 4.6). After 50 days, leachate samples were taken less frequently. This caused the sample size to be affected by evaporation despite attempts to prevent evaporation. Flowrates calculated after 50 days are not considered as accurate as the first 50 days due to evaporation and fraction collector overflow.

The flowrate reduction is similar to results of column studies flushed with hog manure by Fonstad (2004) who reported a reduction in flow rate within 30 days. Fonstad 2004 explained the reduction in flowrate as the result of a thin clogged layer at the manure-soil interface. For this study, the simulated contaminant lacks the organic matter and suspended solids present in the liquid manure; therefore, other explanations for the reduction in flow rate were examined.

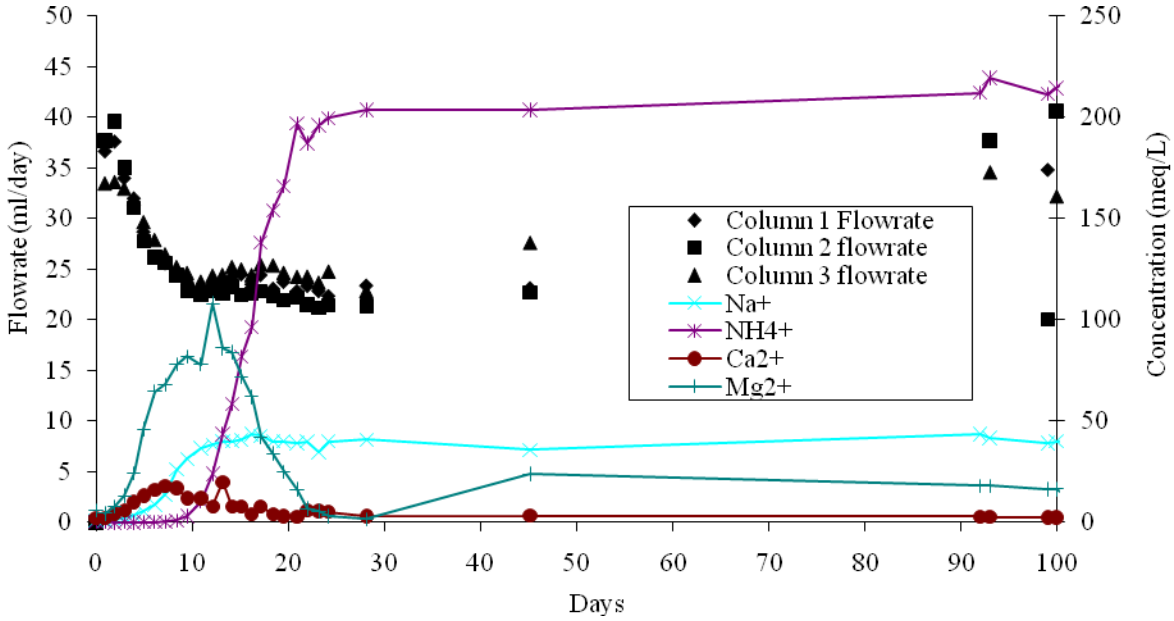

Figure 4.6. Site 1 flowrate during the simulated contaminant flushing stage.

During the simulated contaminant flushing stage for Site 2 (Figure 4.7), the flowrate decreased from approximately 33 ml/day to 12 ml/day within 10 days or approximately 1.5 pore volumes. The flowrate then appeared to remain relatively stable between 10 and 20 ml/day for the remainder of the simulated contaminant flushing stage.

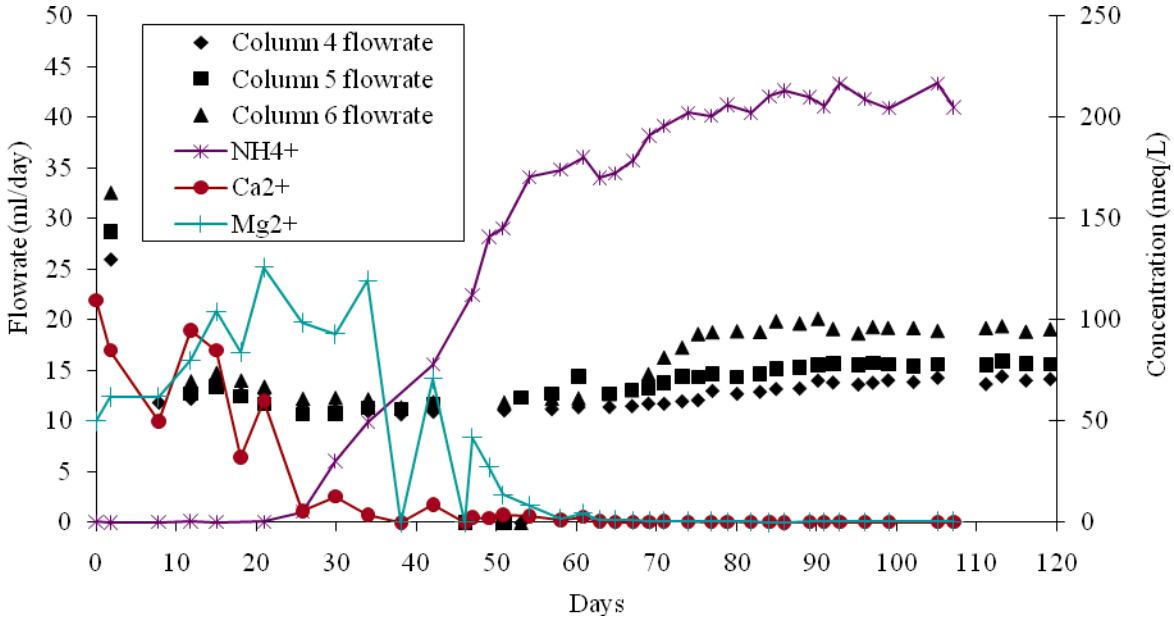

Figure 4.7. Site 2 flowrate during the simulated contaminant flushing stage.

Changes in flowrate of the soil columns is directly related to changes in hydraulic conductivity through Darcy's Law (Equation 3). Four possibilities were examined to explain the change in column flow rate during the simulated contaminant flushing stage and the freshwater flushing stage.

1) Pressure compaction

The Standard Procter test, which has a compactive energy of 594 kN m/m^3, was used to compact the soil into the columns. Since the soil was compacted with a higher energy when the columns were constructed it is assumed that the soil was not further compacted by the pressure at which the leachate was applied.

2) Osmotic flow

Osmotic flow is described in depth by Babour and Fredlund (1989). In short, it is the process where a solvent (water) passes from a solution of lower solute concentration through a semipermeable membrane (clay soil) into a solution of high concentration.

The soil volume changes due to fluid flow that develops within the clay in response to osmotic gradients. As the clay is exposed to a concentrated salt solution, osmotic flow out of the immobile pore spaces occurs. This outward flow causes negative pore fluid pressures which leads to increases in effective stress and causes volume change. A decrease of approximately 0.5-0.7 mm in soil column height was visually observed and measured over the length of testing.

3) Osmotic compressibility (diffuse double layer theory)

As discussed earlier, the ionic strength of the solution influences soil structure by altering the thickness of the diffuse double layer surrounding clay particles. In addition to ionic strength, the type of ion contributing to the ionic strength of the solution is important. This is because the valence and hydrated radius of a cation in solution affects the thickness of the diffuse double layer.

Volume change in the clay that occurs as a result of changes in pore fluid chemistry due to the alteration of the electrostatic interactions between the clay particles. As the diffuse double layer

thickness increases, the repulsive forces between clay interlayers and clay particles increases. Particles with a thick double layer tend to disperse while particles with a thin diffuse double layer tend to flocculate.

During the simulated contaminant flushing stage, the lower ionic strength pore water was replaced by high ionic strength pore water. The increase in pore water concentration causes a decrease in the diffuse double layer thickness. The smaller diffuse double layer causes a decrease in repulsive force between the soil aggregates and causes the soil aggregates to flocculate. The spring confines the soil column and the soil aggregates are forced to approach each other. Also, the introduction of high ionic strength pore water causes water to pass from the lower strength immobile pore space fluid into the mobile pore space (osmotic flow), causing a decrease in the volume of the immobile pore space. Both of these phenomenon cause a smaller area that is available for flow, which results in a decreased hydraulic conductivity. This phenomenon was also seen by Cey et al. (2001), Babour and Yang (1993) and is summarized by Schmitz (2005). The decrease in flow rate was caused by both osmotic flow and osmotic compressibility.

4) Mineral precipitation

Due to the precipitation of carbonate minerals, the soil pores could be blocked by the precipitates causing the flowrates within the columns to decrease.

4.6 Solute Breakthrough Profiles during the Simulated Contaminant Flushing Stage

The breakthrough of major cations during the simulated contaminant flushing stage occurred as a series of fronts and resulted in the elution of Ca^{2+} and Mg^{2+} above input concentrations and the attenuation of K^+, and NH_4^+ by the soil exchange site. This is due to the displacement of Ca^{2+} and Mg^{2+} on the soil exchange sites by K^+ and NH_4^+ present in the simulated contaminant (Fonstad 2004, Thorton et al. 2001). The competition for the soil exchange sites was dependent on mass fraction, ionic charge and ionic size (hydrated radius).

The breakthrough curves, attenuation factors and a mass balance for each species during leachate breakthrough is use to describe the factors affecting the transport of each solute. The data is presented in terms of dimensionless normalized concentration (C/C_0) against pore volumes of fluid eluted from the column. Effluent concentrations of solutes are normalized to concentrations (C_0) in the reservoir.

The mass balance for each column during the simulated contaminant flushing stage is shown in Tables 4.9 and 4.10. Negative numbers indicate mass of solutes retained in the column, while positive numbers indicate solutes released from the columns. The total quantity of retained cations is greater than the total available CEC of the columns and the total quantity of released cations is less than the total available CEC of the columns. This discrepancy is related to a number of factors. These factors are discussed further when the breakthrough curve for each solute is presented separately in the next section.

The mass balance shows that the fraction of cations adsorbed from the simulated contaminant is comparable with the measured column CEC (Tables 4.2 and 4.3).

Table 4.9. Site 1 mass balance at the end of the simulated contaminant flushing stage.

	Column #1 meq/100g	Column #2 meq/100g	Column #3 meq/100g	average meq/100g
chloride	-2.2	-2.0	-1.8	**-2.0**
ammonia	-11.6	-13.3	-11.9	**-12.3**
sodium	-0.2	-0.1	-0.7	**-0.4**
potassium	-3.6	-2.2	-2.3	**-2.7**
sulphate	-2.1	-1.9	-2.3	**-2.1**
calcium	1.2	1.0	1.1	**1.1**
bicarbonate	-7.4	-8.1	-16.1	**-10.5**
magnesium	8.0	7.6	7.3	**7.7**
TOTAL CATIONS RELEASED	**9.2**	**8.7**	**8.5**	**8.8**
TOTAL CATIONS RETAINED	**-15.5**	**-15.6**	**-14.9**	**-15.3**

Table 4.10. Site 2 mass balance at the end of the simulated contaminant flushing stage.

	Column #4 meq/100g	Column #5 meq/100g	Column #6 meq/100g	average meq/100g
chloride	-2.2	0.2	0.3	**-0.6**
ammonia	-10.5	-8.7	-12.1	**-10.5**
sodium	0.5	0.8	1.9	**1.1**
potassium	-3.1	-2.3	-3.0	**-2.8**
sulphate	8.1	7.3	8.3	**7.9**
calcium	2.6	2.6	1.7	**2.3**
bicarbonate	-19.7	-20.5	-20.8	**-20.3**
magnesium	4.9	4.1	7.7	**5.5**
TOTAL CATIONS RELEASED	**8.1**	**7.5**	**11.4**	**9.0**
TOTAL CATIONS RETAINED	**-13.6**	**-11.0**	**-15.1**	**-13.3**

The breakthrough of each solute during the simulated contaminant flushing stage is discussed in the following sections.

4.6.1 Chloride

Figure 4.8 shows the Site 1 Cl^- breakthrough curve during the simulated contaminant flushing stage. Ogata and Banks (1961) analytical solution to the advection dispersion was fit to the Cl^- breakthrough curve as shown in Figure 4.9. In order to estimate the attenuation factor for each reactive ion using the analytical solution to the advection dispersion equation, the coefficient of hydrodynamic dispersion was estimated.

To achieve the best visual fit, a column peclet number of 9.3 and a hydrodynamic dispersion coefficient of 2.3×10^{-9} m^2/s were chosen. These parameters resulted in an attenuation factor of 1.0 for Cl^-.

The shape of the Site 1 Cl^- breakthrough curves suggest a flow pattern where initial breakthrough up to approximately 1.5 pore volumes is associated with macropore flow. There is plateau from approximately 1.5 to 3 pore volumes where a portion of the flow is contributed by the macropores at the same Cl^- concentration as the input solution, while the balance is from the soil matrix where breakthrough has not yet occurred and the Cl^- concentration is much lower. This plateau coincides with the peak of Mg^{2+} concentration in the column (Figure 4.12). The second increase in the C/C_0 curve is associated with the appearance of Cl^- transported through the soil matrix until the effluent Cl^- concentration equals the input solution; this phenomenon was also observed by Camebreco et al. (1996)

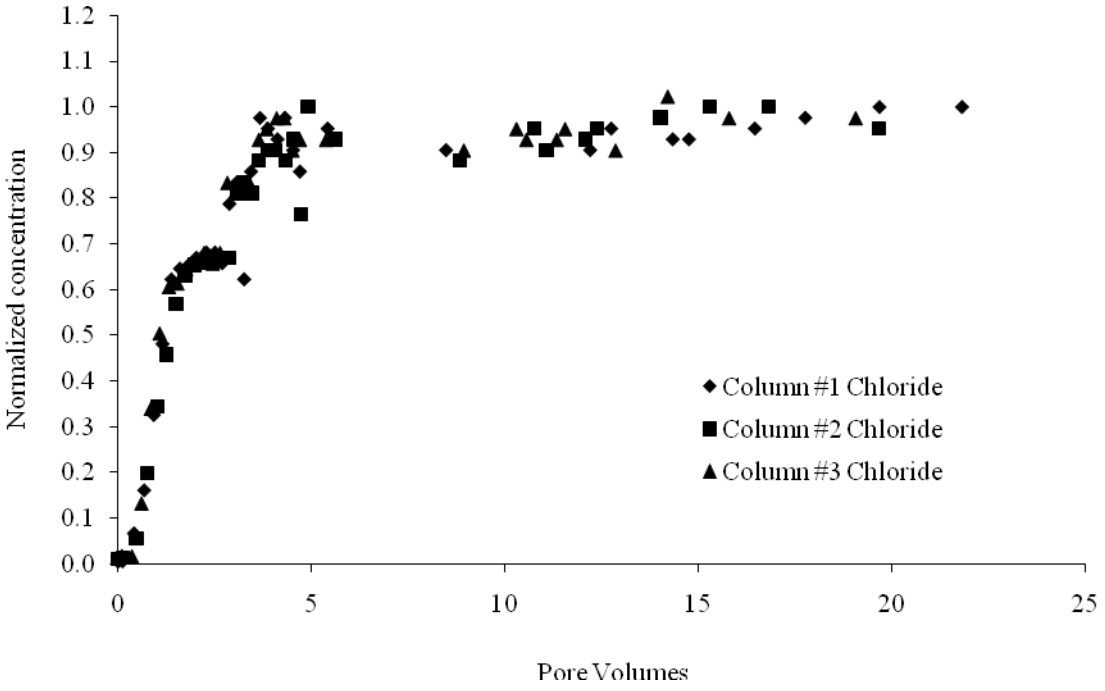

Figure 4.8. Site 1 chloride breakthrough curve during simulated contaminant flushing stage.

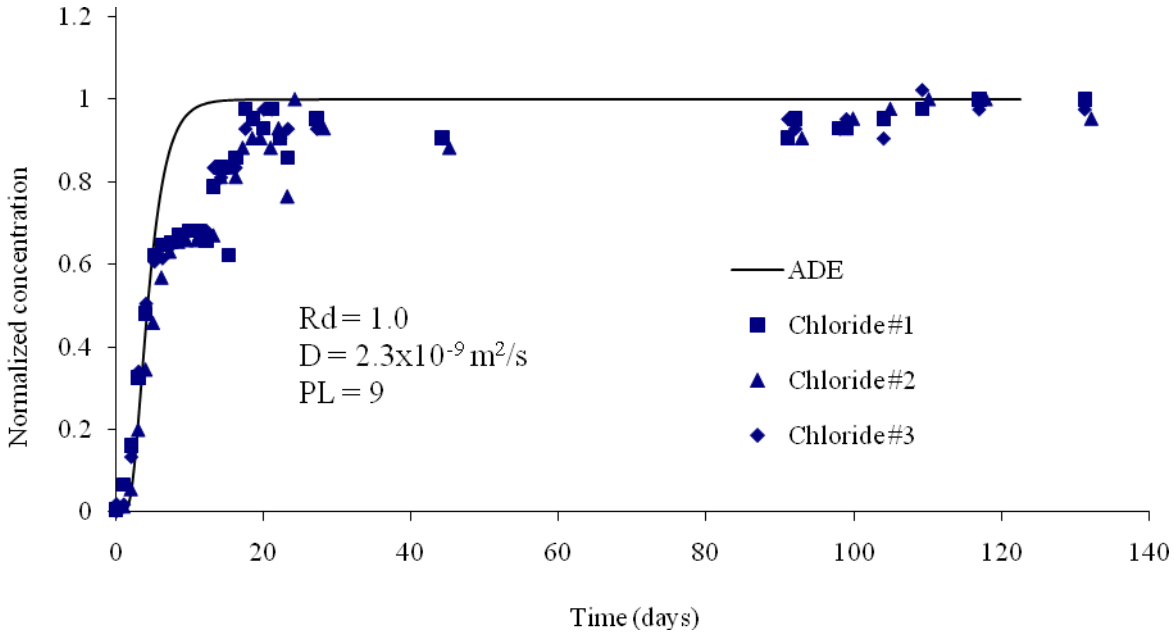

Figure 4.9. Site 1 advection dispersion curve fitting for chloride breakthrough during simulated contaminant flushing stage.

The Cl^- breakthrough curve for Site 2 is shown in Figure 4.10. Site 2 Cl^- breakthrough is attenuated by a factor of 2.1 (Figure 4.11). Generally, an attenuation factor of one is expected for Cl^-, since Cl^- is assumed to be nonreactive ion. The breakthrough curve exhibits extensive tailings characteristics up to 11 pore volumes.

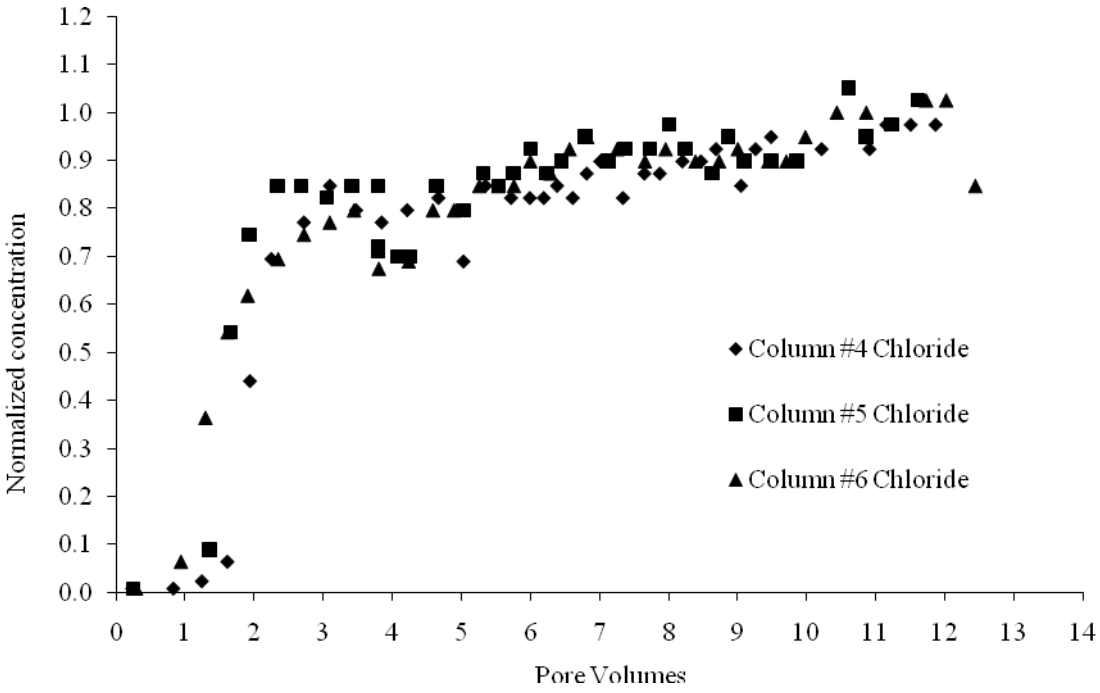

Figure 4.10. Site 2 chloride breakthrough curve during freshwater flushing stage.

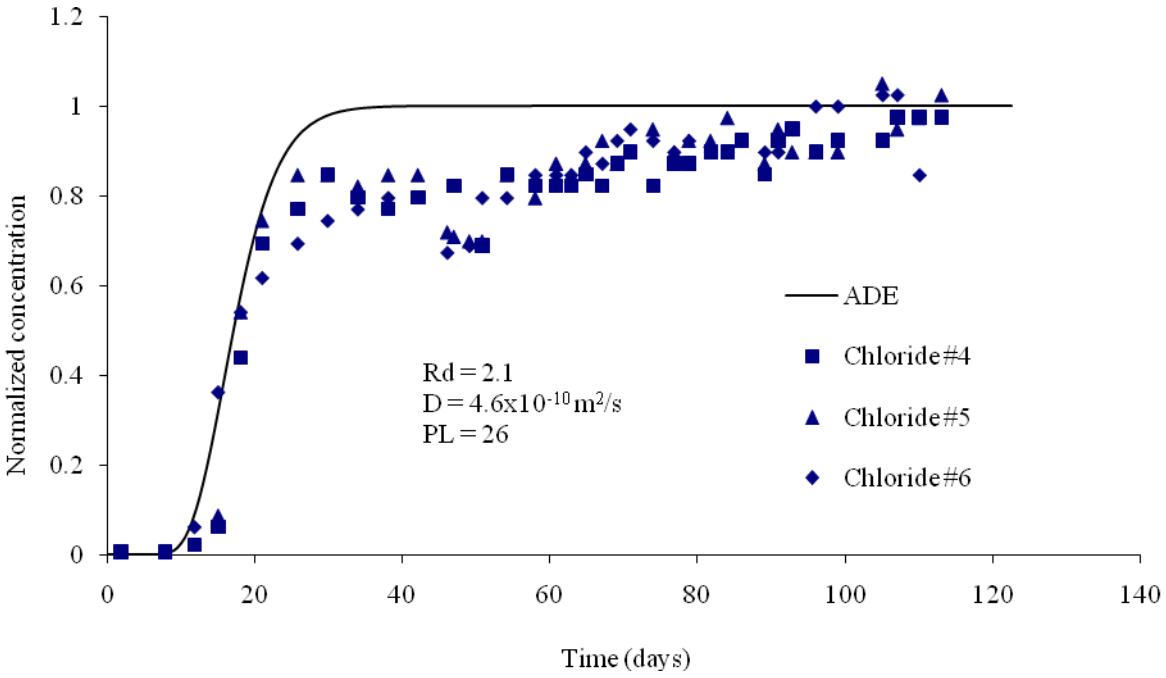

Figure 4.11. Site 2 advection dispersion curve fitting for chloride breakthrough during simulated contaminant flushing stage.

During the simulated contaminant flushing stage, the pore water has high ionic strength caused by high concentrations of NH_4^+ in the simulated contaminant and the Ca^{2+} and Mg^{2+} being displaced by NH_4^+ on the soil exchange sites (Figure 4.12). Chloride is a key component to charge balance this high concentration of cations in the soil pore water. As a result, Cl^- ions would be held back in the soil to achieve a charge balance and would not arrive unattenuated, as expected. This phenomenon was also seen by Chang and Donahue (2007) during radial diffusion cell tests with a livestock effluent similar in chemistry to this test. They showed that Cl^- played a key role in achieving charge balance during NH_4^+ diffusion.

An additional cause of Cl^- attenuation could be a pore water dilution effect caused by osmotic flow. The introduction of a solution of high concentration into a solution of low concentration

causes water to pass through a soil from immobile pore space into the high concentration solution in the mobile pore space. The concentration of Cl^- in the mobile pore space would be temporarily diluted causing an apparent delay or attenuation in the expected Cl^- concentration measured at the end of the column.

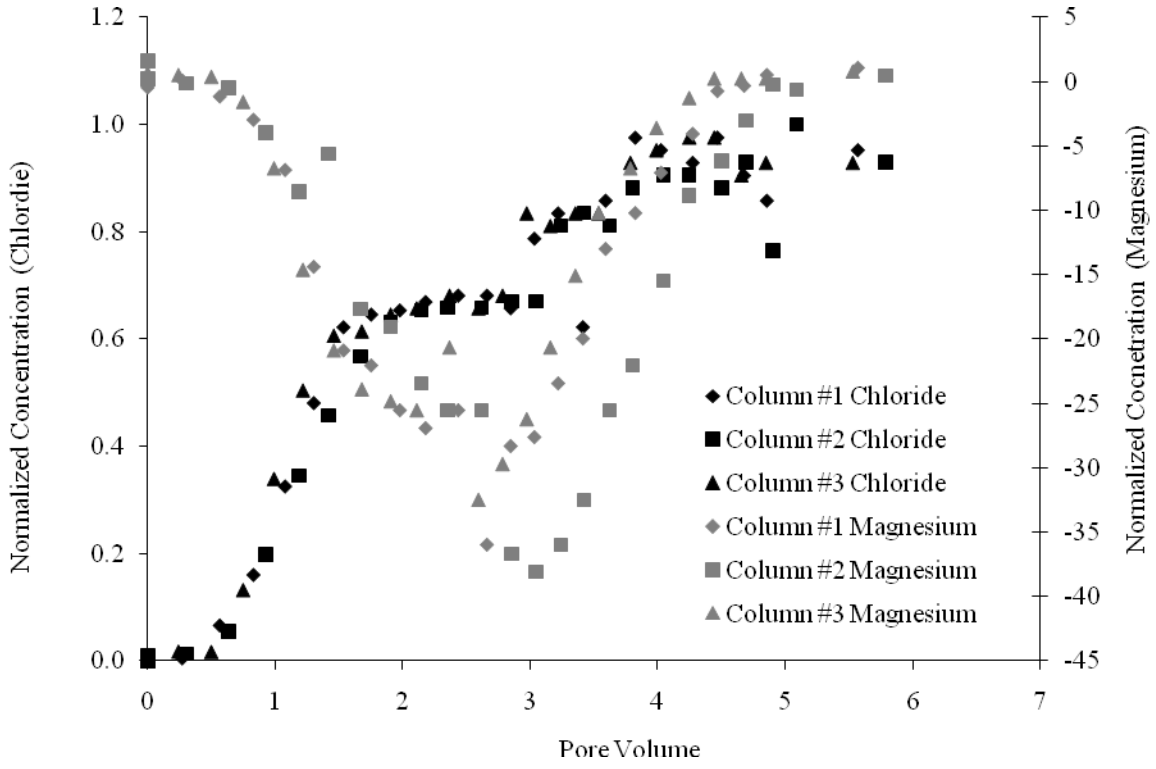

Figure 4.12. Comparison of Site 1 chloride breakthrough curve to the Site 1 magnesium breakthrough curve.

4.6.2 Ammonium

Figure 4.13 shows the Site 1 NH_4^+ breakthrough curve during the simulated contaminant flushing stage. Ammonium ions in the simulated contaminant were attenuated in the columns by a factor of 3.2 for Site 1 (Figure 4.14). Breakthrough (C/C_0=1) was achieved after five pore

volumes. At this point the adsorbed cation composition reached equilibrium with the leachate cation composition and NH_4^+ was no longer attenuated. Nitrates were not detected in the column effluent samples suggesting that the columns were in a reduced oxidation state.

The hydrodynamic diffusion coefficient is lower and the Peclet number is higher for NH_4^+ compared to hydrodynamic dispersion coefficient and resulting Peclet number for Cl^- during the simulated contaminant flushing stage. This is because NH_4^+ transport is attenuated with respect to Cl^- transport and the decrease in diffuse double layer (discussed in Section 4.3) and resulting flocculation of clay particles caused the hydraulic conductivity of the soil to decrease and molecular diffusion became more dominant in ion transport through the column already occurred.

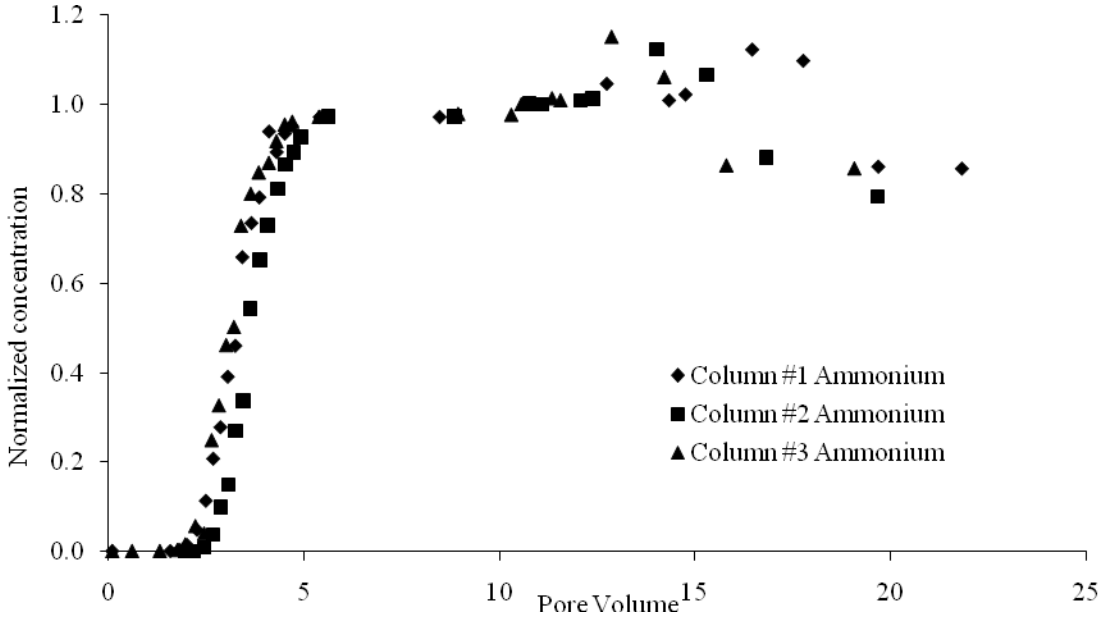

Figure 4.13. Site 1 column breakthrough curve for ammonium.

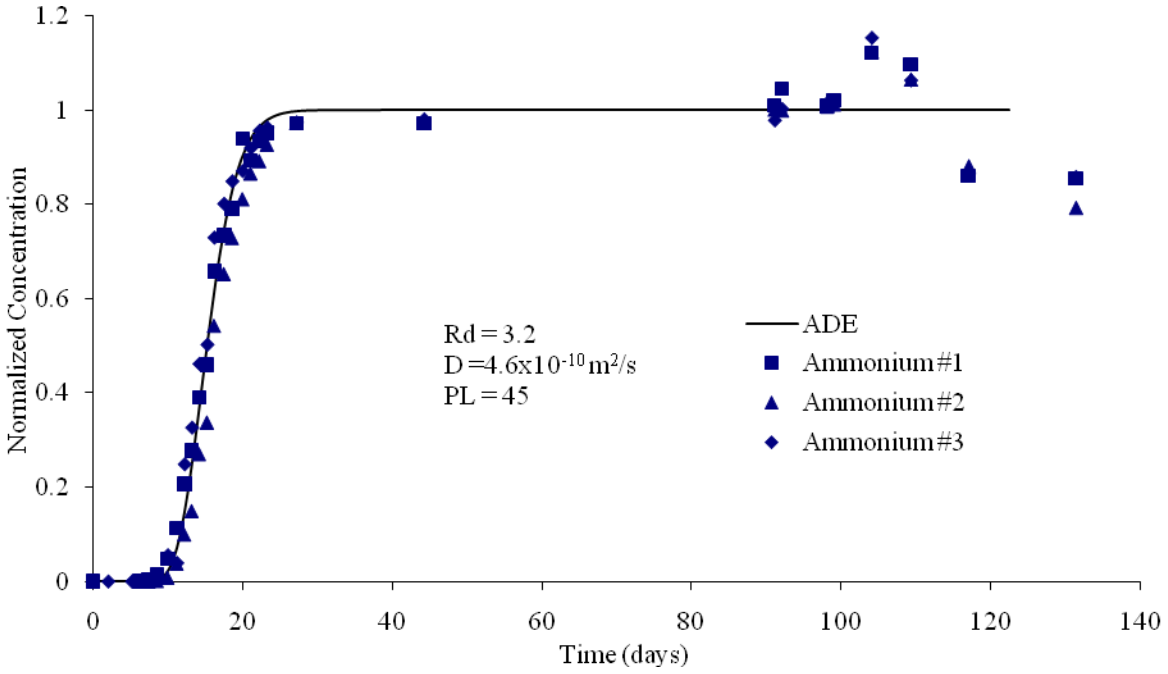

Figure 4.14. Site 1 advection-dispersion curve fitting for ammonium breakthrough.

Figure 4.15 shows the Site 2 NH_4^+ breakthrough curve during the simulated contaminant flushing stage. Ammonium ions in the simulated contaminant were attenuated in the columns by a factor of 6.0 for Site 2 (Figure 4.18). Breakthrough (C/C_0=1) was achieved after approximately eight pore volumes. At this point the sorbed cation composition reached equilibrium with the simulated contaminant cation composition and NH_4^+ was no longer attenuated.

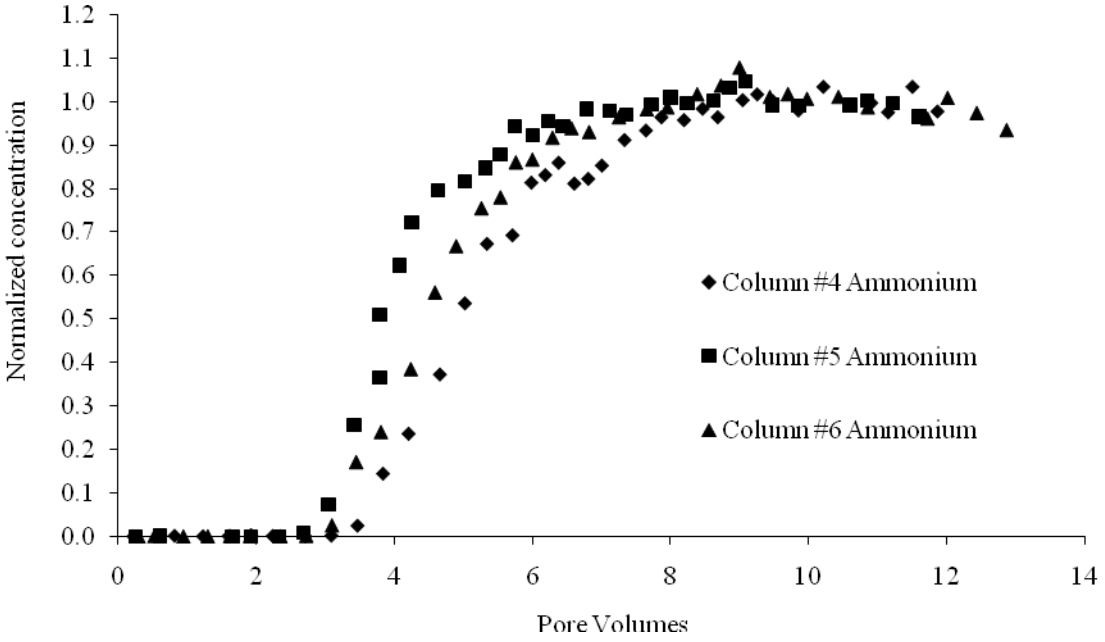

Figure 4.15. Site 2 column breakthrough curve during the simulated contaminant flushing stage.

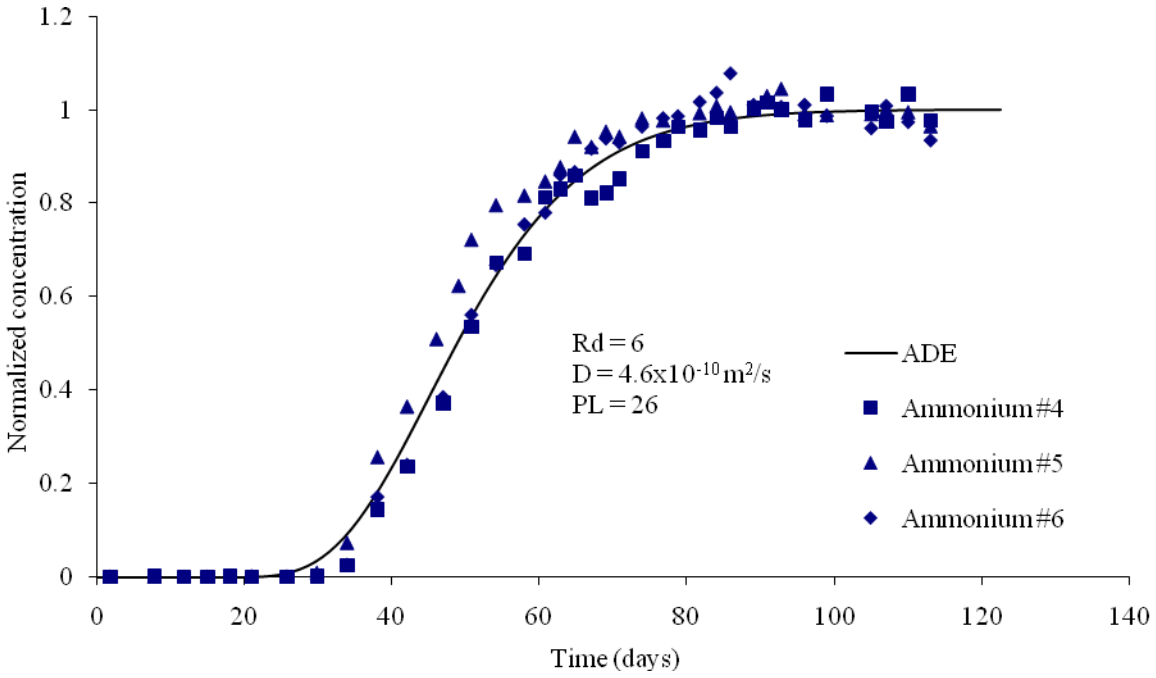

Figure 4.16. Site 2 advection-dispersion curve fitting for ammonium breakthrough during the simulated contaminant flushing stage.

The mass balance on the column influent and effluent concentrations results in an average of 12.3 meq/100 g of NH_4^+ retained in the site 1 soil columns. This does not agree with the CEC analysis completed on column #1 where 3.2 meq/100 g of NH_4^+ was retained on the soil exchange sites. The same is true for Site 2 mass balance where an average of 10.5 meq/100 g of NH_4^+ was retained in the soil column as opposed to 4.9 meq/100 g as calculated from the CEC analysis. It is suspected that the CEC analysis was not able to remove the NH_4^+ adsorbed as interlayer cations. When NH_4^+ replaced Ca^{2+} and Mg^{2+} on the soil exchanges sites it is likely that the clay mineral collapsed, trapping the NH_4^+ and making it unavailable for exchange during freshwater flushing stage and the CEC analysis. A collapsed structure can only exchange through solid state diffusion, which is 3-4 orders of magnitude slower than diffusion in solution (Appelo and Postma 2005).

4.6.3 Potassium

Figures 4.17 and 4.19 show the K^+ breakthrough curve during the simulated contaminant flushing stage for Sites 1 and 2, respectively. Potassium ions in the simulated contaminant were attenuated by a factor of 3.2 for Site 1 (Figure 4.18). This is the same attenuation factor as NH_4^+, although the K^+ breakthrough curve for Site 1 exhibits tailing behaviour. The tailing behaviour indicates that small amounts of K^+ were still being adsorbed even though it appeared that NH_4^+ attenuation was exhausted. A mass balance on the column influent and effluent volumes concentrations results in an average 2.7 meq/100 g of K^+ retained in each soil column. This number from the mass balance agrees with the CEC analysis completed on column #1 which was 2.1 meq/100 g.

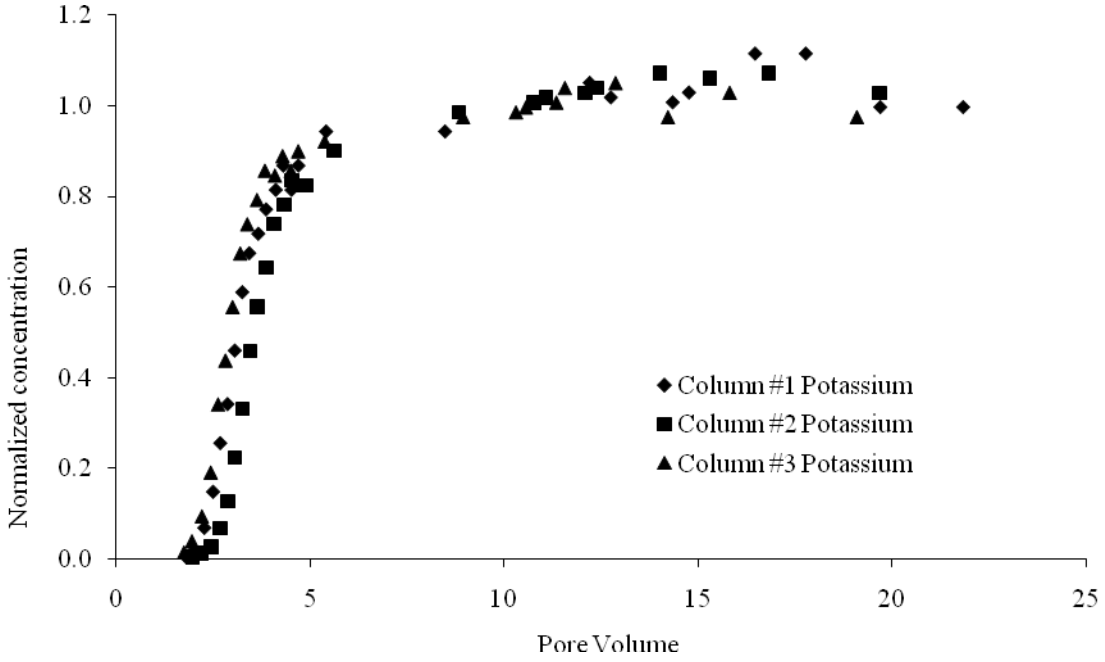

Figure 4.17. Site 1 column breakthrough curve for potassium during simulated contaminant flushing stage.

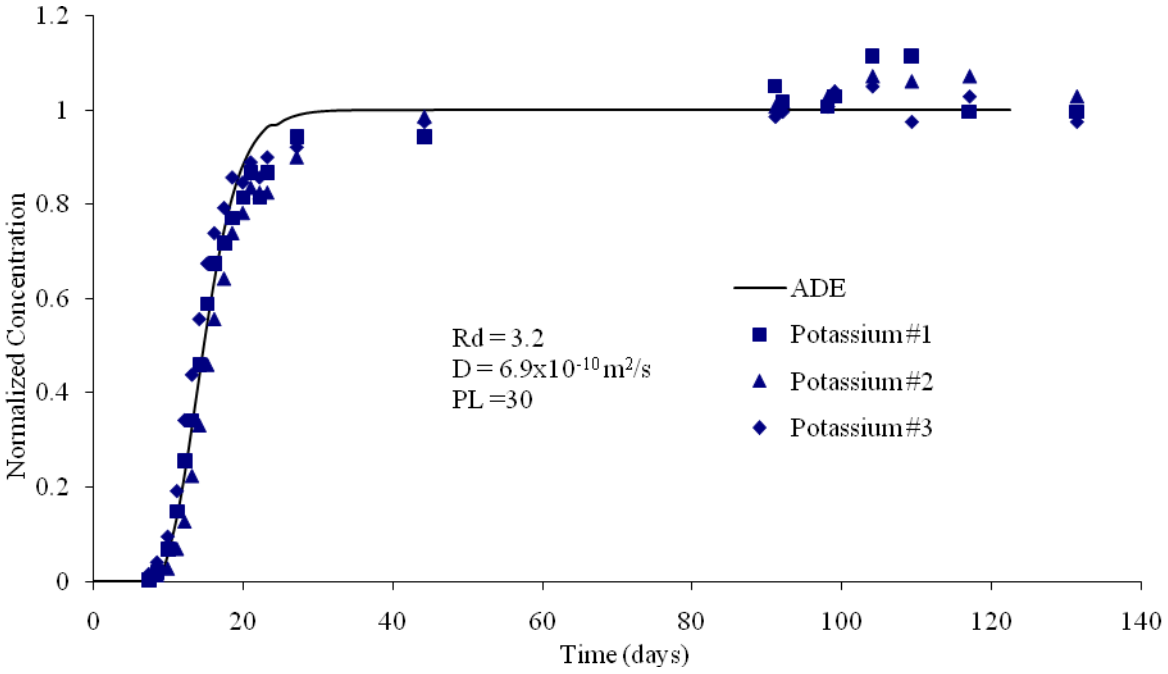

Figure 4.18. Site 1 advection dispersion curve fitting for potassium breakthrough during the simulated contaminant flushing stage.

Potassium ions in simulated contaminant were attenuated by a factor of 5.4 by the Site 2 soil (Figure 4.20). This is the same attenuation factor as NH_4^+, although the K^+ breakthrough curve exhibits tailing concentration behaviour. The tailing behaviour indicates that small amounts of K^+ were still being adsorbed even though it appears that NH_4^+ attenuation was exhausted. A mass balance on the column influent and effluent volumes concentrations results in an average 2.8 meq/100 g of K^+ retained in each soil column. This number from the mass balance agrees with the CEC analysis completed on column #4 which was 2.1 meq/100 g.

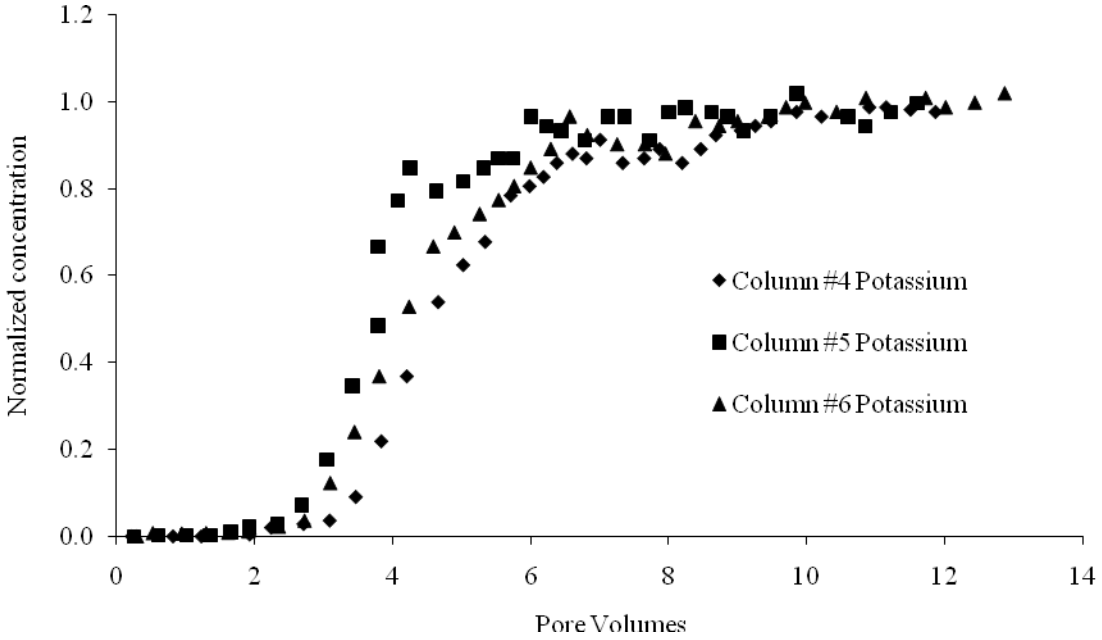

Figure 4.19. Site 2 column breakthrough curve for potassium during the simulated contaminant flushing stage.

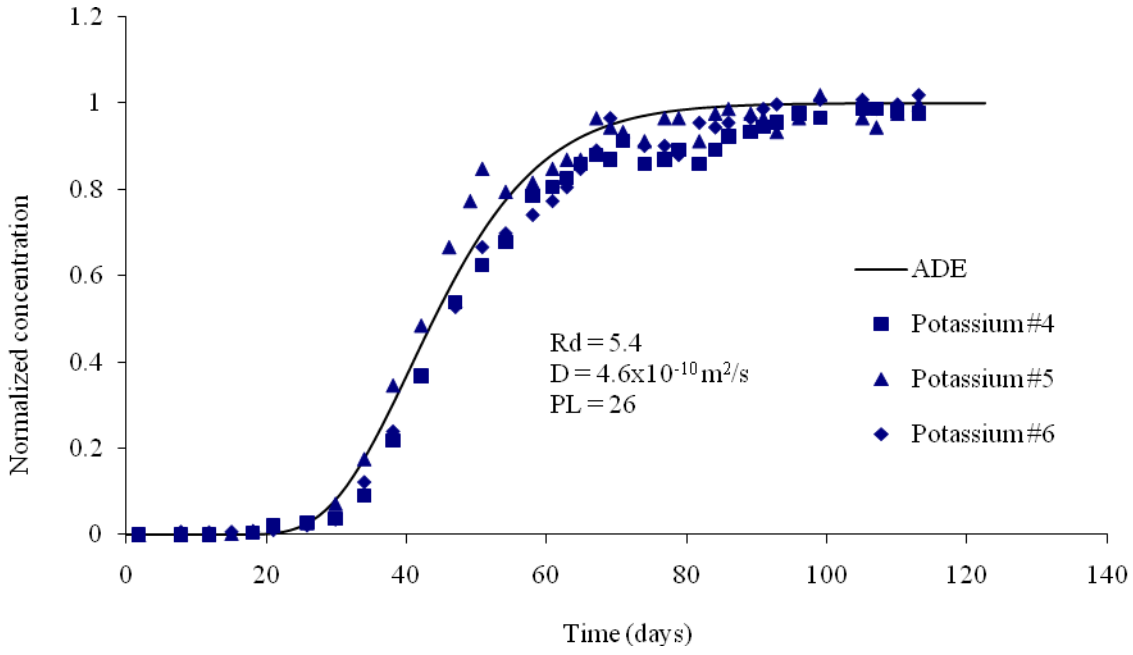

Figure 4.20. Site 2 advection dispersion curve fitting for potassium breakthrough during the simulated contaminant flushing stage.

4.6.4 Sodium

Figures 4.21 and 4.23 show the Na^+ breakthrough curve during the simulated contaminant flushing stage for Site 1 and 2, respectively. Sodium remained relatively unreactive and was attenuated by a factor of 1.6 by the Site 1 soil (Figure 4.22). A mass balance on the column influent and effluent volumes and concentrations results in an average of 0.4 meq/100 g of Na^+ retained in each soil column. This number from the mass balance agrees with the CEC analysis completed on column #1 which as 1.0meq/100 g. The normalized concentration is greater than one for a short period indicating that at this point it is possible that Na^+ is being replaced by any other cations in the solution.

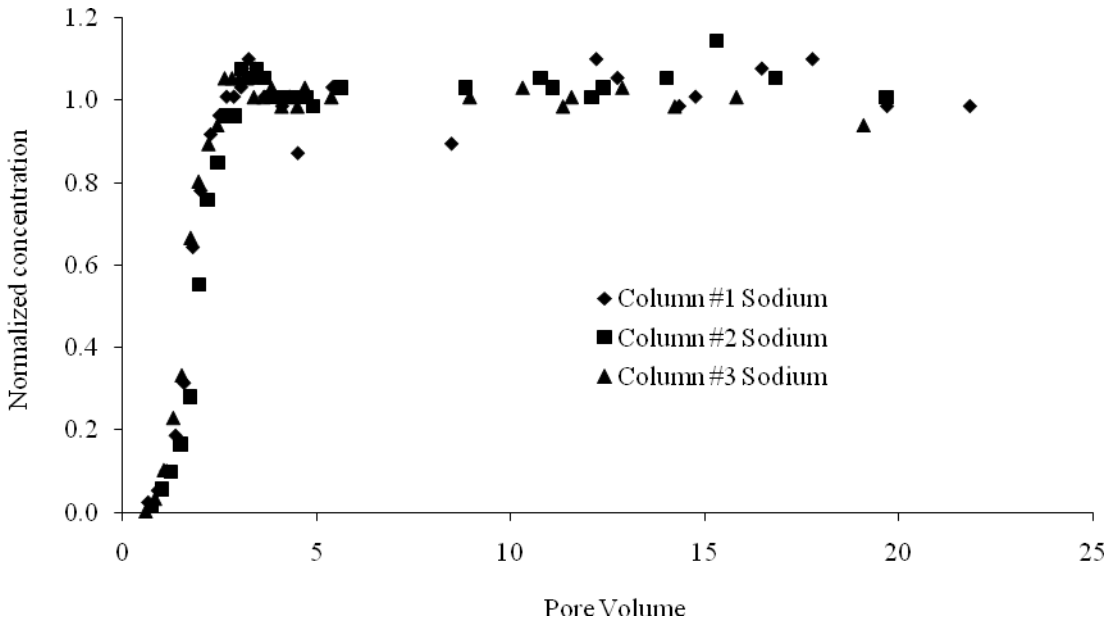

Figure 4.21. Site 1 sodium breakthrough curve during the simulated contaminant flushing stage.

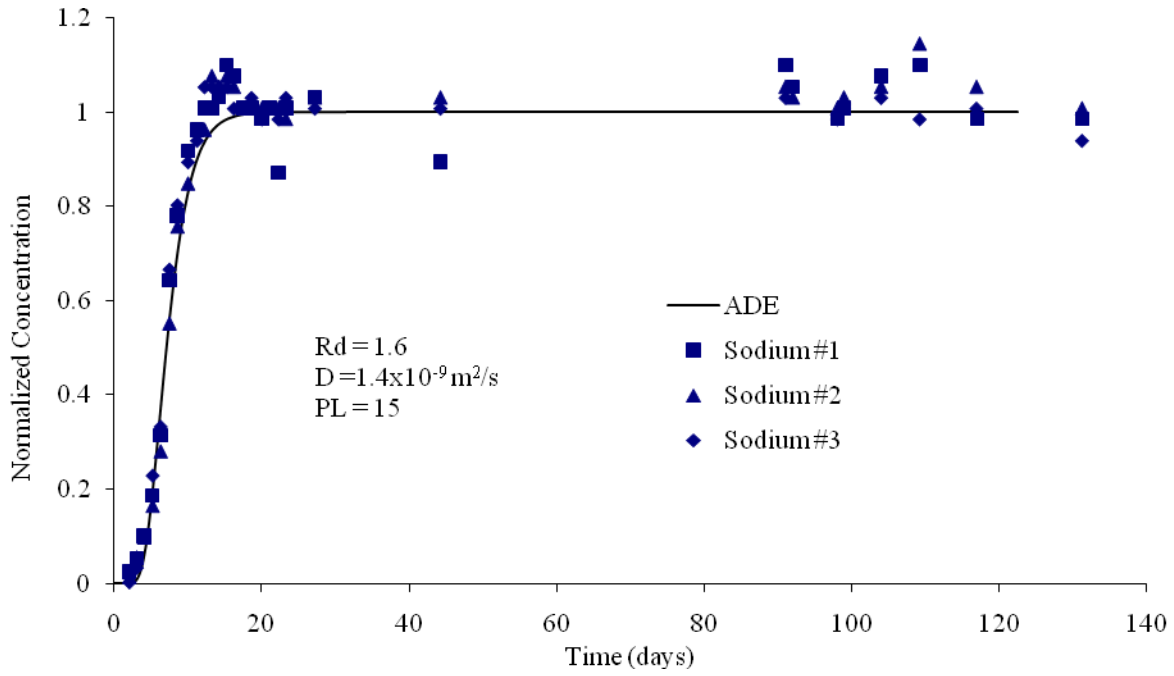

Figure 4.22. Site 1 advection-dispersion curve fitting for sodium breakthrough during the simulated contaminant flushing stage.

Sodium remained relatively unreactive and was attenuated by a factor of 2.4 by the Site 2 soil (Figure 4.24). A mass balance on the column influent and effluent volumes and concentrations results in an average of 2.7 meq/100 g of Na^+ retained in each soil column. This number from the mass balance agrees with the CEC analysis completed on column #1 which as 2.1 meq/100 g. Similar to Site 1, the normalized concentration is greater than one at different periods possibly indicating Na^+ is being replaced intermittently by any other cations in the solution. For both soils, breakthrough times for Na^+ occurred at approximately the same time as Cl^-.

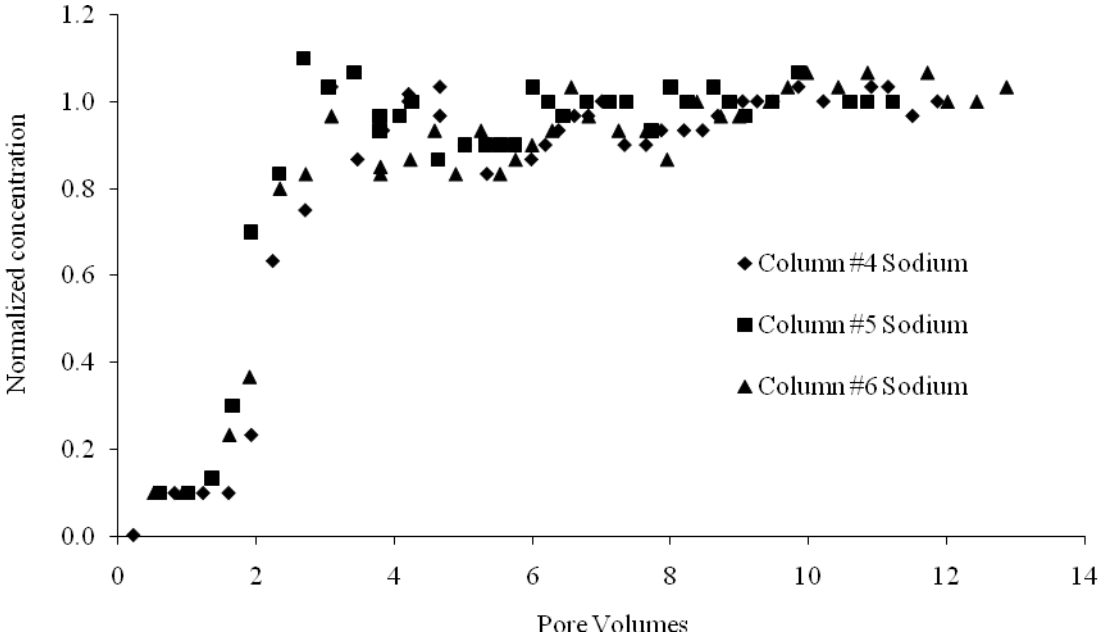

Figure 4.23. Site 2 sodium breakthrough curve during the simulated contaminant flushing stage.

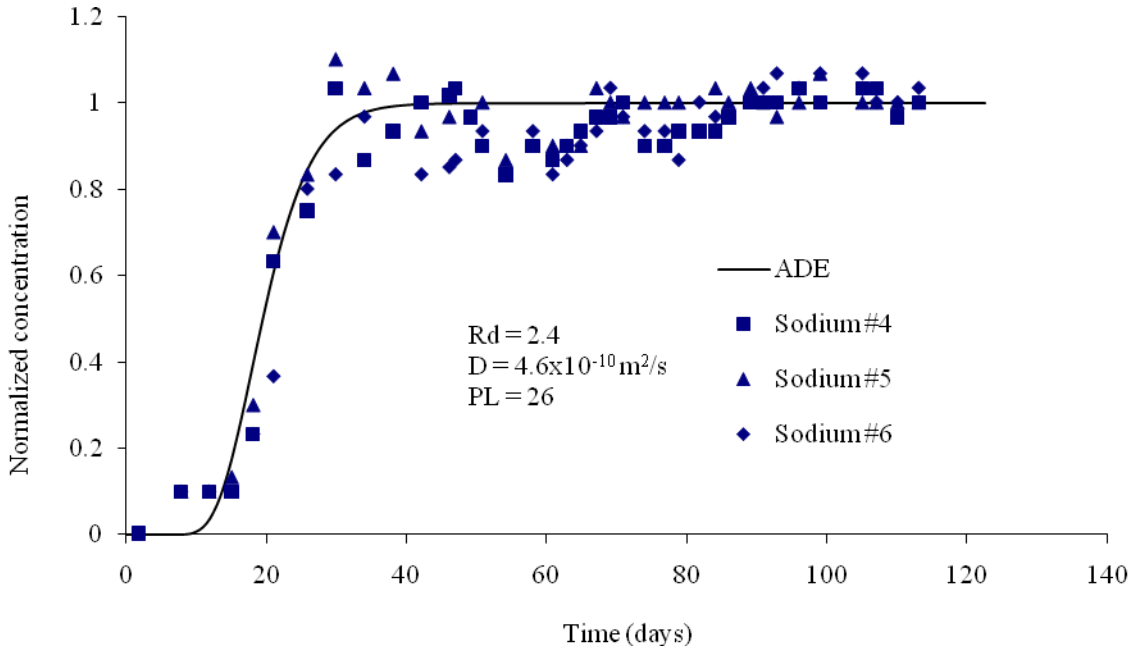

Figure 4.24. Site 2 advection-dispersion curve fitting for sodium breakthrough during the simulated contaminant flushing stage.

4.6.5 Bicarbonate

Figures 4.25 and 4.27 display the HCO_3^- breakthrough curve during the simulated contaminant flushing stage for Sites 1 and 2, respectively. The breakthrough curve for HCO_3^- has an attenuation factor of approximately 3.0 (Figure 4.26) for Site 1 and 6.0 for Site 2 (Figure 4.28). The attenuation of negatively charged HCO_3^- ions was not caused by cation exchange, suggesting that another mechanism is responsible for the apparent attenuation of HCO_3^-. Sass et al. (2001) found that HCO_3^- levels decrease due to the precipitation of calcite. The saturation indices for calcite and other carbonate precipitates are shown in Figure 4.29. Saturation indices greater than zero indicate that the solution is supersaturated with respect to these minerals.

Excess Ca^{2+} and Mg^{2+} from the soil exchange sites will induce the precipitation of carbonate minerals. The mass balance provides further evidence of carbonate precipitation since an average of 10.5 meq/100 g and 20.3 meq/100 g of HCO_3^- were retained in the Site 1 and Site 2 soil columns, respectively.

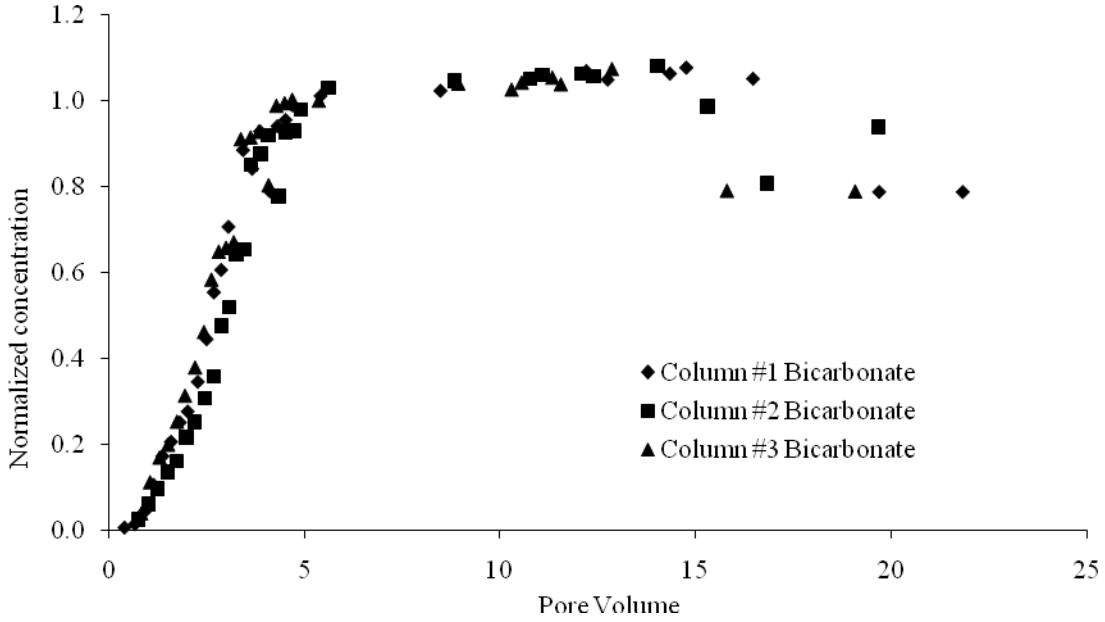

Figure 4.25. Site 1 column breakthrough curve for bicarbonate during the simulated contaminant flushing stage.

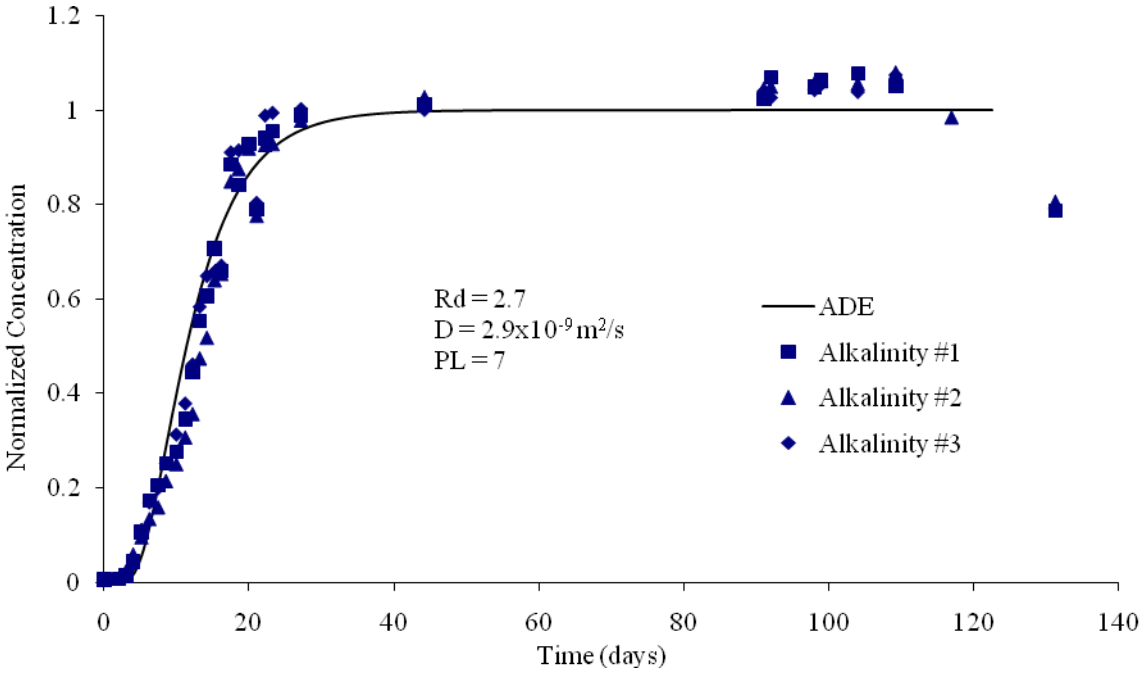

Figure 4.26. Site 1 advection dispersion curve fitting for bicarbonate during the simulated contamiant flushing stage.

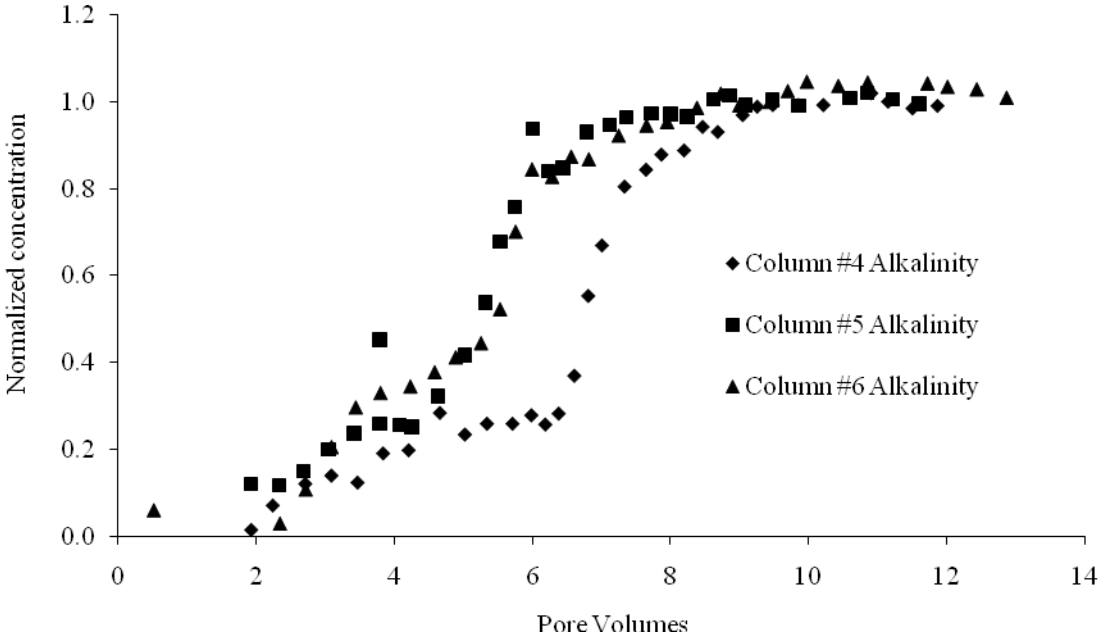

Figure 4.27. Site 2 column breakthrough curve for bicarbonate during the simulated contaminant flushing stage.

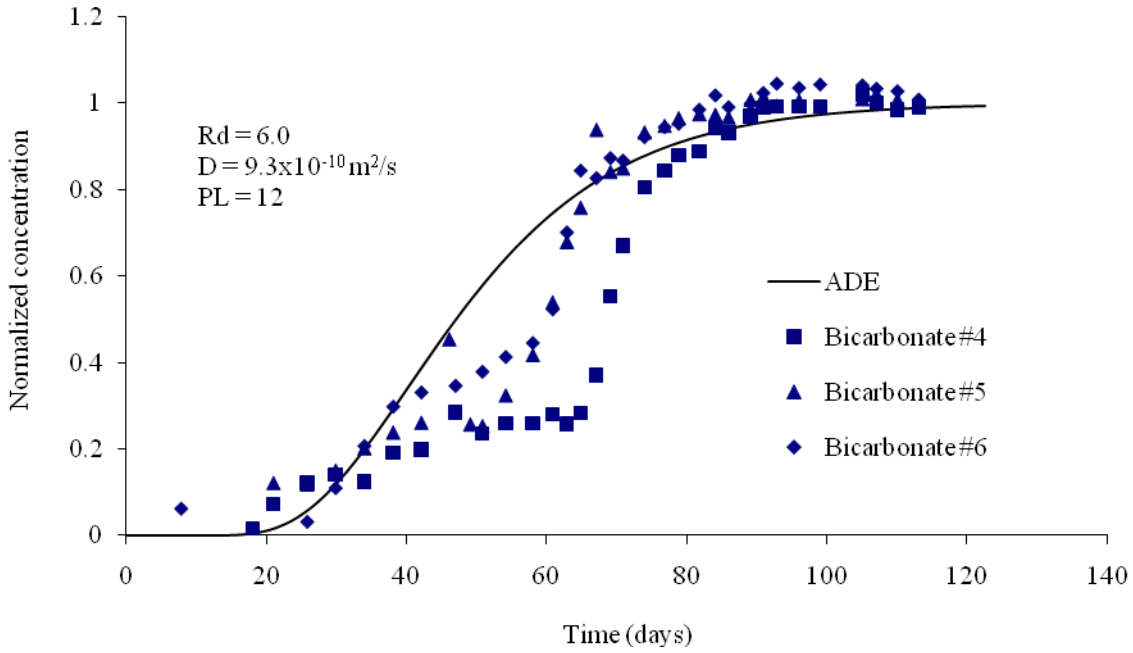

Figure 4.28. Site 2 advection dispersion fitting for bicarbonate breakthrough curve during the simulated contaminant flushing stage.

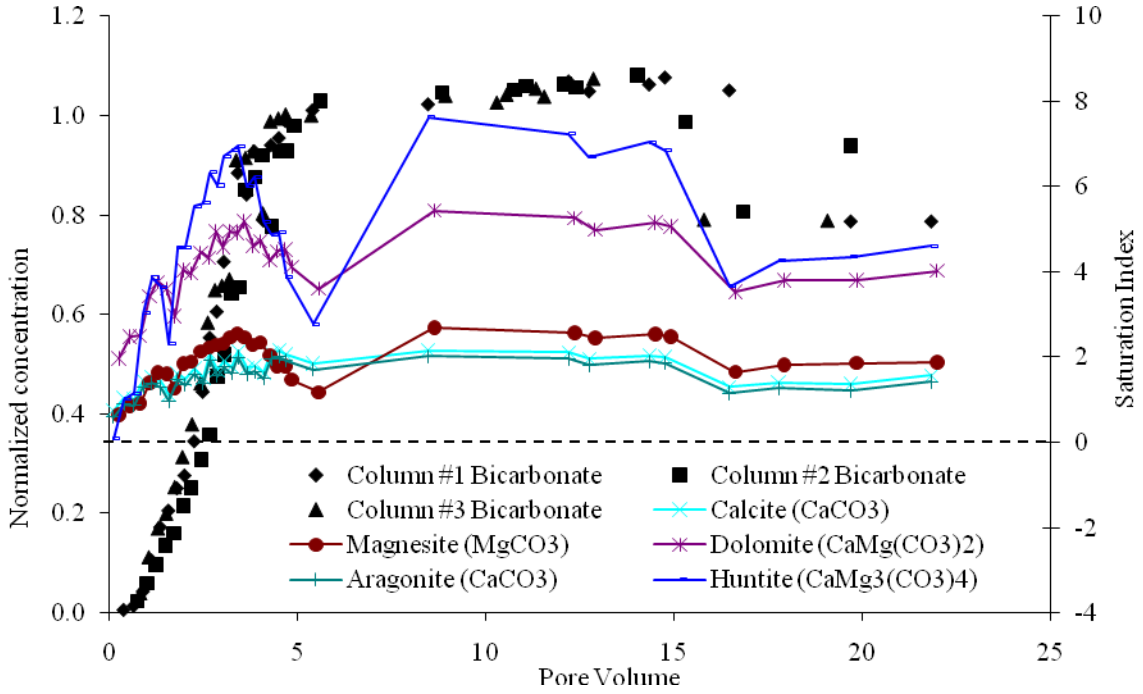

Figure 4.29. Column breakthrough curve for bicarbonate during the simulated contaminant flushing stage compared to the saturation indices for various carbonate minerals at pH=7.

The pH of the solution affects the solubility because is governs the aqueous complexation (ie. H_2CO_3, HCO_3, and CO_3^{2-}). The precipitation of calcite will cause the pH to decrease (Langmuir 1997 p 157) because carbonic acid is produced:

$$Ca^{2+} + 2HCO_3^- = CaCO_3 + H_2CO_3 \qquad (14)$$

The slight drop in pH around 2 to 4 pore volumes for the Site 1 soil columns (Figure 4.30) is another indication that carbonate mineral precipitation is taking place. For Site 2, the pH data is not as tight fitting and no pH trends are discernible (Figure 4.31).

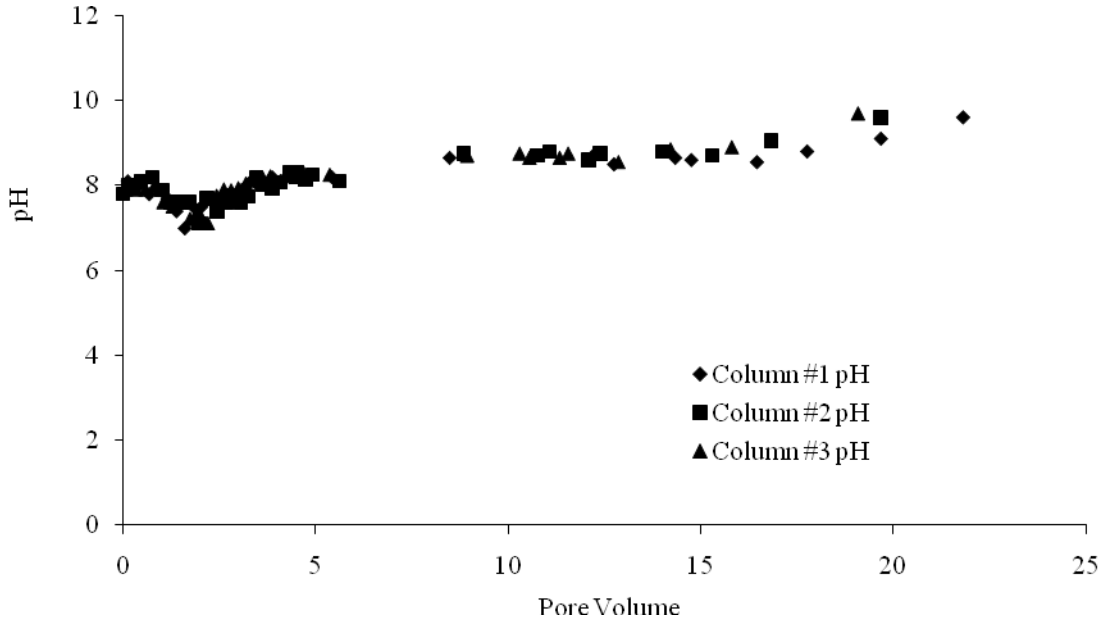

Figure 4.30. pH of Site 1 column effluent during simulated contaminant flushing stage.

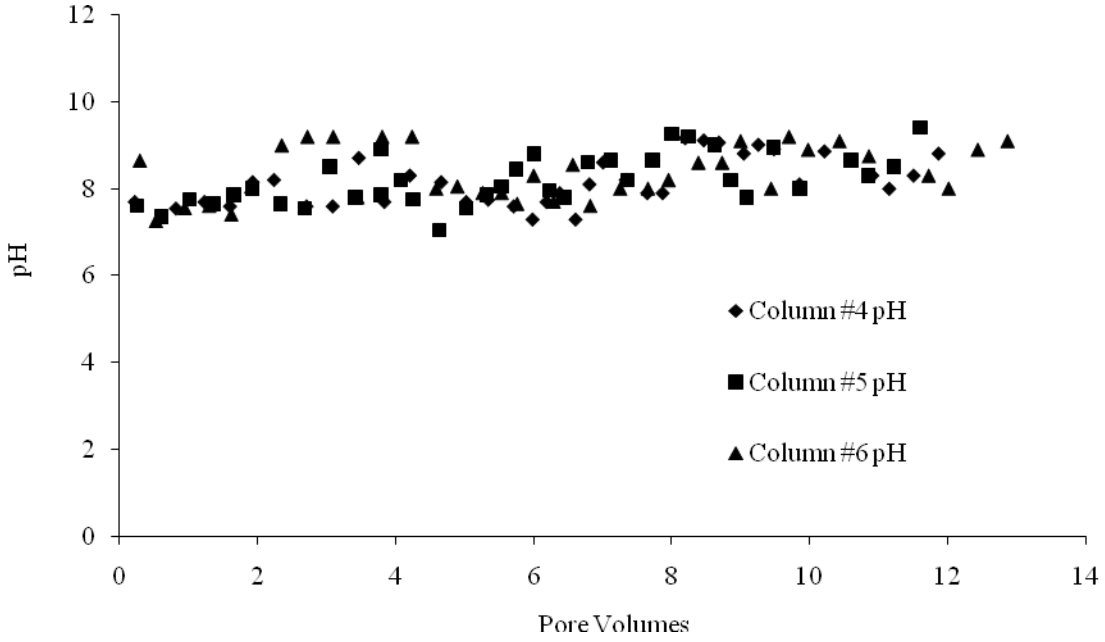

Figure 4.31. pH of Site 2 column effluent during simulated contaminant flushing stage.

4.6.6 Calcium

Figures 4.32 and 4.33 show the Ca^{2+} breakthrough curves during the simulated contaminant flushing stage for Site 1 and 2, respectively. Ammonium and K^{+} adsorption on the soil exchange sites resulted in the release of native Ca^{2+} ions. According the mass balance of column influent and effluent concentrations, an average of 1.1 meq/100g and 2.3 meq/100 g of Ca^{2+} was released from the soil exchange sites for Sites 1 and 2, respectively. According to the CEC analysis 0.8 meq/100 g and 1.5 meq/100 g of Ca^{2+} was released from the soil exchange sites for Sites 1 and 2, respectively. According to the CEC analysis of column #1, 6.6 meq/100 g of Ca^{2+} was originally on the soil prior to leaching with the simulated contaminant; therefore, approximately 12% of

available Ca^{2+} was released from soil exchange sites. For column #4, 6.1 meq/100g of Ca^{2+} was originally on the soil prior to leaching with the simulated contaminant; therefore, approximately 25% of available Ca^{2+} was released from the soil exchange sites.

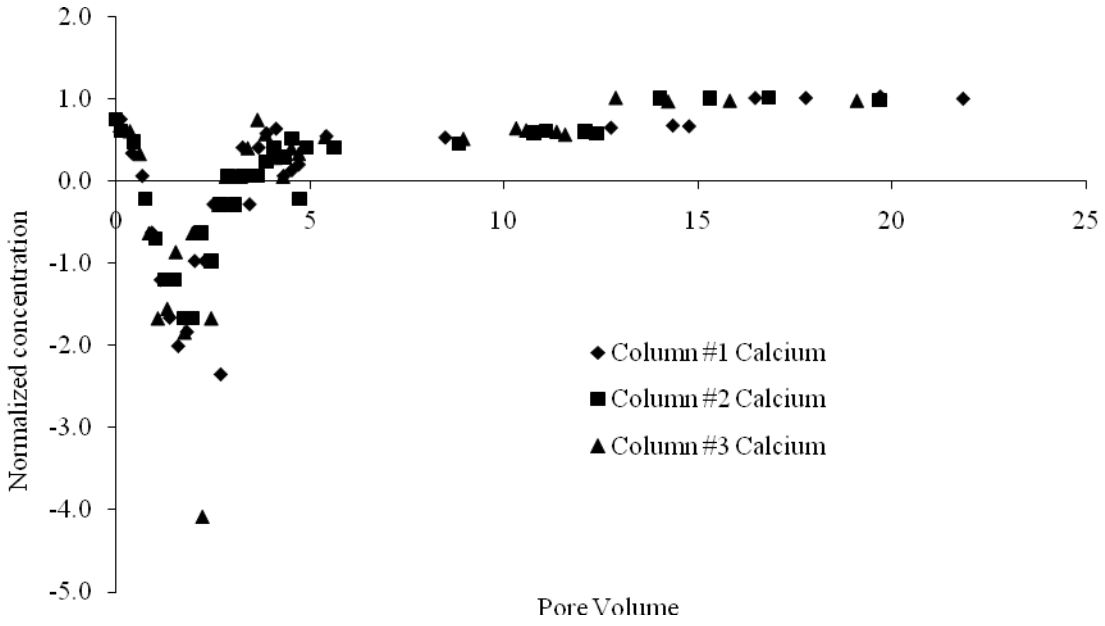

Figure 4.32. Site 1 column breakthrough curve for calcium during the simulated contaminant flushing stage.

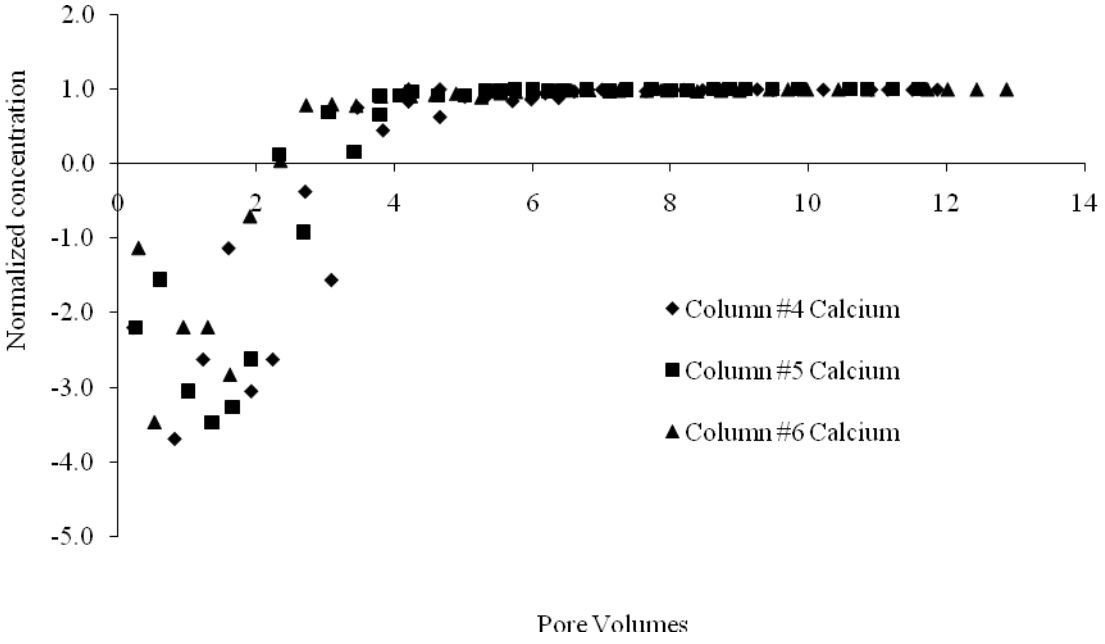

Figure 4.33. Site 2 column breakthrough curve for calcium during the simulated contaminant flushing stage.

Attenuation of HCO_3^- in the soil column was attributed to carbonate mineral precipitation, which is not apparent after examining the transport of Ca in the soil column. However, from the mass balance, the amount of K^+ and NH_4^+ adsorbed was greater than the amount of Ca^{2+} and Mg^{2+} released. This could be caused by the loss of released Ca^{2+} and Mg^{2+} due to carbonate mineral precipitation. As described in Section 4.5.5, it is also postulated that the CEC analysis of Ca^{2+} on the soil exchange sites was overestimated due to the dissolution of calcite during the CEC analysis. This would result in higher than actual amounts of Ca^{2+} assumed to be present on the soil exchange sites.

Figure 4.34 shows that Ca^{2+} is released from the soil exchange sites immediately before NH_4^+ breakthrough.

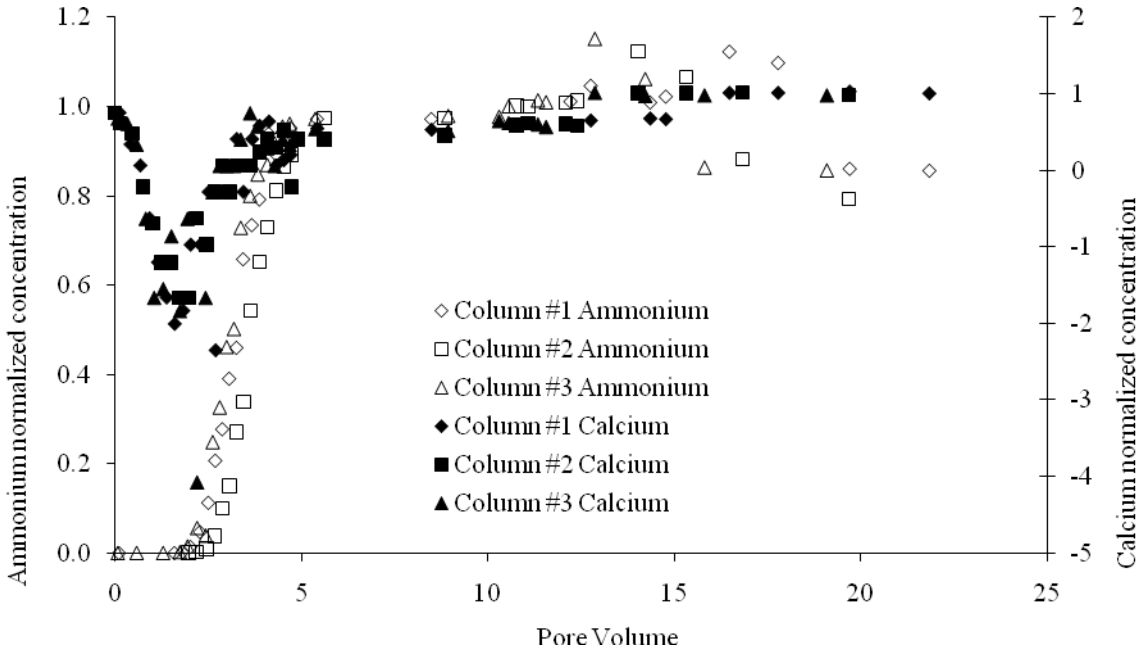

Figure 4.34. Calcium breakthrough curve compared to ammonium breakthrough curve for Site 1.

4.6.7 Magnesium

Figures 4.35 and 4.36 show the Mg^{2+} breakthrough curve during the simulated contaminant flushing stage for Site 1 and 2, respectively. Ammonium and K^+ adsorption on the soil exchange sites resulted in the release of native Mg^{2+} ions. Figure 4.37 shows that peak release of Mg^{2+} for Site 1 is greater than the Ca^{2+} peak but lags behind the Ca^{2+} concentration peak. This means that initially, Ca^{2+} is more easily exchanged but is limited and Mg^{2+} becomes the cation that is more readily exchangeable.

According the mass balance of column influent and effluent concentrations, an average of 7.9 meq/100g and 5.5 meq/100g of Mg^{2+} was released from the soil exchange sites for Site 1 and Site 2, respectively. According to CEC analysis, 3.40 meq/100 g and 5.1 meq/100 g was released from the soil exchange sites for Site 1 and Site 2, respectively. The difference between the mass balance and CEC analysis for Site 1 may be due to barium being ineffective at replacing Mg^{2+} on exchange site during the CEC analysis due to adsorption inside the interlayers of the smectite clay.

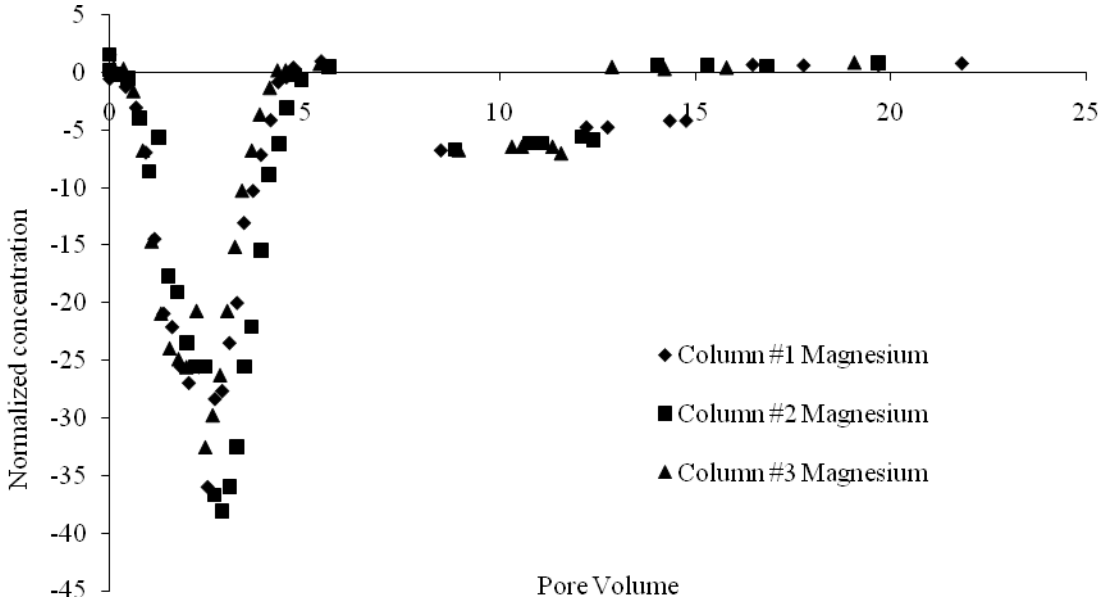

Figure 4.35. Site 1 column breakthrough curve for magnesium during the simulated contaminant flushing stage.

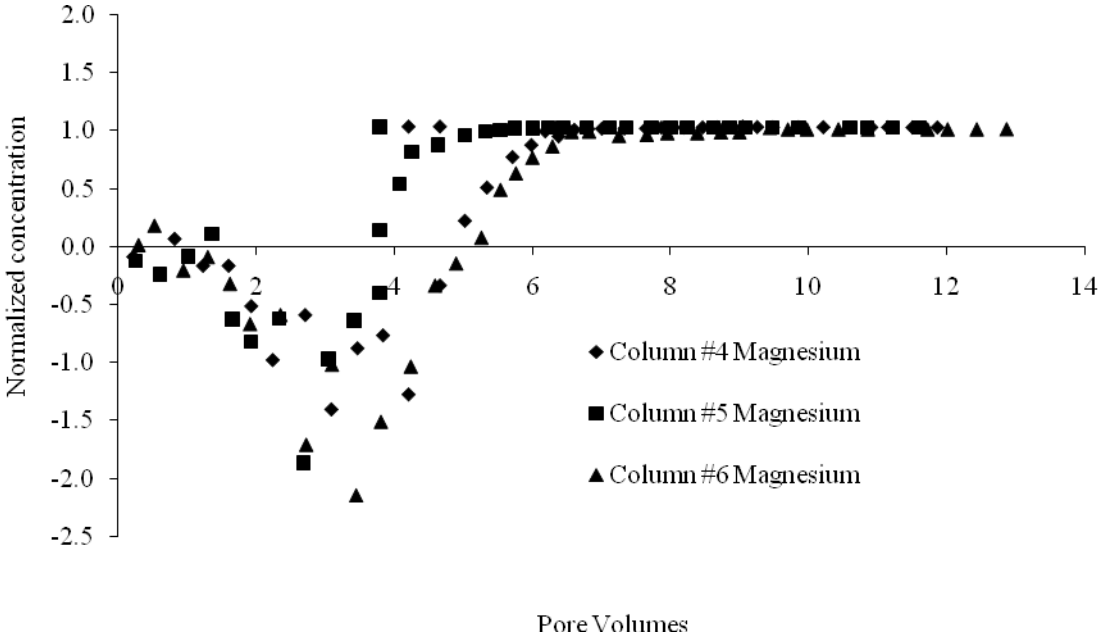

Figure 4.36. Site 2 column breakthrough curve for magnesium during the simulated contaminant flushing stage.

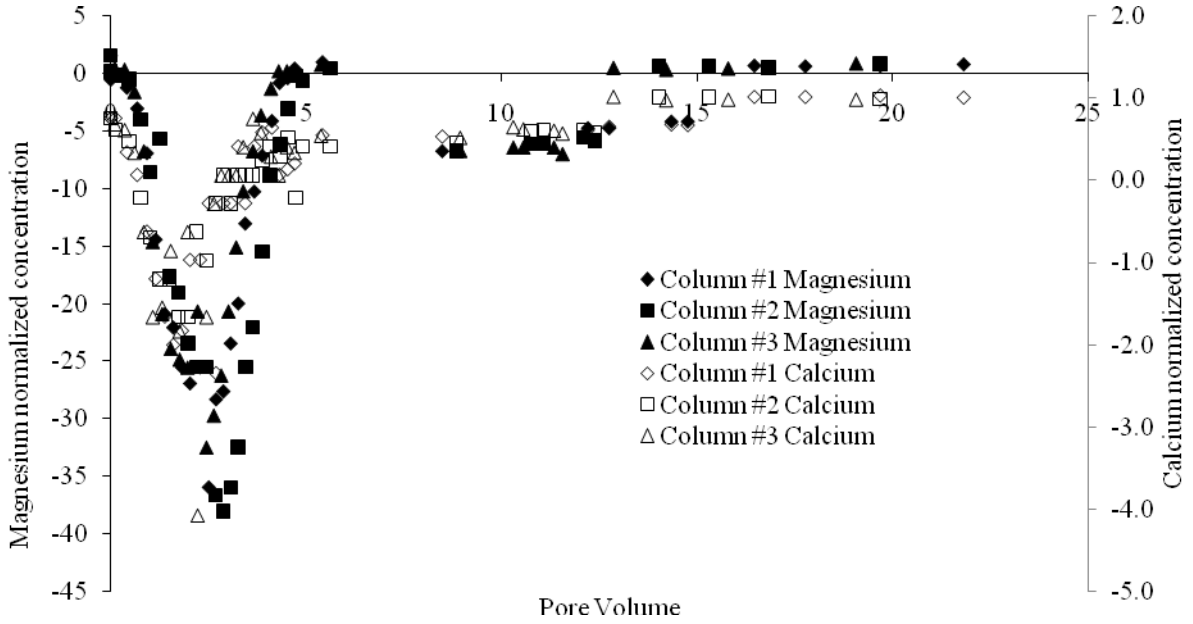

Figure 4.37. Site 1 magnesium breakthrough curve compared to ammonium breakthrough curve during the simulated contaminant flushing stage.

Figure 4.38 shows that for Site 2, Mg^{2+} release lags behind Ca^{2+}, although the Ca^{2+} peak is larger, more Mg^{2+} is exchanged according to the mass balance (7.9 meq/100 g of Mg^{2+} compared to 2.3 meq/100 g of Ca2+). For Site 1, the Ca^{2+} peak is appears barely ahead of the Mg^{2+} peak, as shown in Figure 4.39.

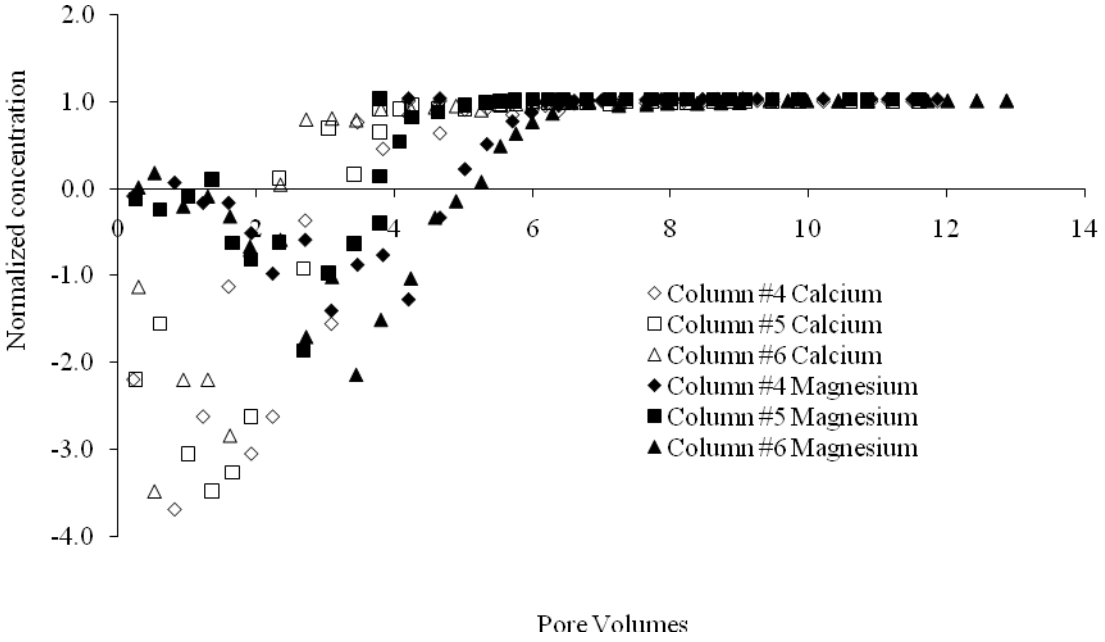

Figure 4.38. Site 2 magnesium breakthrough curve comparted to the calcium breakthrough curve during the simulated contaminant flushing stage.

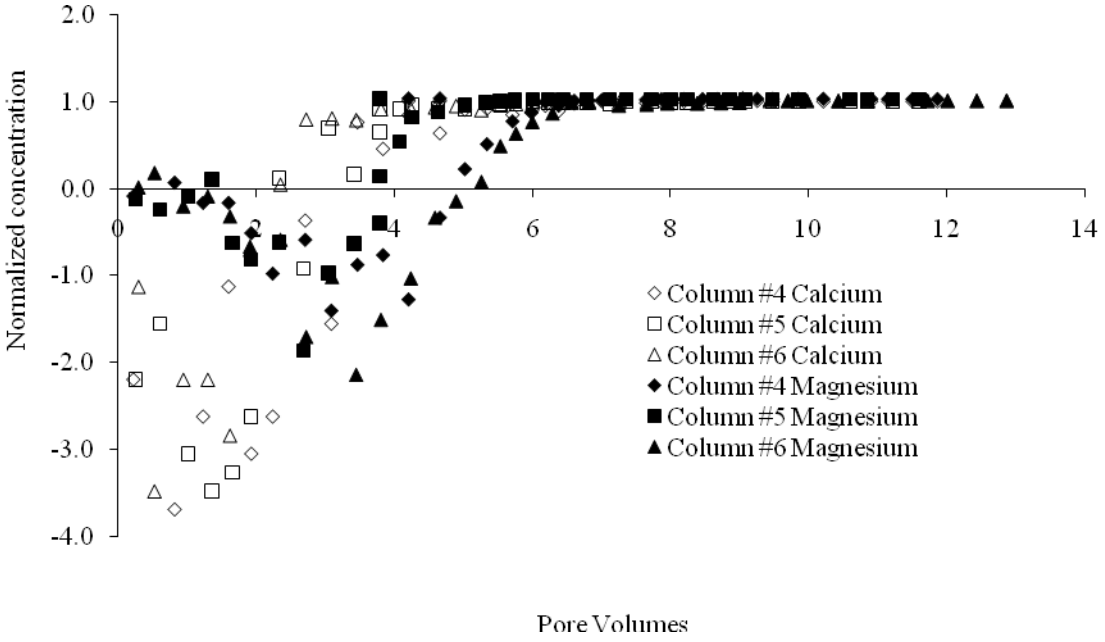

Figure 4.39. Site 2 magnesium breakthrough curve comparted to the calcium breakthrough curve during the simulated contaminant flushing stage.

4.6.8 Sulphate

The column breakthrough curves for SO_4^{2-} are shown in Figures 4.40 and 4.41 for Sites 1 and 2, respectively. Sulphate transport through the column is unattenuated for both soils.

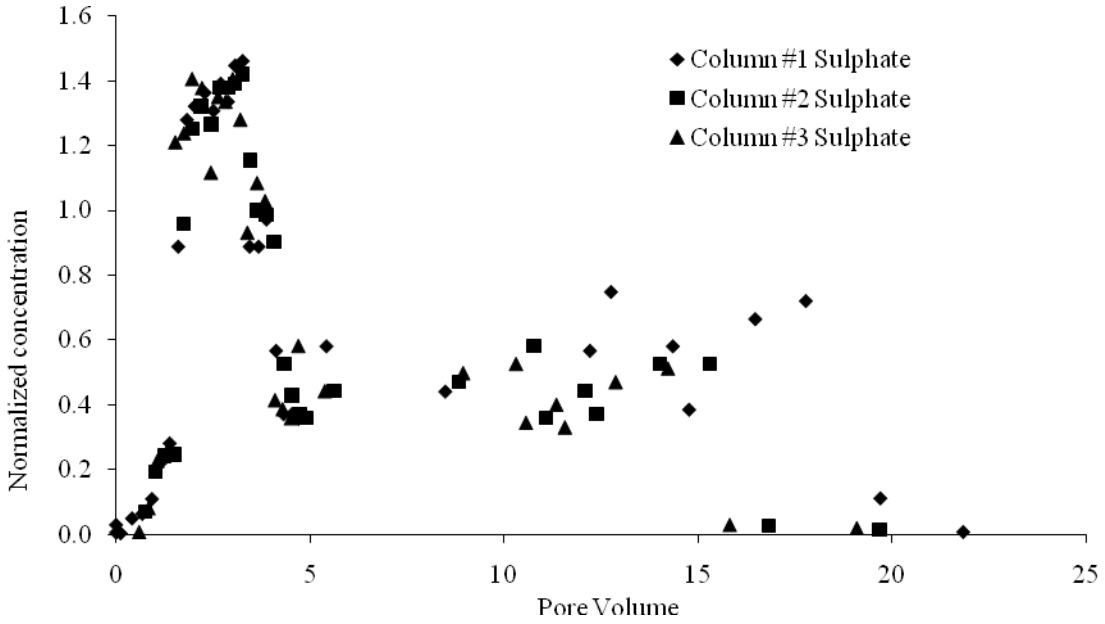

Figure 4.40. Site 1 column breakthrough curve for sulphate during simulated contaminant flushing stage.

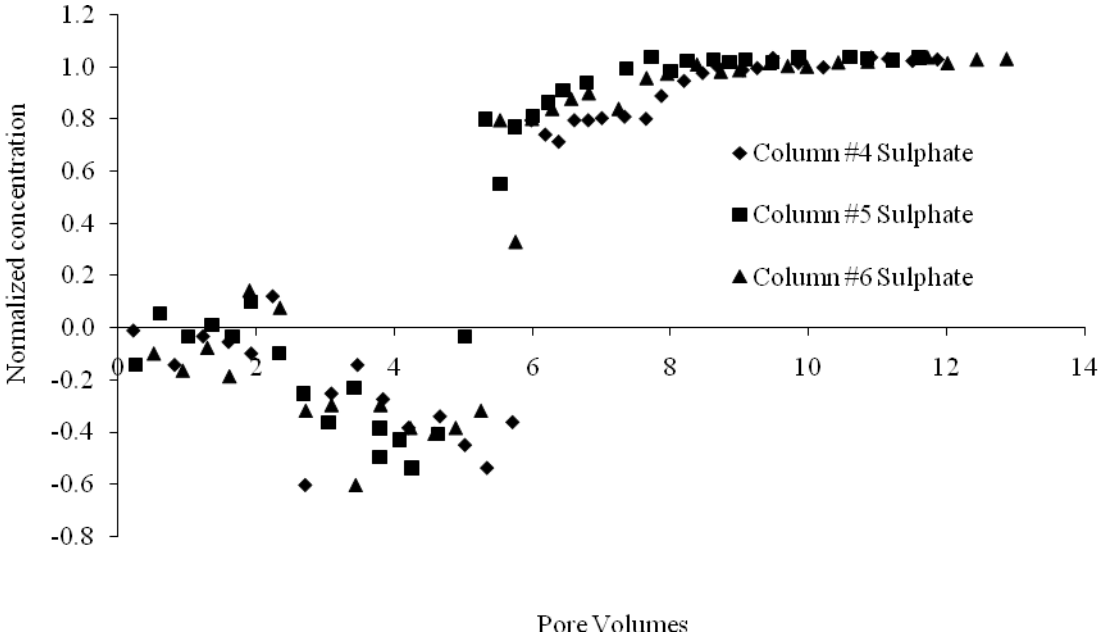

Figure 4.41. Site 2 column breakthrough curve for sulphate during simulated contaminant flushing stage.

For Site 1, SO_4^{2-} periodically reaches concentrations higher than the simulated contaminant. This period of SO_4^{2-} concentrations with C/C_0 greater than one coincide with the peak of Mg^{2+}. Dissolution of gypsum that occurs naturally in the soil may cause the concentration of SO_4^{2-} to exceed of the simulated contaminant. After approximately four pore volumes, SO_4^{2-} concentrations remained below in put levels, suggesting that it is controlled by mineral phase precipitation and/or biological processes (Thornton et al. 2000).

During column studies eluted with sea water Gomis-Yagues (1997) observed calcium sulphate precipitation. High concentrations of Ca^{2+} and SO_4^{2-} in the first stages of intrusion produce precipitation of gypsum. Its subsequent dissolution causes the concentration of SO_4^{2-} to be

higher than C_0. This does not appear to be the case because gypsum is undersaturated, as shown in Figure 4.42.

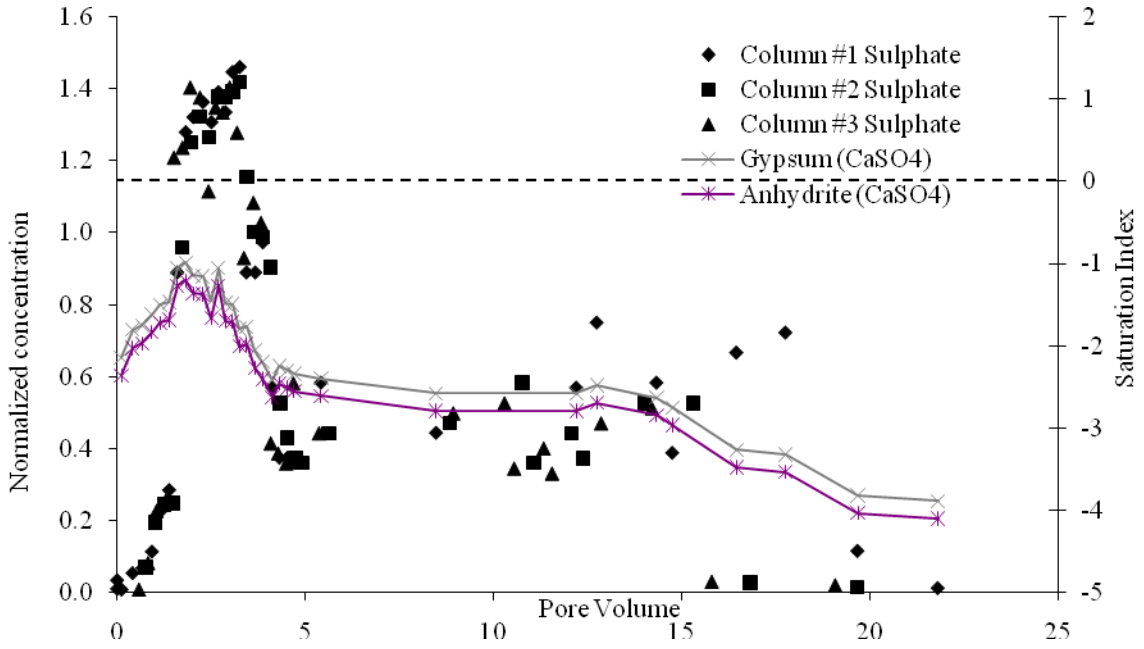

Figure 4.42. Site 1 column breakthrough curve for sulphate compared to saturation indices for gypsum and anhydrite.

After five pore volumes, SO_4^{2-} concentrations decrease to less than the simulated contaminant concentrations which may be due to SO_4^{2-} reduction. Black precipitates were visibly evident in the columns which could possibly be black precipitates of iron sulfide by SO_4^{2-} reducing bacteria (Thorton et al. 2000).

For Site 2 soil and freshwater, SO_4^{2-} behavior is approached differently. The concentration of SO_4^{2-} in the freshwater (4,200 mg/L) is higher than in the simulated contaminant (560 mg/L). The normalized concentration for SO_4^{2-} is negative for approximately five pore volumes. This is

because the effluent leaving the column has a higher SO_4^{2-} concentration than the freshwater. Eventually, the SO_4^{2-} concentration in the effluent decreases and approaches a normalized concentration of 1 (or the concentration of SO_4^{2-} in the simulated contaminant). The initial concentration of SO_4^{2-} that are higher then the freshwater SO_4^{2-} concentration could be caused by the dissolution of gypsum in the soil.

4.7 Freshwater Flushing Stage

The freshwater flushing stage started on September 15, 2005 for the Site 1 columns and on November 28, 2005 for the Site 2 columns. In continued until May 15, 2006 for columns 2 and 4, respectively, until December 12, 2005 for column 3 and until April 4, 2006 for column 6.

During the freshwater flushing stage (Figure 4.43), the flowrate initially decreased and then recovered to a stable flowrate.

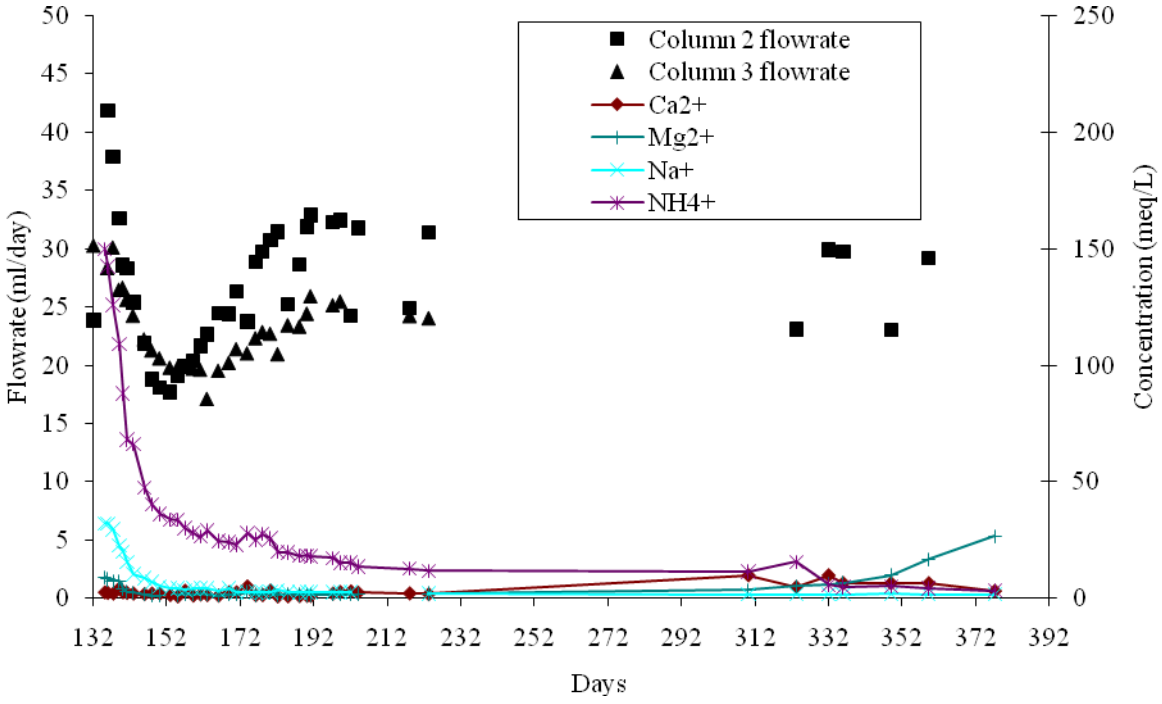

Figure 4.43. Site 1 flowrate during freshwater flushing stage.

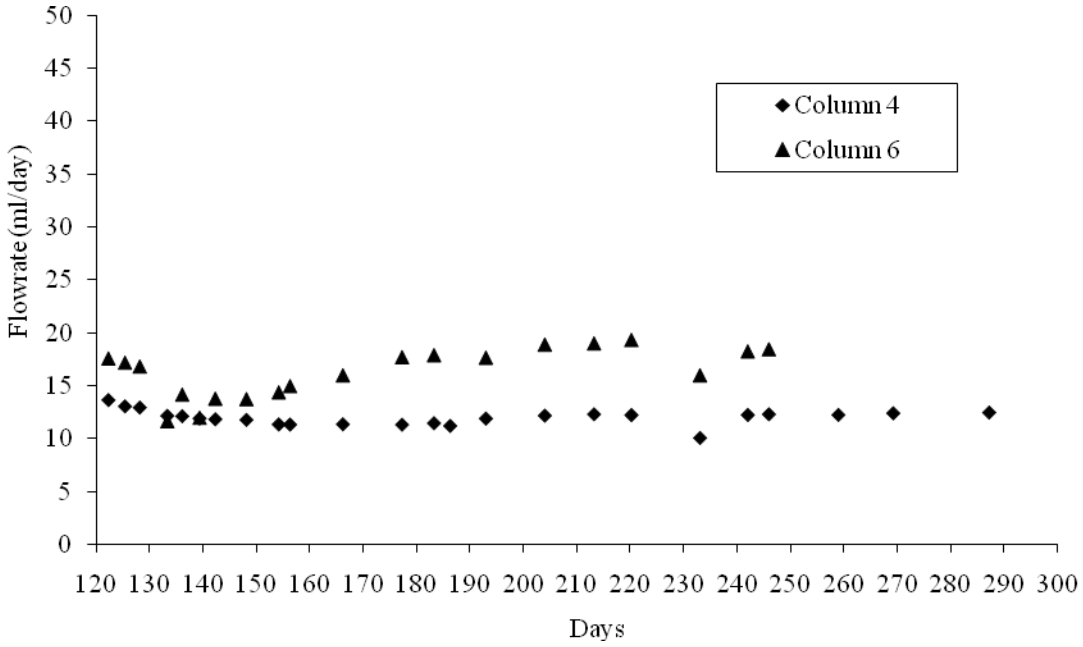

Figure 4.44. Site 2 flowrate during the freshwater flushing stage.

During the fresh water flushing stage, the high ionic strength simulated contaminanqt is replaced by the lower ionic strength freshwater. This is comparable to Barbour and Yang (1993) when the pore fluid of a sample prepared with brine is replaced by distilled water. They found that the "decrease in concentration causes a reduction in the shear strength between the soil aggregates. This resulted in an initial "collapse" of the soil structure and an increase in compressibility." The compression of the soil sample causes an additional decrease in hydraulic conductivity. Eventually, expansion of the diffuse double layers leads to an increase in repulsive force between soil aggregates, the clay particles separate and a larger area is available to flow. This causes an overall increase in hydraulic conductivity.

The Site 2 soil experienced a decrease in flowrate during the simulated contaminant flushing stage but the hydraulic conductivity of the soil did not recover (Figure 4.44) during the freshwater flushing stage. Site 1 soil contains 9% clay and the Site 2 soil contained 30% clay. The lower amount of clay in Site 1 soil allowed Site 1 soil to be more dynamic than the till from Site 2 and the hydraulic conductivity could recover. For Site 2 it is postulated that the high clay content of the soil caused pore blockages when the soil dispersed in the freshwater flushing stage and the hydraulic conductivity was unable to recover.

4.8 Solute Breakthrough Profiles during the Freshwater Flushing Stage

The mass balance for each column during the freshwater flushing stage are shown in Tables 4.11 and 4.12. Negative numbers indicate mass of solutes retained in the column, while positive numbers indicate solutes released from the columns. The total quantity of retained cations is greater than the total available CEC of the columns and the total quantity of released cations is less than the total available CEC of the columns. This discrepancy is related to a number of factors. These factors are discussed further when the breakthrough curve for each solute is presented separately in the next section.

The mass balance shows that the fraction of cations sorbed from the leachate is comparable with the column CEC.

Table 4.11. Site 1 mass balance during the freshwater flushing stage.

	Column #2 meq/100g	Column #3 meq/100g	average meq/100g

chloride	4.9	2.6	**3.8**
ammonia	9.9	6.6	**8.3**
sodium	0.8	0.6	**0.7**
potassium	1.7	1.1	**1.4**
sulphate	-0.3	-0.3	**-0.3**
calcium	-3.6	-1.9	**-2.8**
bicarbonate	6.7	5.8	**6.2**
magnesium	-2.2	-1.4	**-1.8**
TOTAL CATIONS RELEASED	**9.2**	**8.7**	**8.5**
TOTAL CATIONS RETAINED	**-15.5**	**-15.6**	**-14.9**

Table 4.12. Site 2 mass balance during the freshwater flushing stage.

	Column #4 meq/100g	Column #6 meq/100g	average meq/100g
chloride	0.9	0.9	**0.9**
ammonia	8.3	7.1	**7.7**
sodium	0.5	0.6	**0.5**
potassium	-3.1	1.6	**-0.8**
sulphate	4.4	0.9	**2.7**
calcium	-10.7	-12.3	**-11.5**
bicarbonate	1.2	0.6	**0.9**
magnesium	-5.4	-6.7	**-6.1**
TOTAL CATIONS RELEASED	**8.8**	**9.2**	**9.0**
TOTAL CATIONS RETAINED	**-19.2**	**-19.0**	**-19.1**

4.8.1 Chloride

Chloride breakthrough data for Site 1 is shown in Figure 4.45. The advection dispersion equation was used to estimate an attenuation factor for Cl^- of 1 (Figure 4.46). This is expected because Cl^- is a non-reactive ion and should travel through the soil unattenuated. In the simulated contaminant flushing stage, Cl^- was attenuated due to Cl^- being held back in the soil to achieve a charge balance with the high concentration of cations taking part in cation exchange reactions and dilution of pore water due to osmotic flow.

Compared to the simulated contaminant flushing stage, the coefficient of hydrodynamic dispersion higher resulting in a Peclet number of 1.6 compared to 15. Lower Peclet numbers occur with higher coefficient of hydrodynamic dispersion which is caused by higher velocities and/or longer flow paths (Fetter 1999).

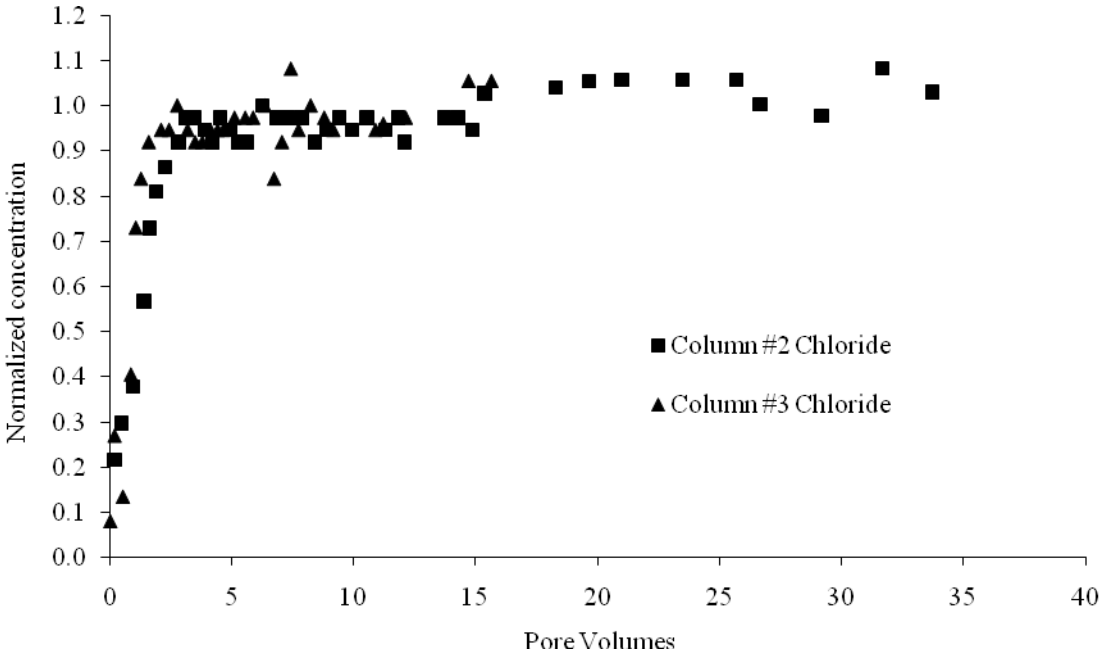

Figure 4.45. Site 1 column breakthrough curve for chloride during the freshwater flushing stage.

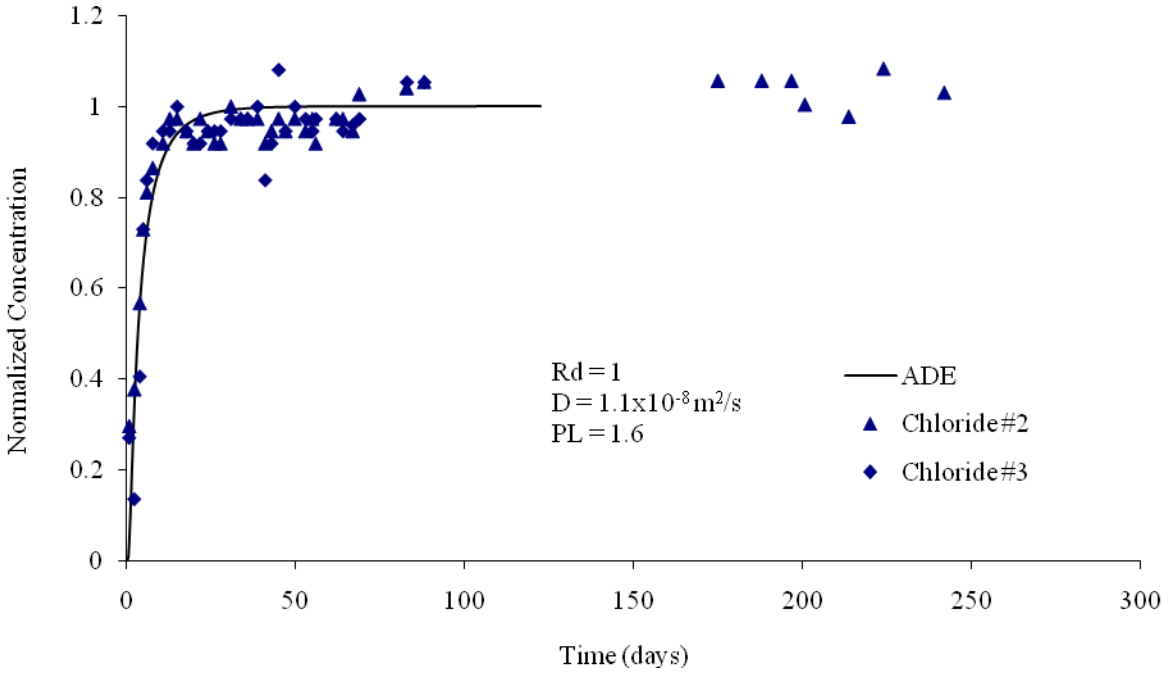

Figure 4.46. Site 1 advection dispersion equation curve fitting for chloride breakthrough during freshwater flushing stage.

The chloride breakthrough curve for Site 2 is shown in Figure 4.47. The advection dispersion equation was used to estimate the attenuation factor for Cl^- which was 0.7. (Figure 4.48). The breakthrough of Cl^- occurs early because the velocity of liquid in the moble region increases when the volume of the stagnant zone is inaccessible. (Appelo and Postma 2005) The hydrodynamic dispersion coefficient increases and the Peclet number decreases.

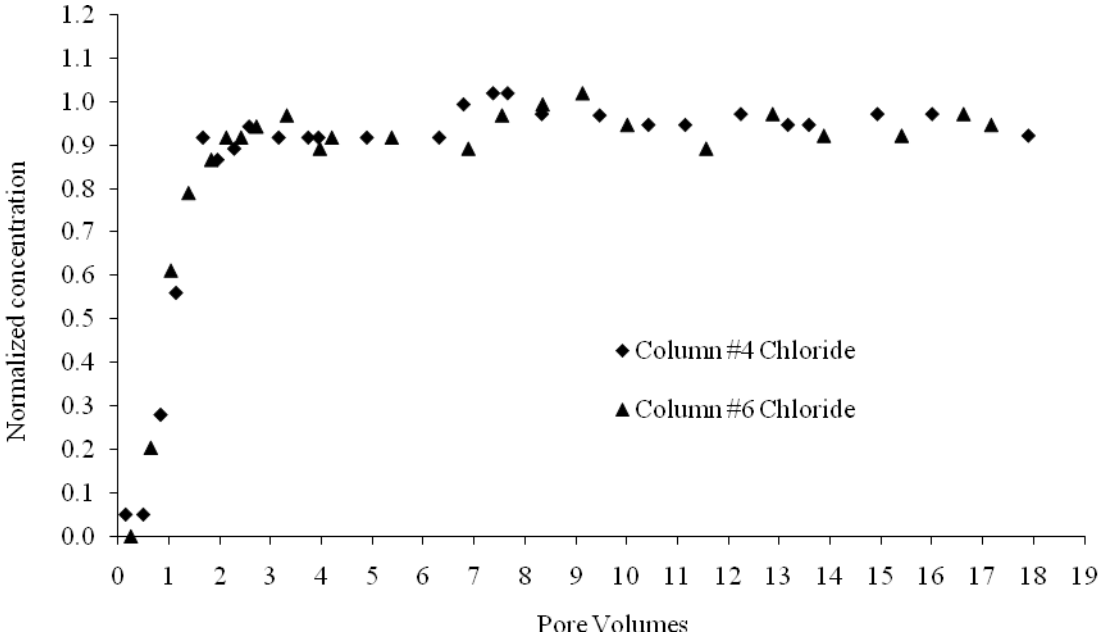

Figure 4.47. Site 2 column breakthrough curve for chloride during the freshwater flushing stage.

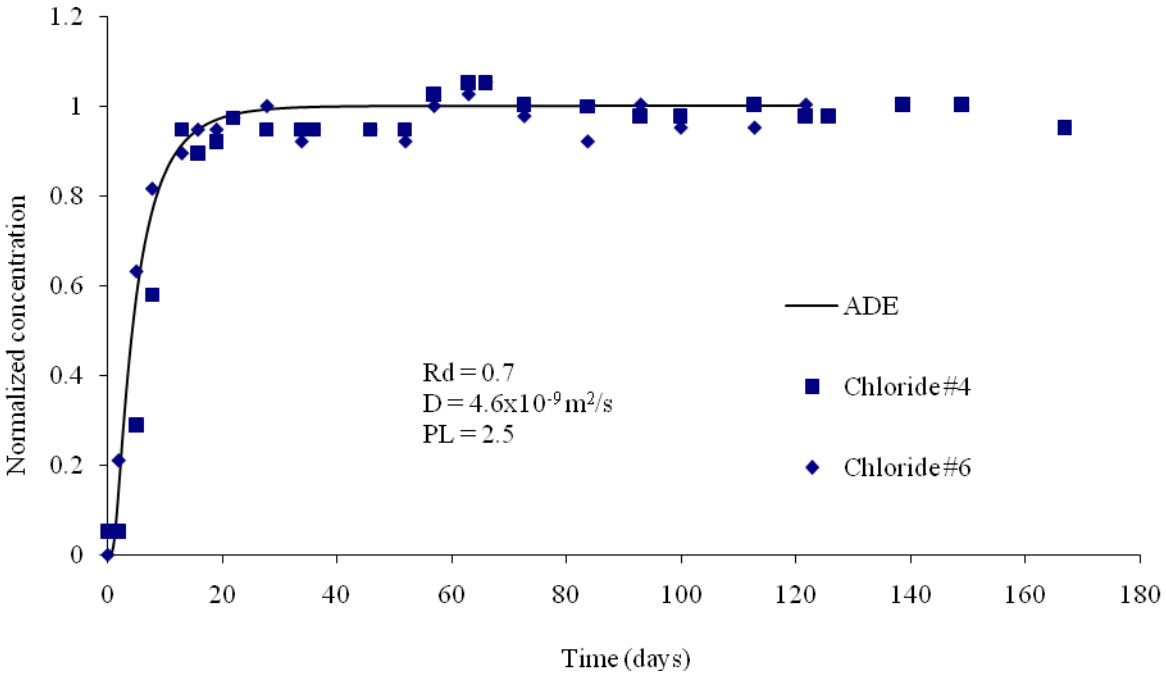

Figure 4.48. Site 2 advection dispersion equation curve fitting for chloride breakthrough during freshwater flushing stage.

4.8.2 Ammonium

Figures 4.49 and 4.50 show the NH_4^+ breakthrough curve during the freshwater flushing stage for Site 1 and Site 2, respectively. Ammonium is released from Site 1 soil exchange sites with an attenuation factor of 4.3 and 2.5 for Sites 1 and 2, respectively. Ammonium was replaced on the soil exchange sites by the Ca^{2+} and Mg^{2+} in the native groundwater. This suggests that replacement of native cations by NH_4^+ was a mass action effect because flushing with NH_4^+ free groundwater resulted in desorption of NH_4^+ and K^+. According the mass balance, the amount of NH_4^+ released from the Site 1 soil exchange sites was 75% and 55 % from columns #2 and #3, respectively. The CEC analysis resulted in 77% of NH_4^+ being released from the soil. The experiments did not proceed long enough to allow all of NH_4^+ to be released from the soil but the

extensive tailing in the breakthrough curve suggests that NH_4^+ is still being replaced on the soil exchange sites for both Site 1 and Site 2 soils.

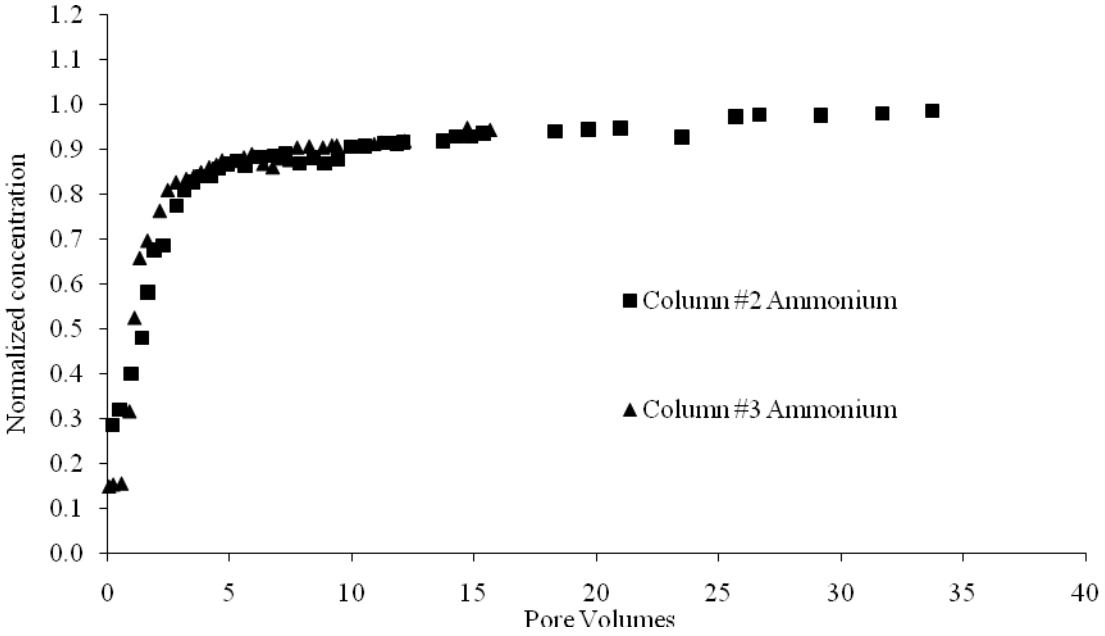

Figure 4.49. Site 1 column breakthrough curve for ammonium during the freshwater flushing stage.

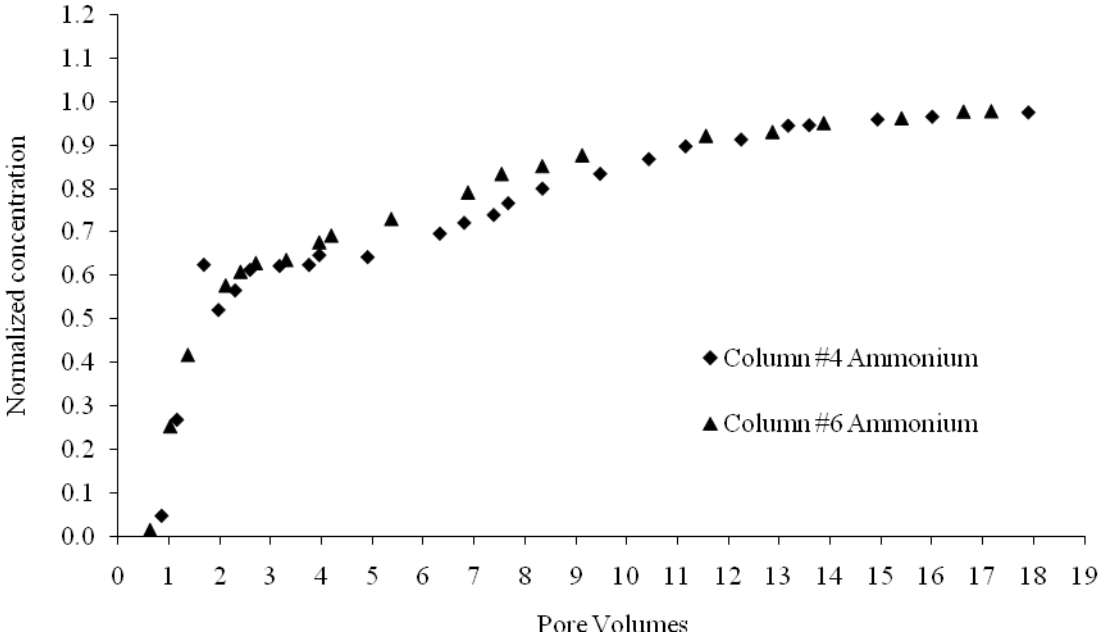

Figure 4.50. Site 2 column breakthrough curve for ammonium during the freshwater flushing stage.

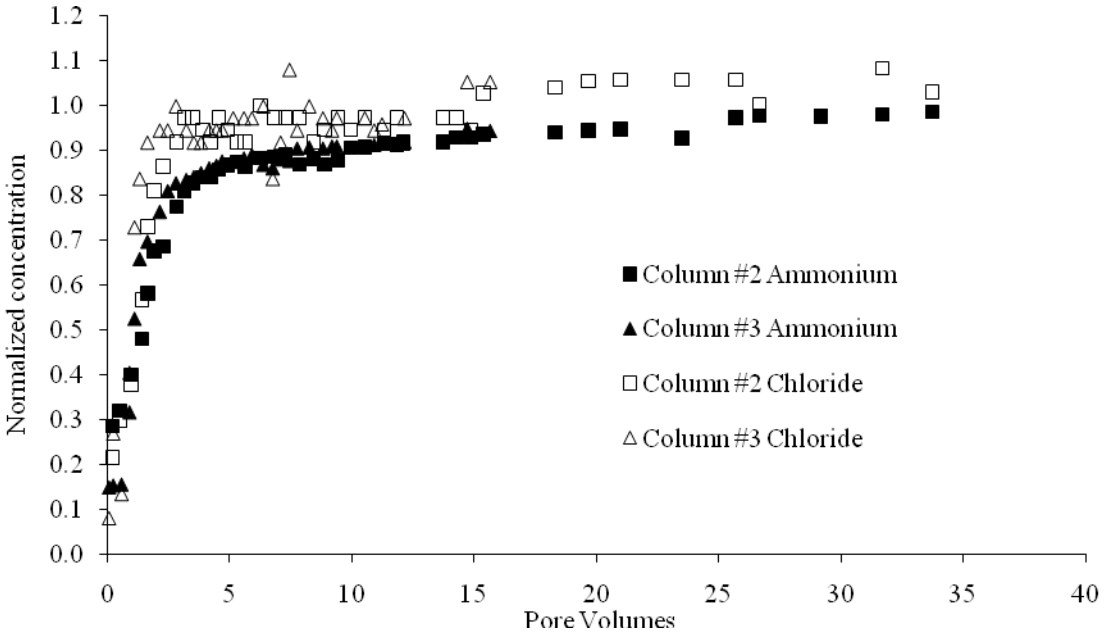

Figure 4.51. Site 1 column breakthrough curve for ammonium compared to the column breakthrough curve for Cl^-.

When compared to the Cl^- breakthrough curve (Figure 4.51), NH_4^+ is initially released at the same rate as unreative Cl^- ions travel through the column. After approximately two pore volumes, the rate of NH_4^+ release decreases. This could be due to the remaining NH_4^+ being adsorbed inter-layers of the clay where it is harder for Ca^{2+} and Mg^{2+} (with a larger hydrated radius) to replace NH_4^+. Ca^{2+} is effective in extracting the NH_4^+ present within the clay structure due to its ability to expand the clay interlayers (Allison et al. 1953).

4.8.3 Potassium

The column breakthrough curve for K^+ is shown in Figures 4.52 and 4.53 for Sites 1 and 2, respectively. Potassium is released from Site 1 soil exchange sites with an attenuation factor of 1.4 and 2.5 for Sites 1 and 2, respectively.

For Site 1, this indicates that K^+ on the soil exchange sites was more easily replaced than NH_4^+. The column breakthrough curves for K^+ do not exhibit the extent of tailing as the NH_4^+ breakthrough curve. According to the mass balance, the amount of K^+ released from the soil exhange site was 80% and 50 % from columns #2 and #3 respectively. The CEC analysis (saturated paste) results in 66% of K^+ being released from the soil.

For Site 2, NH_4^+ and K^+ were released at the same rate and K^+ exhibits extensive tailing.

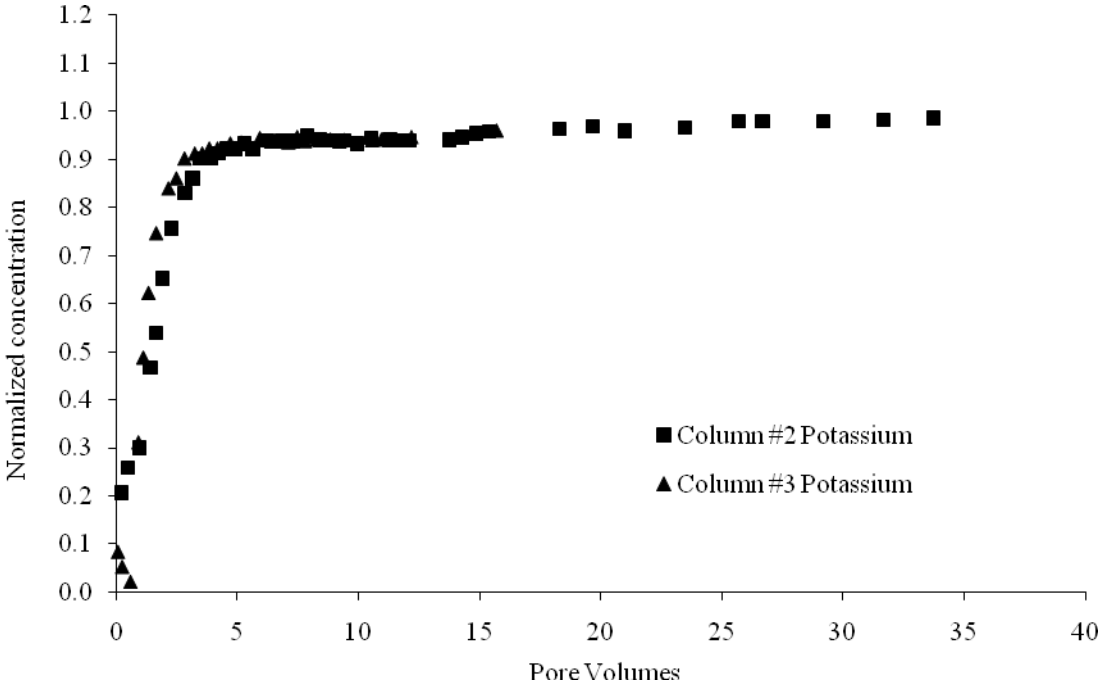

Figure 4.52. Site 1 column breakthrough curve for potassium during freshwater flushing stage.

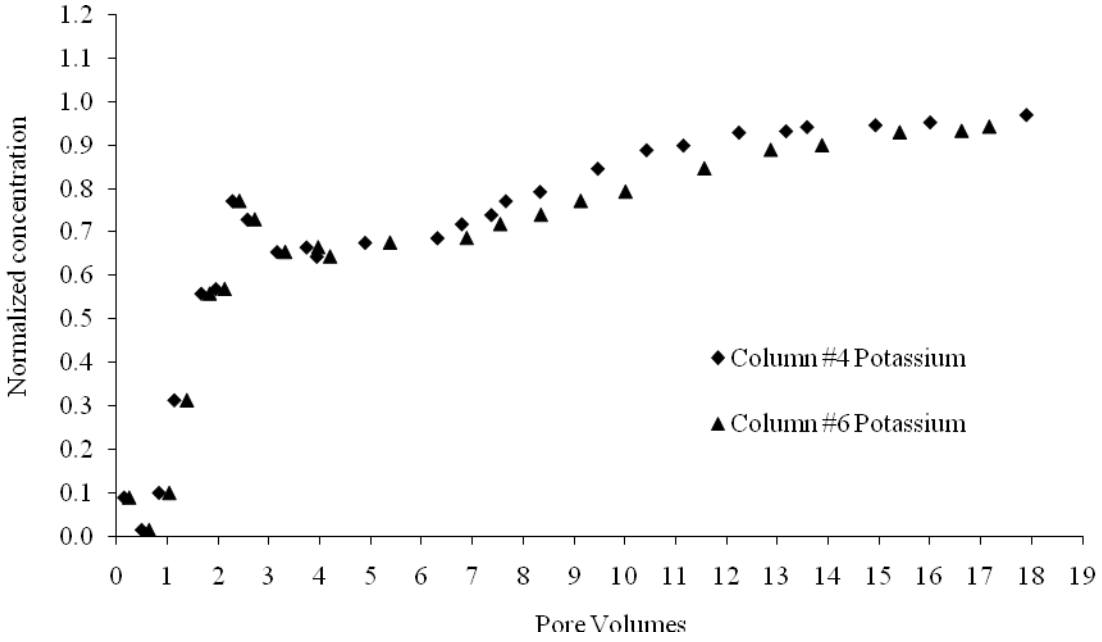

Figure 4.53. Site 2 column breakthrough curve for potassium during the freshwater flushing stage.

4.8.4 Magnesium

The Site 1 column breakthrough curve for Mg^{2+} is shown in Figure 4.54. The normalized concentration numbers are negative because the concentration of Mg^{2+} leaving the column is less than the concentration of Mg^{2+} that was initially in the soil pore water at the stage of the freshwater flushing stage. Magnesium concentrations are less than column influent because Mg^{2+} is effective at replacing NH_4^+ and K^+ on the soil exchange sites. After 20 pore volumes passed through the column, Mg^{2+} concentrations surpassed column influent concentrations. The saturation indices for huntite and magnesium carbonates past 20 pore volumes indicate that these minerals are undersaturated; therefore, it will be thermodynamically possible for them to

dissolve. The Mg^{2+} and Ca^{2+} carbonate minerals precipitated during the simulated contaminant flushing stage could now be dissolving as the ionic strength of the solution decreases.

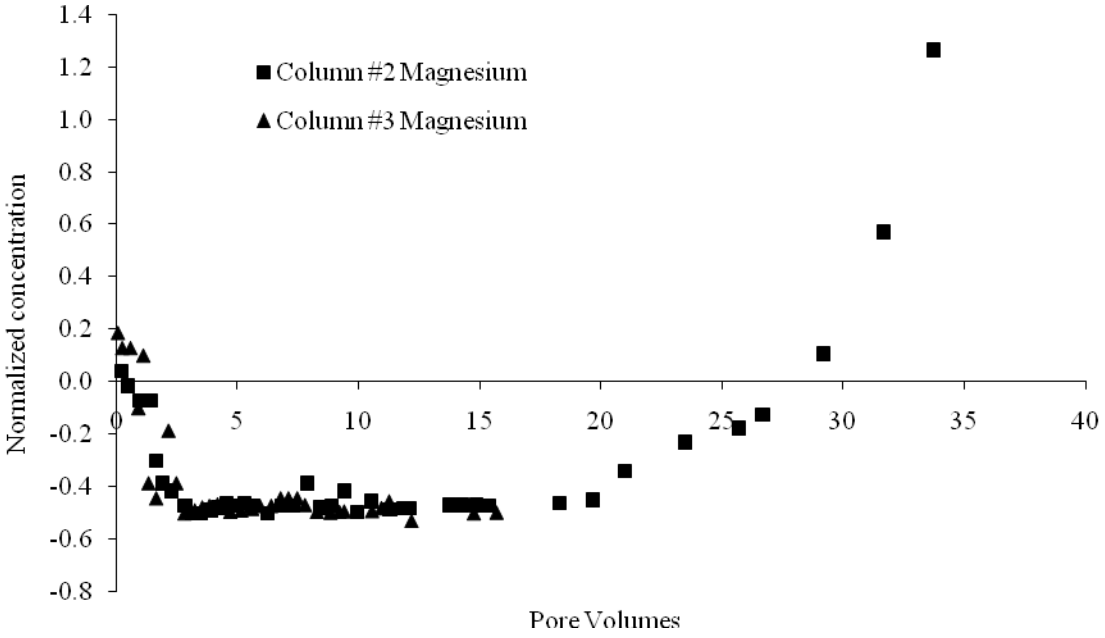

Figure 4.54. Site 1 column breakthrough curve for magnesium during freshwater flushing stage.

For Site 1, an average of 0.9 meq/100g of Mg^{2+} was retained in the soil column. The CEC analysis shows that 1.6 meq/100 g of Mg^{2+} was retained in the soil column. After 35 pore volumes, attenuation of Mg^{2+} appears to be exhausted.

The Site 2 column breakthrough curve for Mg^{2+} is shown in Figure 4.55. For Site 2 soil, Mg^{2+} attenuation is exhausted after approximately 12 pore volumes, at the same point where NH_4^+ concentrations in the column effluent start to decline significantly. According to the mass

balance an average of 6.1 meq/100 g of Mg^{2+} was retained in the soil column. This agrees closely with the CEC analysis which gives 5.6 meq/100 g of Mg^{2+} retained in the soil columns.

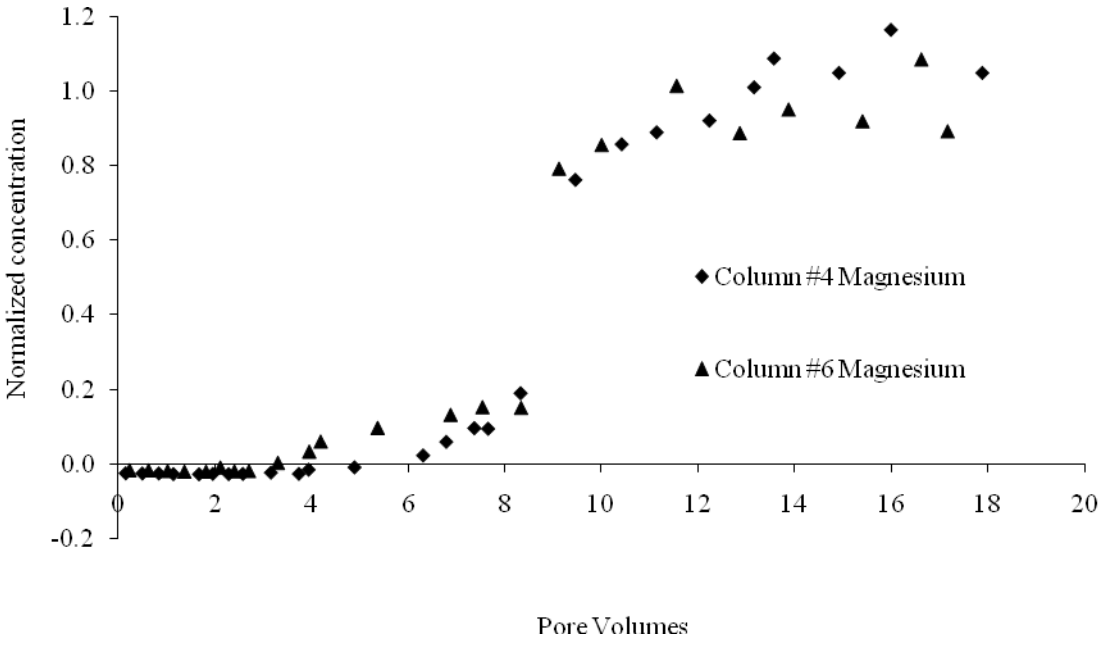

Figure 4.55. Site 2 column breakthrough curve for magnesium during the freshwater flushing stage.

4.8.5 Calcium

The Site 1 column breakthrough curve for Ca^{2+} is shown in Figure 4.56. Calcium concentrations are less than column influent because Ca^{2+} is effective at replacing NH_4^+ and K^+ on the soil exchange sites. After 20 pore volumes passed through the column, Ca^{2+} concentrations start to rise but do not reach original freshwater concentrations by the end of the test. The incomplete

breakthrough curve for NH_4^+ shows that Ca^{2+} is still replacing NH_4^+ on the soil exchange sites. Even though magnesium carbonates are undersaturated near the end of the tests, the saturation indices for calcium carbonates remain above zero (Figure 4.57). Calcium is still replacing NH_4^+ and K^+ on the exchange sites and has become more effective than Mg^{2+} after 20 PV. The mass balance shows that more NH_4^+ and K were released than Ca^{2+} and Mg^{2+} adsorbed. This number is not the same because of the dissolution of calcium and magnesium carbonates.

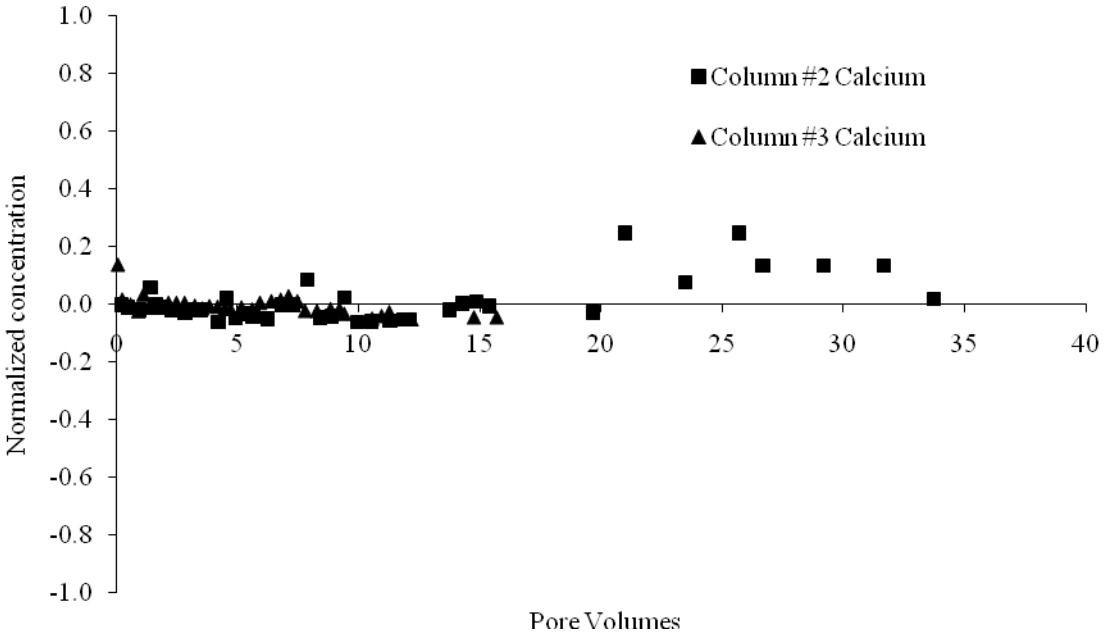

Figure 4.56. Site 1 column breakthrough curve for calcium during the freshwater flushing stage.

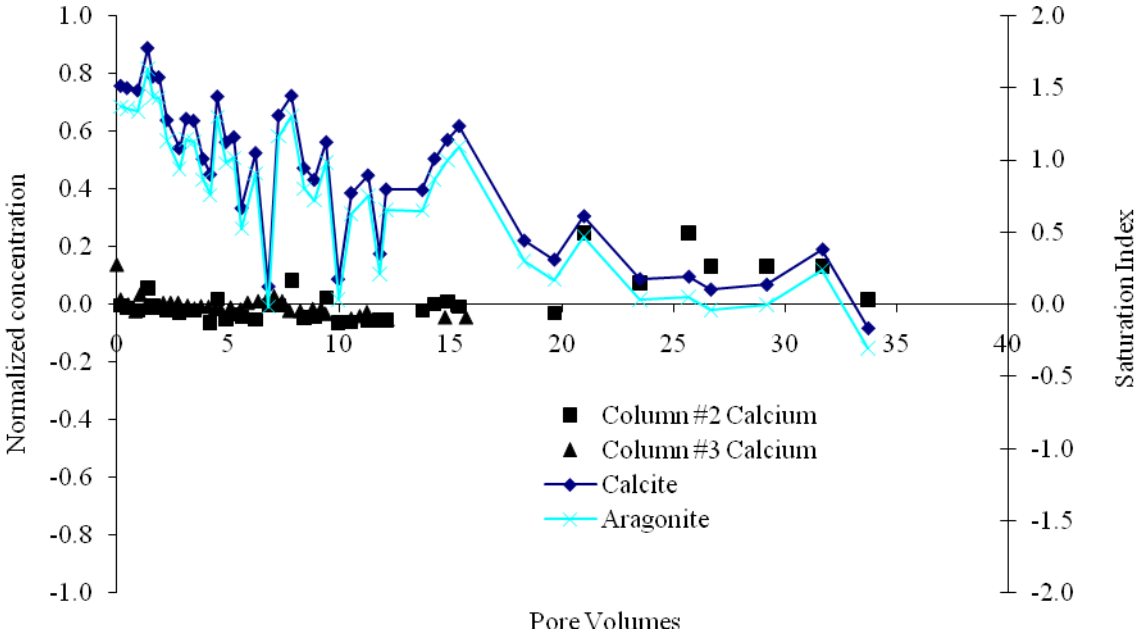

Figure 4.57. Site 1 column breakthrough curve for calcium compared to saturation indices for calcium carbonates.

The Site 2 column breakthrough curve for Ca^{2+} is shown in Figure 4.58. For Site 2, Ca^{2+} is attenuated by a factor of 9.5 (Figure 4.59). This shows that Ca^{2+} is slightly more effective at replacing K^+ and NH_4^+ than Mg^{2+} which was attenuated by a factor of 8.

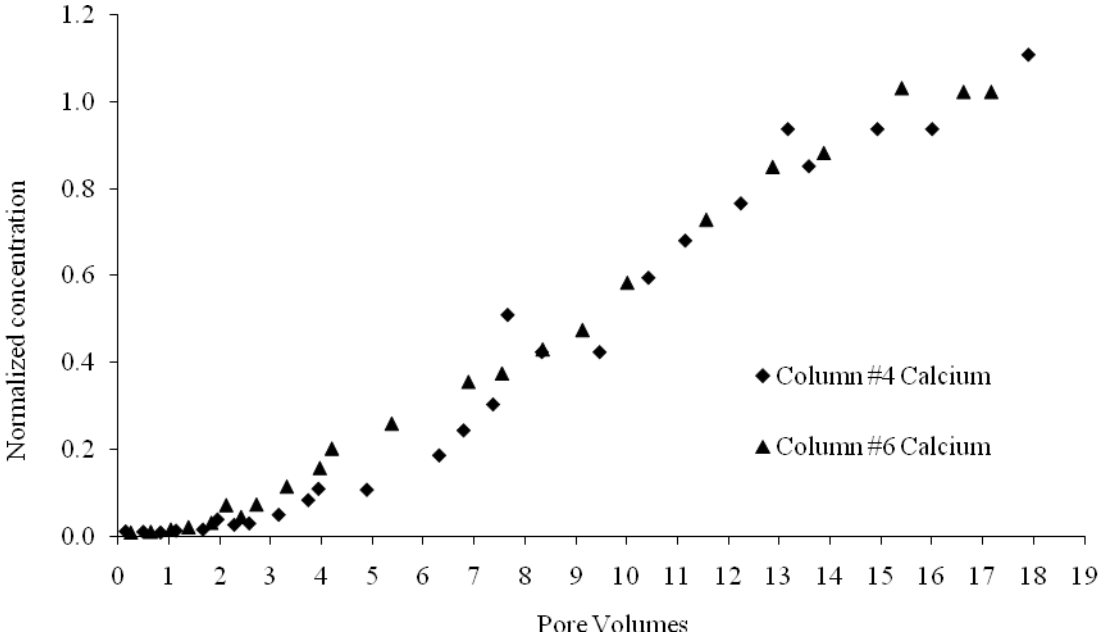

Figure 4.58. Site 2 column breakthrough curve for calcium during the freshwater flushing stage.

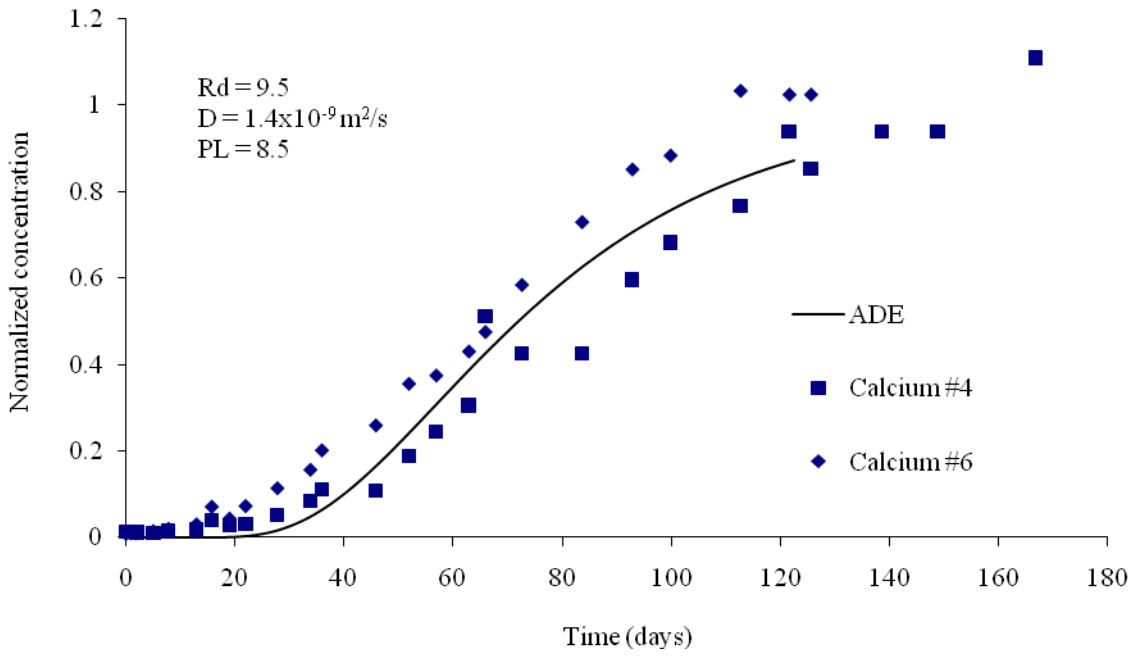

Figure 4.59. Site 2 advection dispersion curve fitting for calcium during the freshwater flushing stage.

4.8.6 Bicarbonate

The Site 1 column breakthrough curve for HCO_3^- is shown in Figure 4.60. The breakthrough of HCO_3^- is attenuated with respect to Cl^- breakthrough by a factor of 2.5 (Figure 4.61). This suggests the HCO_3^- is actively participating in mineral precipitation and dissolution reactions. It is likely that magnesium and calcium bicarbonates are precipitating near the beginning of the freshwater flushing stage, but start to dissolve towards the end of the fresh water flushing stage.

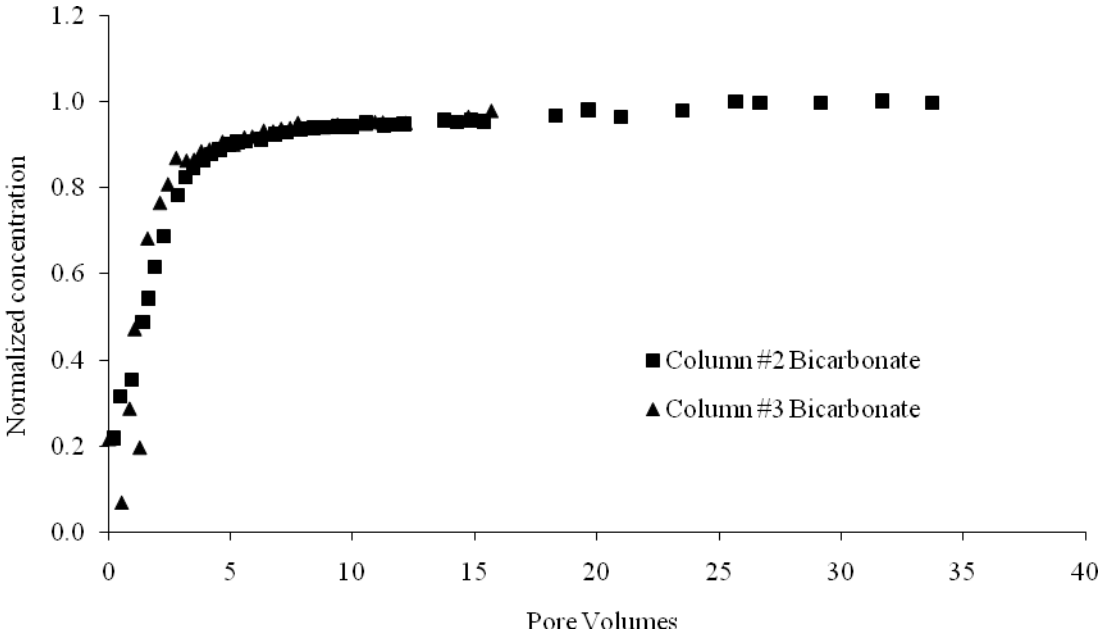

Figure 4.60. Site 1 column breakthrough curve for bicarbonate during freshwater flushing stage.

The mass balance shows that an average of 6.2 meq/100g of HCO_3^- exited the columns which did not enter the columns during the freshwater flushing stage. This further supports the theory of magnesium carbonate dissolution during the latter portion of the freshwater flushing stage. For column #1 there were 70 meq of NH_4^+ and K released from the soil and 24 meq of Ca and Mg^{2+} adsorbed onto the soil. The difference is 46 meq which is nearly equal to the extra 43 meq of HCO_3^- eluded from the column.

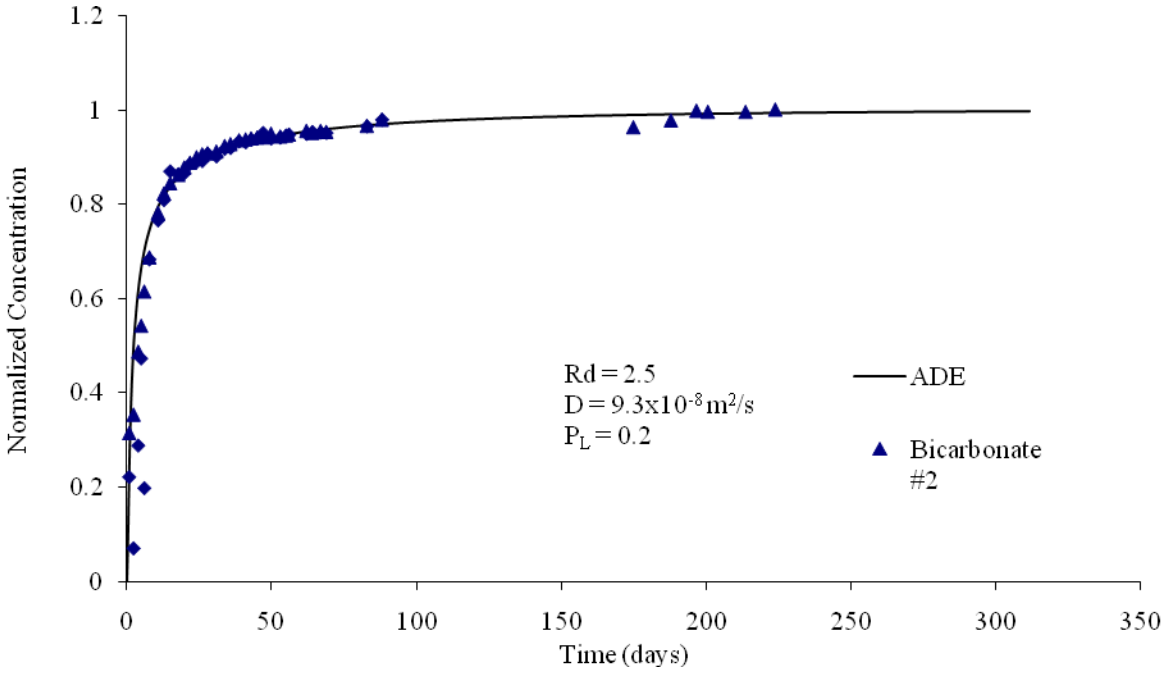

Figure 4.61. Site 1 advection dispersion curve fitting for bicarbonate during the freshwater flushing stage.

The Site 2 column breakthrough curve for HCO_3^- is shown in Figure 4.62. For Site 2, alkalinity broke through the column unattenuated (Figure 4.63), which indicates that mineral precipitation/dissolution reactions were not taking place.

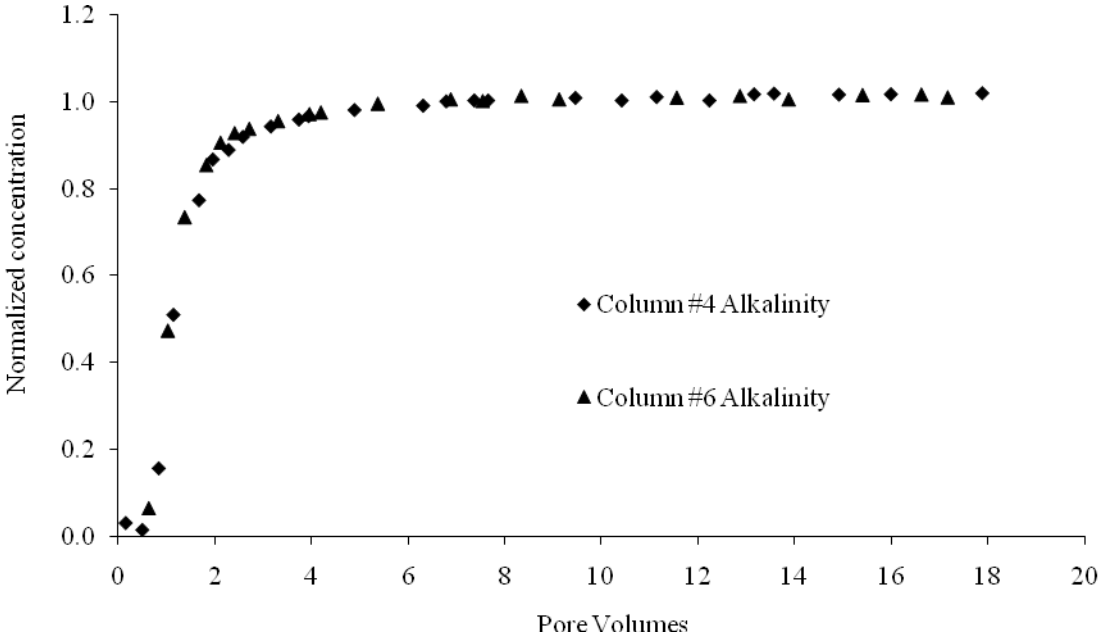

Figure 4.62. Site 2 column breakthrough curve for alkalinity during the freshwater flushing stage.

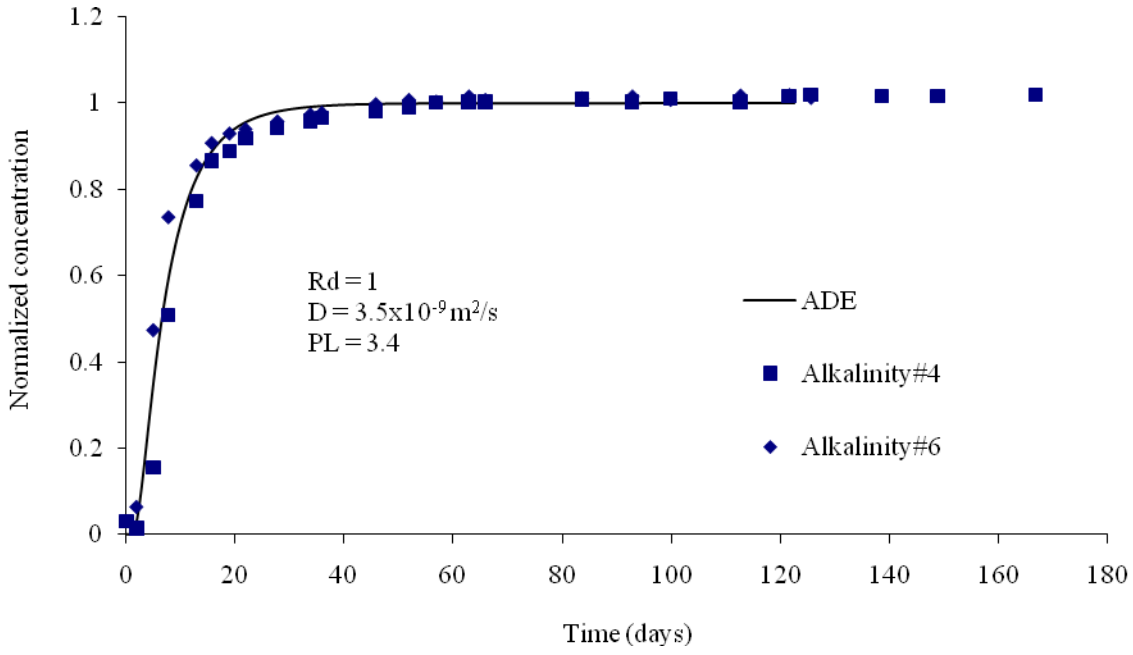

Figure 4.63. Site 2 advection dispersion curve fitting for alkalinity during the freshwater flushing stage.

4.8.7 Sulphate

The Site 1 column breakthrough curve for SO_4^{2-} is shown in Figure 4.64. Sulphate appears to breakthrough immediately at C/ C_0=1 at zero pore volumes. During the simulated contaminant flushing stage, it appeared the SO_4^{2-} reduction was taking place; therefore the concentration of SO_4^{2-} leaving the column at the end of the simulated contaminant stage was approximately the same concentration as SO_4^{2-} in the groundwater. 0.3 meq/100 g of SO_4^{2-} were retained in each column during the freshwater flushing stage (as opposed to 13 meq during simulated contaminant flushing stage); therefore, it appears that during the freshwater flushing stage SO_4^{2-} reduction ceased.

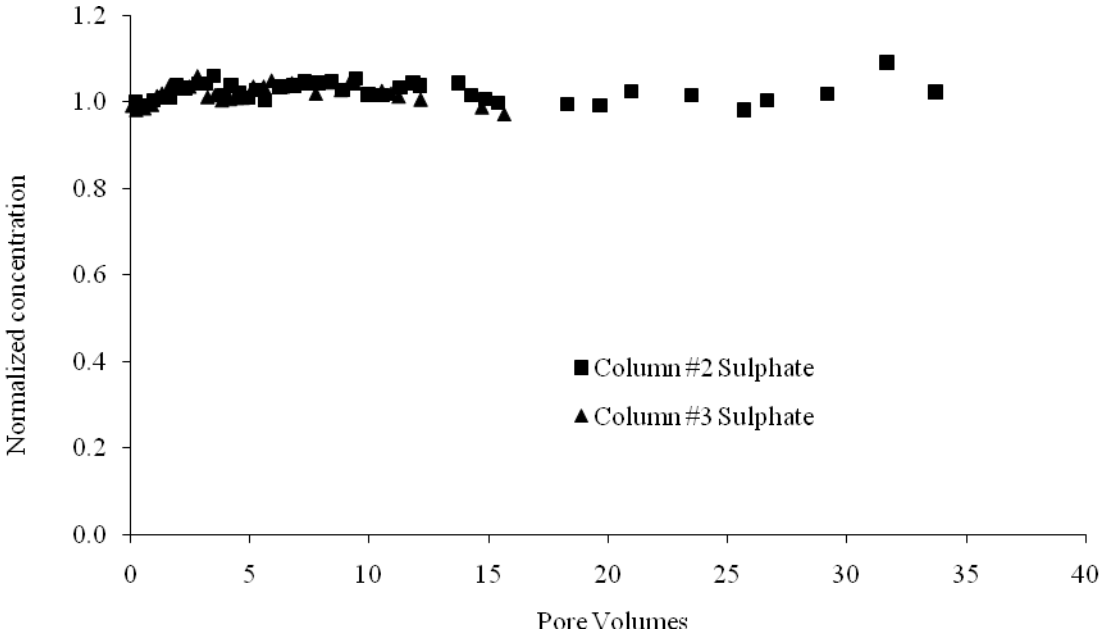

Figure 4.64. Site 1 column breakthrough curve for sulphate during the freshwater flushing stage.

The Site 2 column breakthrough curve for SO_4^{2-} is shown in Figure 4.65. Sulphate appears to breakthrough unattenuated. As mentioned in the simulated contaminant flushing stage, the concentration of SO_4^{2-} in the freshwater for Site 2 is greater than the concentration of SO_4^{2-} in the simulated contaminant so this is an increase in SO_4^{2-} concentration.

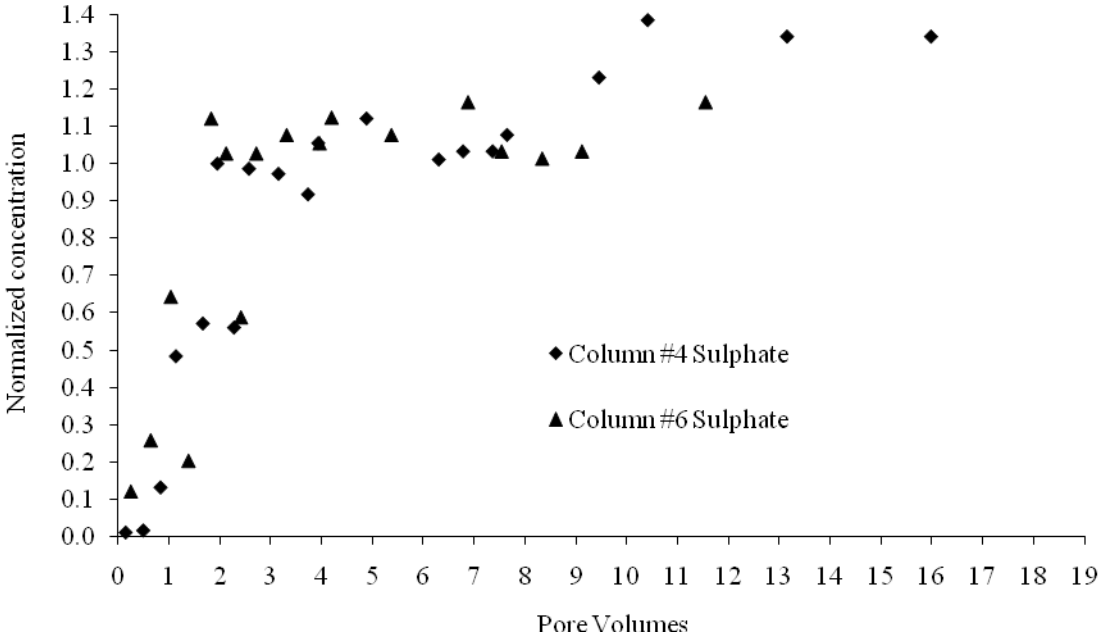

Figure 4.65. Site 2 column breakthrough curve for sulphate during the freshwater flushing stage.

4.8.8 Sodium

The Site 1 column breakthrough curve for Na^+ is shown in Figure 4.66. Sodium remained relatively unreactive and was attenuated by a factor of 1.4 (Figure 4.66). A mass balance on the column influent and effluent volumes and concentrations results in an average of 0.7 meq/100 g of Na^+ released from the cation exchange sites in each soil column. This number from the mass balance agrees with the CEC analysis completed on column #3 which was 0.35 meq/100 g.

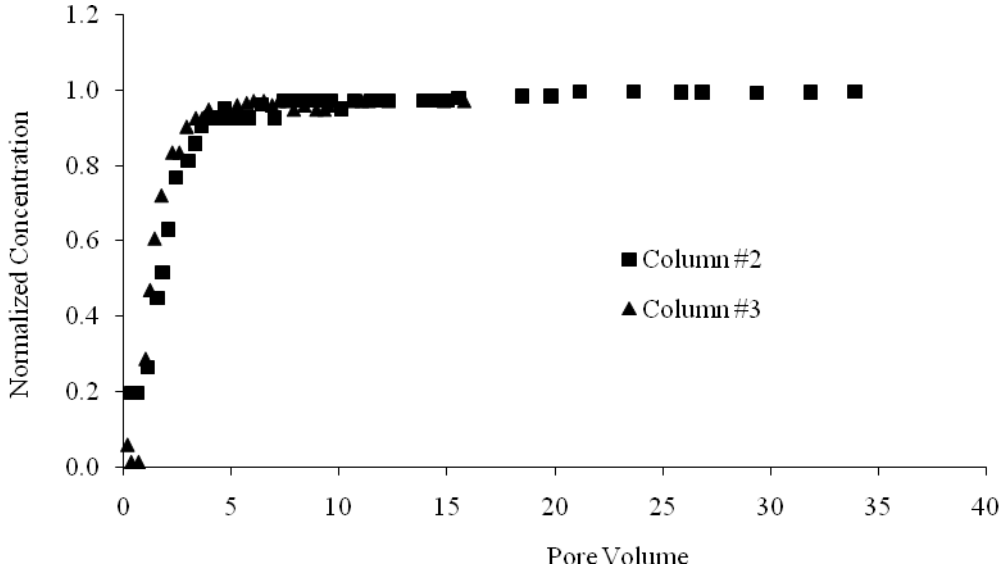

Figure 4.66. Site 1 column breakthrough curve for sodium during freshwater flushing stage.

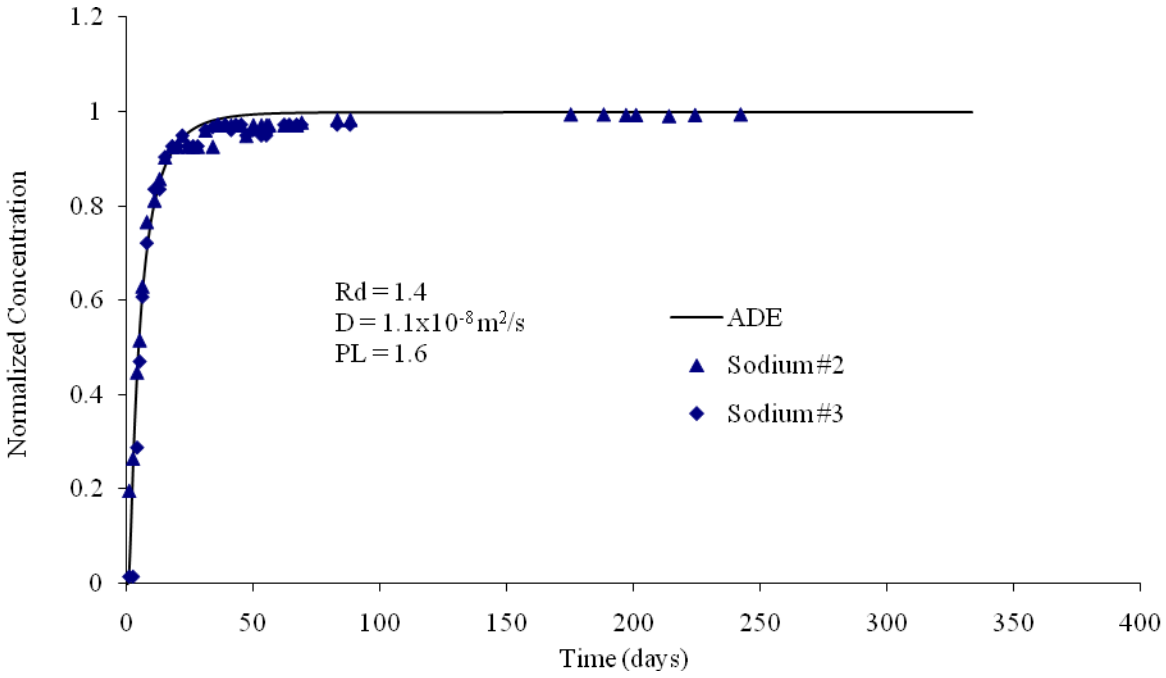

Figure 4.67. Site 1 advection dispersion curve fitting for sodium during freshwater flushing stage.

The Site 2 column breakthrough curve for Na^+ is shown in Figure 4.68. Sodium was attenuated by a factor of 1 (Figure 4.69), but the concentration decreased from 2 to 9 pore volumes, indicating that Na^+ was taking part in ion exchange reactions. According to the mass balance, 0.5 meq/100 g of Na^+ was released from the soil exchange sites. This number agrees closely with the CEC analysis of 0.6 meq/100 g.

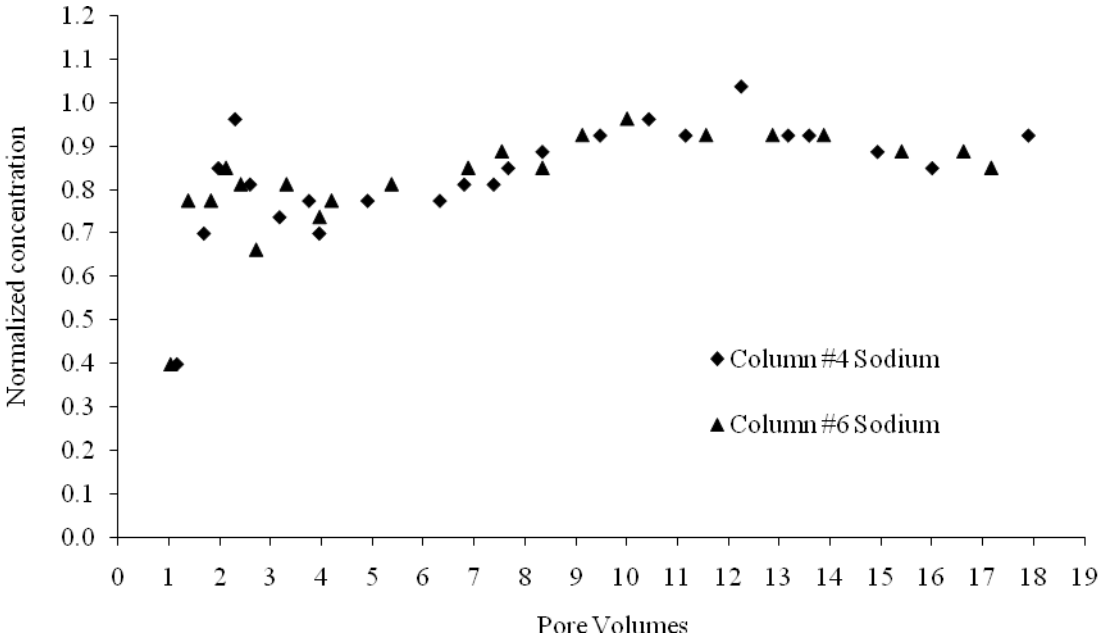

Figure 4.68. Site 2 column breakthrough curve for sodium during the freshwater flushing stage.

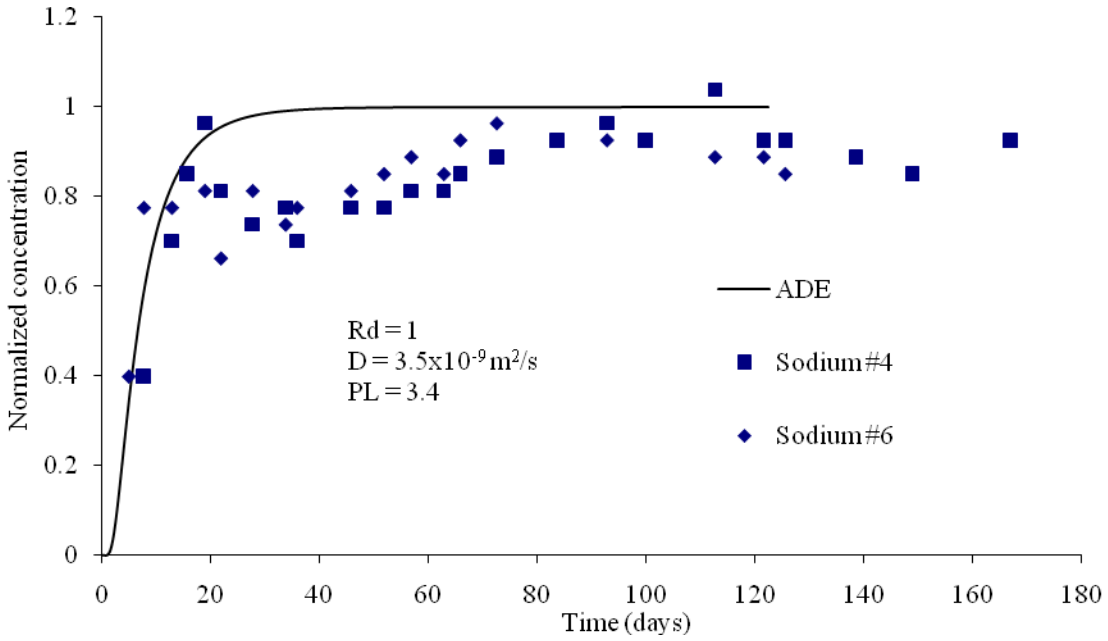

Figure 4.69. Site 2 advection dispersion curve fitting for sodium during the freshwater flushing stage.

4.9 Summary

This study has examined the attenuation and release of inorganic contaminants in laboratory columns containing clay soils from two earthen manure storage sites. Simple transport modeling, mass balance approaches and an aqueous speciation modeling has been used to indentify the important processes and geochemical properties which control the transport of key contaminants (NH_4^+ and K^+).

Attenuation of NH_4^+ and K^+ occurred by cation exchange with the clay in the soil during leaching with the simulated contaminant. This sorption is finite. The transport of these ions and other

cations in the leachate could be described by an analytical solution to the advection dispersion transport equation using attenuation factors (Table 4.13 and Table 4.14). Ammonium and K^+ were more strongly adsorbed than Na^+. The dissolution and precipitation of carbonates contributed to the transport mechanisms.

Mass balance calculation indicate that comparable amounts of NH_4^+ are adsorbed by the two different soils (Table 4.9 and 4.10). The fraction of cations adsorbed from the simulated contaminant is comparable with the CEC of the column, implying close to complete turnover of the soil exchange complex.

The clay structure of the soil was altered by chemical changes in the soil solution. During the simulated contaminant flushing stage the soil structure collapsed causing a decrease in flowrate or hydraulic conductivity of both soil types.

Table 4.13. Modeled transport parameters for Site 1 during the simulated contaminant flushing stage.

Constituent	Attenuation Factor, Rd	Hydrodynamic Dispersion, Hd (m^2/s)	Peclet Number
Cl^-	1.0	$2.3x10^{-9}$	9
NH_4^+	3.2	$4.6x10^{-10}$	45
K^+	3.2	$6.9x10^{-10}$	30
Na^+	1.6	$1.4x10^{-9}$	15
HCO_3^-	2.7	$2.0x10^{-9}$	7

Table 4.14. Modeled transport parameters for Site 2 during the simulated contaminant flushing stage.

Constituent	Attenuation Factor, Rd	Hydrodynamic Dispersion, Hd (m^2/s)	Peclet Number
Cl^-	2.1	$4.6x10^{-10}$	26
NH_4^+	6.0	$4.6x10^{-10}$	26
K^+	5.4	$4.6x10^{-10}$	26
Na^+	2.4	$4.6x10^{-10}$	26
HCO_3^-	6.0	$9.3x10^{-10}$	12

The freshwater flushing stage showed that attenuated inorganic contaminant may be mobilized from the soil during contact with freshwater. Flushing with NH_4^+ free freshwater easily liberated most of the adsorbed NH_4^+ and K^+. The elution of NH_4^+ and K^+ was accompanied by a decrease of Ca^{2+} and Mg^{2+}. This shows that these divalent ions in the freshwater displaced NH_4^+ and K^+ adsorbed onto the soil. The transport of these ions and other cations in the leachate could be described by an analytical solution to the advection dispersion transport equation using attenuation factors (Table 4.15 and Table 4.16)

Mass balance calculations showed that the milliequivalents of NH_4^+ and K^+ that were eluted from the column nearly equaled that of Ca^{2+} and Mg^{2+} removed from the freshwater.

The clay structure of the soil was altered by chemical changes in the soil solution. During the freshwater flushing stage the Site 1 soil structure was able to recover causing a slight increase in flow rate or hydraulic conductivity. The Site 2 soil structure did not recover and the flow rate through the column remained the same as the simulated contaminant flushing stage.

Table 4.15. Modeled transport parameters for Site 1 during the fresh water flushing stage.

Constituent	Attenuation Factor, Rd	Hydrodynamic Dispersion, Hd (m^2/s)	Peclet Number
Cl^-	1.0	$1.1x10^{-8}$	1.6
NH_4^+	4.3	$1.7x10^{-7}$	0.1
K^+	1.4	$1.1x10^{-8}$	1.8
Na^+	1.4	$1.1x10^{-8}$	1.8
HCO_3^-	2.5	$9.3x10^{-8}$	0.2

Table 4.16. Modeled transport parameters for Site 2 during the fresh water flushing stage.

Constituent	Attenuation Factor, Rd	Hydrodynamic Dispersion, Hd (m^2/s)	Peclet Number
Cl^-	1.1	$4.6x10^{-9}$	2.5
NH_4^+	0.7	$4.6x10^{-9}$	2.5
K^+	2.5	$1.2x10^{-8}$	1.0
Na^+	1.0	$3.5x10^{-9}$	3.4
HCO_3^-	1.0	$3.5x10^{-9}$	3.4
Ca^{2+}	9.5	$1.4x10^{-9}$	8.5
Mg^{2+}	8.0	$4.6x10^{-10}$	25.5

CHAPTER 5
CONCLUSION

5.1 Simulated Contaminant Flushing Stage Summary

This portion of the study examined the attenuation of inorganic contaminants in a simulated contaminant in laboratory soil columns containing two different soils. Simple transport modeling and mass balance approaches were used to indentify important processes and geochemical properties which control the fate of the contaminants. The experiments showed the ion-exchange processes controlled the rate of transport of the contaminants. Secondary processes included dissolution/precipitation of solid phases and the effect of soil solution chemistry on clay soil structures.

During the simulated contaminant flushing stage, ammonium and potassium replaced calcium and magnesium on the soil exchange sites. Generally, ions with higher valency will exchange for those of lower valency, but in this case the majority of the ions (ammonium and potassium) in the solution have a lower valency and will exchange with those of higher valency by mass action. Calcium is first to be replaced, followed by magnesium once the ionic strength of the solution increases.

The displacement of calcium and magnesium created a concentration pulse of these cations that coincides with the chloride breakthrough curve. Calcium and magnesium concentrations reached

up to approximately 275% and 2000%, respectively, higher than the freshwater originally in the column. The observed concentration pulse agrees with the results from Fonstad (2004) who concluded that hard water front can be an early indicator of contaminant from a source that is high in non-native cations.

The cations are attenuated with respect to chloride in the following order: $Na < NH_4^+ < K^+$. Even though the soil was able to attenuate the transport of ammonium and potassium, the exchange capacity of the soil was eventually exhausted and these constituents were able to leave the column at the same concentration as the influent.

The mass of NH_4^+ and K^+ retained in the column (101 meq) was twice of Ca^{2+} and Mg^{2+} released from the column (55 meq) which suggests a loss of Ca and Mg^{2+} released from the soil which happens to be equal to the amount of bicarbonate lost in the system which suggests calcite precipitation (lost 115 meq of bicarbonate which is equal to 57.5 mmol 57.5 meq Ca^{2+}).

5.2 Freshwater Flushing Stage Summary

Freshwater flushing was leached through the soil columns to assess the permanency of contaminant attenuation and to identify the mechanisms and geochemistry of contaminant release. Concentrations of NH_4^+ and K^+ declined quickly. 95% of attenuated NH_4^+ was released by the soil. Therefore, the attenuation of NH_4^+ is reversible but this occurs over several pore volumes at concentrations which are much lower than those in the leachate and therefore would not result in a mass loading (Thorton 2001). There is good agreement between the fraction of

cations sorbed to and desorbed from the soil during freshwater flushing, suggesting cation exchange as the mechanism responsible.

5.3 Environmental Implications

Both soils possess a considerable capacity to attenuate the inorganic contaminants in manure leachate and will significantly attenuate the transport of NH_4^+ and K^+, in agreement with previous studies (Fonstad 2004). However, both materials have a finite sorption capacity and when exhausted, NH_4^+ passes through the sediment unattenuated at leachate concentrations. Furthermore, when fresh water is introduced the sorbed ions are liberated from the soil.

Attenuation of NH_4^+ occurred by cation exchange with the sediment materials but this attenuation is finite. Attenuated inorganic contaminants may be mobilized from clay liners during contact with fresh water after leachate through-flow has ceased in the longer term. Attenuated NH_4^+ and K^+ will be released but the groundwater loadings will be manageable.

This work provides greater understanding of leachate pollutant fate and an improved basis for the risk assessment of aquifer vulnerability for lined and unlined lagoons.

LIST OF REFERENCES

American Public Health Association. 1999. Standard methods for the examination of water and wastewater. American Water Works Association, Water Environment Federation.

Appelo, C.A.J. 1996. Multicomponent ion exchange and chromatography in natural systems. In: P.C. Lichtner, C.I. Steefel, and E.H. Oelkers (eds), Reviews in Mineralogy 34: 193-227.

Appelo, C.A.J. and D. Postma. 1999. Geochemistry, Groundwater, and Pollution. A.A. Balkema, Rotterdam, Netherlands.

Barbour, S.L. and N. Yang. 1993. A review of the influence of clay-brine interactions on the geotechnical properties of Ca-montmorillonitic clayey soils from western Canada. Canadian Geotechnical Journal 30: 920-934.

Barbour, S.L. and D.G. Fredlund. 1989. Mechanisms of osmotic flow and volume change in clay soils. Canadian Geotechnical Journal 26: 551-562.

Beekman, H.E. and C.A.J. Appelo. 1990. Ion chromatography of fresh- and salt-water displacement: laboratory experiments and multicomponent transport modelling. Journal of Contaminant Hydrology 7: 21-37.

Carter, M.R. 1993. Soil Sampling and Methods of Analysis. Canadian Society of Soil Science. Lewis Publishers.

Ceazan, M.L, E.M. Thurman and R. L. Smith. 1989. Retardation of ammonium and potassium transport through a contaminated sand and gravel aquifer: the role of cation exchange. Environmental Science and Technology 23: 1402-1408.

Chang, W.J. and R. Donahue. 2007. Cation exchange due to the diffusion of ammonium from livestock effluent through glacial clay soils. Applied Geochemistry 22: 53-68.

Ciravolo, T.G. et al. 1979. Pollutant movement of shallow ground water tables from anaerobic swine waste lagoons. Journal of Environmental Quality 8 (1): 126-130.

Dohrmann, R. 2006. Cation Exchange Capacity Methodology I: An Efficient Model for the Detection of Incorrect Cation Exchange Capacity and Exchangeable Cation Results. Applied Clay Science 34: 31-37.

Erksine, A.D. 2000. Transport of ammonium in aquifers: retardation and degradation. Quarterly Journal of Engineering Geology and Hydrogeology, 33: 161-170.

Fetter, C.W. 1999. Contaminant Hydrogeology 2nd Edition. Prentice-Hall, Upper Saddle River, New Jersey, USA.

Fonstad, T.A. 2004. Transport and fate of nitrogen from earthen manure storage effluent seepage. Ph.D. Thesis. Saskatoon, SK. Department of Civil Engineering, University of Saskatchewan.

Fonstad, T.A. and C. Rinas. 2006. Geochemistry and hydrogeology near earthen manure storages. ADF Final Report Agricultural and Bioresource Engineering, University of Saskatchewan, May 2006.

Freeze, R.A. and J.A. Cherry. 1979. Groundwater. Prentice Hall, Upper Saddle River, New Jersey, USA.

Gelhar, L.W., C. Welty, K.R. Rehfeldt. 1992. A critical review of data on field-scale dispersion in aquifers. Water Resources Research 28(7): 1955-1974.

Goodall, D.C. and R.M. Quigley. 1977. Pollutant migration from two sanitary landfill sites near Sarnia, Ontario. Canadian Geotechnical Journal 14: 223-236.

Griffioen, J., C.A.J. Appelo and M. Van Veldhuizen. 1992. Practice of chromatography: deriving isotherms from elution curves. Soil Science Society of America Journal 56: 1429-1436.

Hendershot, W.H. and Duquette M. 1986. A simple barium chloride method for determining cation exchange capacity and exchangeable cations. Soil Science Society of America Journal 50: 605-608.

Islam, J. and N. Singhal. 2002. A one-dimensional reactive multi-component landfill leachate transport model. Environmental Modelling and Software. 17(2): 531-543.

Jones, D.D. and R. Koelsch. 1999. Closure of earthen manure storages (including holding ponds and anaerobic lagoons).

Kennedy, C.A. and W.C. Lennox. 2001. A stochastic interpretation of the tailing effect in solute transport. Stochastic Environmental Research and Risk Assessment 15(4): 325-340.

Keren, R. and M. Ben-hur. 2003. Interaction effects of clay swelling and dispersion and CaCO3 content on saturated hydraulic conductivity. Australian Journal of Soil Research 41(5): 979-989.

Koelsch, R. 2006. Abandonment planning for earthen manure storages, holding ponds, and anaerobic lagoons. University of Nebraska-Lincoln Extension, Institute of Agriculture and Natural Resources.

Levy, M. and B. Berkowitz, 2003. Measurement and analysis of non-Fickian dispersion in heterogeneous porous media. Journal of Contaminant Hydrology 64 (3-4): 203-226.

Ludwig, B. and A. Kolbl. 2002.Modelling cation exchange rates in an undisturbed subsoil at different flux rates. Soil Science 168(4): 253-266.

McMillan, R.J. and A. Woodbury. 2000. Investigation of seepage from earthen animal manure storages. Winnipeg, Manitoba: Manitoba Livestock Manure Management Initiative Inc.

Ogata, A. and R.B. Banks. 1961. A solution of the differential equation of longitudinal dispersion porous media. Professional Paper No. 411-A-USGS Geological Survey, Washington, D.C.

Ritter, W.F. and A.E.M Chirnside. 1990. Impact of animal waste lagoons on ground-water quality. Biological Wastes 34: 39-54.

Saskatchewan Agriculture Food and Rural Revitalization. 2005. Site Characterization Manual for the development of Intensive Livestock Operations and Earthen Manure Storage. Saskatchewan Agriculture Food and Rural Revitalization, Government of Saskatchewan, Canada, January 2005.

Saskatchewan Pork. Saskatchewan Statistics. <http://www.saskpork.com/html/industry_info/industry_stats/index.cfm> (14 March 2011)

Schmitz, R.M. 2006. Can the diffuse double layer theory describe changes in hydraulic conductivity of compacted clay? Geotechnical and Geological Engineering 24: 1835-1844.

Shackleford, C.D. 1995. Cumulative mass approach for column testing. Journal of Geotechnical Engineering 19: 696-703.

Shackleford, C.D. and P.L. Redmond. 1995. Solute breakthrough curves for processed kaolin at low flow rates. Journal of Geotechnical Engineering 121(1): 17-32.

Stephens, D.B., K. Hsu, M.A. Prieksat, M.D. Ankeny, N. Blandford, T.L. Roth, J.A. Kelsey, and J.R. Whitworth. 1998. A comparison of estimated and calculated effective porosity. Hydrogeology Journal 6(1): 156-165.

Teppen, B.J. and D.M. Miller. 2006. Hydration energy determines isovalent cation exchange selectivity by clay minerals. Soil Science Society of America Journal 70: 31-40.

Thornton, S.F. 2001. Attenuation of landfill leachate by clay liner materials in laboratory columns: 2. Behavior of inorganic contaminants. Waste Management and Research 19(1): 70-88.

Thornton, S.F., J.H. Tellam, D.N. Lerner. 2005. Experimental and modelling approaches for the assessment of chemical impacts of leachate migration from landfills: a case study of a site on the Triassic sandstone aquifer in the UK East Midlands. Geotechnical and Geological Engineering 23: 811-829.

van der Kamp, G., Van Stempvoort, D.R., Wassenaar, L.I., 1996. The radial diffusion method. Using intact cores to determine isotopic composition, chemistry and effective porosities for groundwater in aquitards. Water Resources Research 32: 1815–1822.

Voegelin, A., V.M. Vulvava, F. Kuhnen, and R. Kretzschmar. 2000. Multicomponent transport of major cations predicted from binary adsorption experiments. Journal of Contaminant Hydrology. 46: 319-388.

Vulvava, V.M, R. Kretzschmar, U. Rusch, D. Grolimund, J.C. Westall, M. Borkovec. 2000. Cation competition in a natural subsurface material: modeling of sorption equilibria. Environment, Science and Technology 34: 2149-2155.

Westerman et al. 1995. Swine lagoon seepage in sandy soil. Transactions of the ASAE 38 (6): 1749-1760.